PERFORMANCE ANALYSIS OF HEAT PIPE HEAT EXCHANGER USING BINARY WORKING FLUIDS

MR. ATIPOANG NUNTAPHAN

A Thesis Submitted in Partial Fulfillment of the Requirements for the Degree of Doctor of Philosophy Thermal Technology Program School of Energy and Materials King Mongkut's University of Technology Thonburi 2000

Performance Analysis of Heat Pipe Heat Exchanger Using Binary Working Fluids

Mr. Atipoang Nuntaphan M.Eng. (Mechanical Engineering)

A Thesis Submitted in Partial Fulfillment of the Requirements for the Degree of Doctor of Philosophy Thermal Technology Program School of Energy and Materials King Mongkut's University of Technology Thonburi 2000

Thesis Committee	
(Prof. Dr. Tanongkiat Kiatsiriroat)	Chairman
(Dr. Jirawan Tiansuwan)	Co-Chairman
(Prof. Dr. Prida Wibulswas)	Member
(Assoc. Prof. Dr. Pojanie Khummongkol)	Member
(Dr. Chi-Chuan Wang)	Member

Copyright reserved

Thesis Title Performance Analysis of Heat Pipe Heat Exchanger Using

Binary Working Fluids

Thesis Credits 42

Candidate Mr. Atipoang Nuntaphan

Supervisors Prof. Dr. Tanongkiat Kiatsiriroat

Dr. Jirawan Tiansuwan

Degree of Study Doctor of Philosophy

Department Thermal Technology

Academic Year 2000

Abstract

This research work studies the performance of the thermosyphon heat exchanger using binary of working fluids. It can be divided into two parts, thermal behavior of thermosyphon heat pipe using binary working fluids and thermal performance enhancement of thermosyphon heat exchanger using various types of working fluids.

The first part is the study of thermal behavior of thermosyphon heat pipe using ethanol-water and TEG-water and the affecting parameters such as the mixture content, the pipe aspect ratio and the working temperature. From the experiments, it is found that at low temperature of heat source, ethanol-water mixture has higher heat transfer rate than that of water, however the ethanol-water mixture gives lower heat transfer rate than that of pure ethanol. In case of TEG-water mixture, the heat transfer rate of the thermosyphon varies with the content of TEG in the mixture and it is found that TEG in the mixture can enlarge the critical heat flux due to the flooding limit of the small size of the thermosyphon.

The boiling equation of Rohsenow and the condensation equation of Nusselt are modified to predict the heat transfer coefficients of the boiling and the condensation inside the thermosyphon. In case of the binary mixtures, it is found that the weighted average of the heat transfer coefficient of each component can be used to predict the total heat transfer coefficient. Furthermore, it is found that ESDU's equation can be used

to predict the critical heat flux due to the flooding limit of the thermosyphon with pure working fluids and binary mixtures.

The second part concerns an investigation of the concept of introducing two-fluid thermosyphons. Calculations were performed for both low and high temperature ranges with parallel and counter flow arrangements by using simulation programs. For lower temperature application, 50 °C < T_{hi} < 100 °C, use of ethanol in some rows and water in the rest of the thermosyphon can slightly improve the associated heat transfer performance of the heat exchanger. However, for balanced parallel flow arrangement, the concept of using two-fluid thermosyphons may not be feasible.

For thermosyphon heat exchanger operating at high temperature applications, it is found that with selected mixture content of TEG-water in each row of the thermosyphon the performance of the system could be increased approximately 30-80% compared with pure TEG for parallel flow and 60-115% for counter flow configurations. The performances also increase approximately 80-160% for parallel flow and 140-220% for counter flow compared with those of pure dowtherm A which is the common working fluid at high temperature applications.

Keywords: Thermosyphon heat pipe / Boiling and Condensation of Binary Mixtures /
Heat transfer Enhancement of Heat Exchanger

หัวข้อวิทยานิพนธ์

การวิเคราะห์สมรรถนะของเครื่องแลกเปลี่ยนความร้อนแบบท่อความร้อน

ที่ใช้สารทำงานคู่ผสม

หน่วยกิตของวิทยานิพนธ์ 42 หน่วย

ON AND IN HOUSE

โดย

นายอติพงศ์ นันทพันธ์

อาจารย์ที่ปรึกษา

ศ. คร. ทนงเกียรติ เกียรติศิริ โรจน์

คร. ชีรวรรณ เคียรถ์สุวรรณ

ระดับการศึกษา

ปรัชญาคุษฎีบัณฑิต

สายวิชา

เทคโนโลยีอุณหภาพ

ปีการศึกษา

2543

บทกัดย่อ

งานวิจัยนี้ศึกษาเกี่ยวกับสมรรถนะของเครื่องแลกเปลี่ยนความร้อนแบบเทอร์โมไซฟอนที่ใช้ สารทำงานคู่ผสม โดยสามารถแบ่งออกเป็นสองส่วนคือ การศึกษาพฤติกรรมทางความร้อนของท่อ ความร้อนแบบเทอร์โมไซฟอนที่ใช้สารทำงานคู่ผสม และ การศึกษาสมรรถนะทางความร้อนของ เครื่องแลกเปลี่ยนความร้อนแบบท่อความร้อนที่ใช้สารทำงานหลายๆ ประเภท

งานวิจัยในส่วนแรกทำการศึกษาพฤติกรรมทางความร้อนของท่อความร้อนแบบเทอร์โมไซ ฟอนที่ใช้สารทำงาน เอธานอล-น้ำ และ ไตรเอธิลีนไกคอล-น้ำ โดยทำการศึกษาผลของพารามิเตอร์ที่ เกี่ยวข้องคือ สัดส่วนผสมของสารทำงาน ขนาดของท่อความร้อน และ อุณหภูมิการทำงาน จากการ ทดลองพบว่า ในกรณีที่อุณหภูมิของแหล่งความร้อนมีค่าต่ำกว่าประมาณ 80°C สารทำงานผสมเอธา นอล-น้ำ ให้ค่าอัตราการการถ่ายเทความร้อนที่สูงกว่าในกรณีของน้ำ แต่อย่างไรก็ตามต่ำกว่าในกรณีของเอธานอลบริสุทธิ์ ในกรณีของสารทำงาน ไตรเอธิลีนไกคอล-น้ำ อัตราการถ่ายเทความร้อนจะแปร ผกผันกับปริมาณของไตรเอธิลีนไกคอล แต่อย่างไรก็ตามพบว่าการใช้สารทำงานผสม ไตรเอธิลีนไก คอล-น้ำ สามารถช่วยลดภาวะวิกฤติเนื่องจากการท่วมของสารทำงานในท่อความร้อนขนาดเล็กได้

สมการการเดือดของ Rohsenow และสมการการควบแน่นของ Nusselt ได้ถูกคัดแปลงเพื่อ นำมาใช้ในการคำนวณค่าสัมประสิทธิ์การถ่ายเทความร้อนของการเดือดและการควบแน่นของสาร ทำงานภายในท่อความร้อน ในกรณีของสารทำงานผสม พบว่าการเฉลี่ยแบบถ่วงน้ำหนักของค่า สัมประสิทธิ์การถ่ายเทความร้อนสารทำงานแต่ละประเภทในสารผสม สามารถทำนายค่าสัมประสิทธิ์ การถ่ายเทความร้อนของสารทำงานคู่ผสมได้ และยังพบว่า สมการของ ESDU สามารถนำมาใช้ใน งานวิจัยในส่วนที่สองเป็นการนำเอาสารทำงานสองชนิคมาใช้ในเครื่องแลกเปลี่ยนความร้อน แบบเทอร์ โมไซฟอนแบบไหลตามกันและไหลสวนทางกันโดยแบ่งออกเป็นสองส่วนคือ ช่วงอุณหภูมิ การทำงานต่ำและสูง ในการคำนวณจะใช้โปรแกรมคอมพิวเตอร์เพื่อจำลองสถานการณ์ต่างๆ ในช่วง อุณหภูมิการทำงานต่ำ (50 °C < T_{hl} < 100 °C) พบว่าการใช้เอธานอลหรือน้ำในแถวของท่อความ ร้อนที่เหมาะสมสามารถเพิ่มสมรรถนะของเครื่องแลกเปลี่ยนความร้อนได้เล็กน้อย แต่อย่างไรก็ตามวิธี การนี้ไม่สามารถใช้ได้กับเครื่องแลกเปลี่ยนความร้อนแบบไหลตามกันที่มีอัตราการไหลของกระแสร้อนและกระแสเข็นเท่ากัน

ในกรณีเครื่องแลกเปลี่ยนความร้อนแบบเทอร์โมไซฟอนที่มีอุณหภูมิการทำงานสูง พบว่าการ เลือกใช้อัตราส่วนผสมของไตรเอธิลีนไกคอลที่เหมาะสมเป็นสารทำงานในแต่ละแถวของท่อความ ร้อนสามารถเพิ่มสมรรถนะการถ่ายเทความร้อน 30-80% ในกรณีเครื่องแลกเปลี่ยนความร้อนแบบ ไหลสวนทางกัน และ 60-115% ในกรณีเครื่องแลกเปลี่ยนความร้อนแบบไหลตามกันเมื่อเทียบกับ การใช้โครเอธิลีนไกคอลอย่างเคียว และสามารถเพิ่มสมรรถนะการถ่ายเทความร้อน 80-160% ใน กรณีเครื่องแลกเปลี่ยนความร้อนแบบไหลตามทางกัน และ 140-220% ในกรณีเครื่องแลกเปลี่ยน ความร้อนแบบไหลสวนทางกัน เมื่อเทียบกับการใช้สารทำงาน ดาวเทอร์ม เอ ซึ่งเป็นสารทำงานที่ใช้ กันในช่วงอุณหภูมิการทำงานนี้

คำสำคัญ (Keywords) : ท่อความร้อนแบบเทอร์โมไซฟอน / การเดือดและการควบแน่นของสาร ทำงานคู่ผสม / การเพิ่มสมรรถนะทางความร้อนของเครื่องแลกเปลี่ยนความ ร้อน

ACKNOWLEDGEMENTS

The author wishes to express his gratitude and appreciation to his adviser, Professor Dr. Tanongkiat Kiatsiriroat for his valuable guidance and kindly suggestion throughout the research work. A sincere thanks is extended to Dr. Jirawan Tiansuwan, his co-adviser, for her helpful and gives useful comment entire the period of this thesis.

Grateful acknowledgements are made to the members of the Ph.D. Program Committee, Professor Dr. Prida Wibulswas and Associate Professor Dr. Pojanie Khummongkol for their valuable comments. The author is greatly indebted to Dr. Chi-Chuan Wang from Industrial Technology Research Institute, Taiwan R.O.C. not only for his kindly agreed to serve as the External Examiner but also his very kind helpful and take care when the author stayed in Taiwan.

Acknowledgement is due to the Royal Jubilee Ph.D. Program from the Thailand Research Fund for awarding the scholarship for his study in KMUTT. A heartfelt thanks is also extended to the Electricity Generating Authority of Thailand for giving the great opportunity to join the Ph.D. course.

Cordial Thanks is extended to Assistant Professor Dr. Pornapit Darasawang for correcting the English in this thesis.

The author is grateful thank to Department of Mechanical Engineering, Chiang Mai University for all facilities and accommodations and the helpful of all students in Thermal System Research Unit, CMU. are also appreciated.

Finally, the author wishes to thank to all guidance and encouragement of his parents, which made this work both possible and worthwhile.

CONTENTS

			Page
English Abs	stract		ii
Thai Abstra			iv
Acknowledg	gement	<u>:</u>	vi
Content	-		vii
List of Table	es		x
List of Figur	res		xii
Nomenclatu	re		xvi
Chapter 1	Intro	oduction	1
	1.1	State of Problems and Background	1
	1.2	Research Objectives	2
	1.3	Scope of Work	3
	1.4	Methodology	3
	1.5	Expected Benefits	4
Chapter 2	Perf	formance Analysis of Thermosyphon Heat Pipe Using	5
	Bin	ary Working Fluids	
	2.1	Introduction	5
	2.2	Literature Reviews	5
		2.2.1 Boiling and Condensation of Binary Mixtures	5
		2.2.2 Boiling and Condensation Heat Transfer	8
		Coefficient of the Thermosyphon	
		2.2.3 Suitable Filling Ratio of the Thermosyphon	11
	2.3	Experimental Set-up	12
		2.3.1 Working Fluid Selection	12
		2.3.2 Experimental Apparatus and Test Procedure	13
	2.4	Heat Transfer Analysis	14
	2.5	Results and Discussion	17

	2.5.1 Temperature Distributions Inside the Thermosyphon	17
	2.5.2 Heat Transfer Rate	18
	2.5.3 Thermal Resistance	19
	2.5.4 Effectiveness	23
	2.5.5 Heat Transfer Model of Pure Working Fluid	23
	2.5.6 Heat Transfer Model of Binary Working Fluids	27
	2.6 Conclusion	29
Chapter 3	Flooding Limit of Thermosyphon Heat Pipe	30
	3.1 Introduction	30
	3.2 The Experimental Set-up	30
	3.3 Theoretical Background	32
	3.4 Results and Discussion	32
	3.5 Conclusion	35
Chapter 4	Design and Construction of Thermosyphon Heat Exchanger	36
	4.1 Introduction	36
	4.2 Literature Reviews	36
	4.3 Design of Thermosyphon Heat Exchanger	37
	4.3.1 Suitable Size of Thermosyphon Heat Exchanger	37
	4.3.1 Details of the Thermosyphon Heat Exchanger	40
	4.3.3 Nozzle Box	44
	4.4 Testing Procedure	45
	4.4.1 The Thermosyphon Heat Pipe	45
	4.4.2 Test of Thermosyphon Heat Exchanger	46
Chapter 5	Simulation Program of the Thermosyphon Heat Exchanger	48
	5.1 Introduction	48
	5.2 Theoretical Background	48
	5.2.1 Air-side Thermal Resistances	48
	5.2.2 Wall Resistances	55
	5.2.3 Tube-side Thermal Resistances	55
	5.2.4 Overall Thermal Resistance	56

	5.3 Simulation Program for Single Working Fluid	57
Chapter 6	Selection of Working Fluids for Air-to-Air Thermosyphon	66
	Heat Exchanger	
	6.1 Introduction	66
	6.2 Selection of Working Fluids for Low Operating	67
	Temperature Thermosyphon Heat Exchanger	
	6.2.1 Simulation Program	67
	6.2.2 Simulation Results and Discussion	70
	6.2.3 Testing of Thermosyphon Heat Exchanger	77
	6.3 Selection of TEG Content in Thermosyphon	79
	Heat Exchanger	
	6.3.1 Simulation Program	79
	6.3.2 Results and Discussion	83
	6.4 Conclusion	86
Chapter 7	Second Law Analysis of Thermosyphon Heat Exchanger	89
	7.1 Introduction	8 9
	7.2 Theoretical Background	89
	7.3 Second Law Efficiency of Thermosyphon Heat Exchanger	90
	. 7.3.1 Low Operating Temperature	90
	7.3.2 High Operating Temperature	96
Chapter 8	Conclusion	104
	8.1 Summary of the Research Work	104
	8.1.1 Thermal Behavior of the Thermosyphon	104
	Heat Pipe using binary mixtures	
	8.1.2 Performance Analysis of Thermosyphon Heat	105
	Exchanger Using Various Kinds of Working Fluids	
	8.2 Recommendation	105
References	-	107
Appendix A	Simulation Programs	111
В	Publications	151

LIST OF TABLES

Table		Page
2.1	Factors C ₁ and C ₂ from the experiments	. 24
2.2	The correlation coefficient C ₃ and C ₄	26
2.3	Factors C ₅ and C ₆ from the experiments	26
5.1	Zhukauskas constants for tube bank in cross flow	51
5.2	Correction factor of Equation (5.3) at low number of tube rows	52
5.3	Testing conditions of the simulation programs for calculate the	61
	performance of thermosyphon heat exchanger	
6.1	Testing conditions and related geometrical parameters of the	68
	thermosyphon heat exchanger	
6.2	Results of simulation in the case of balanced counter flow	73
	arrangement for low temperature application	
6.3	Results of simulation in the case of unbalanced counter flow	74
	arrangement for low temperature application	
6.4	Results of simulation in the case of balanced parallel flow	75
	arrangement for low temperature application	
6.5	Results of simulation in the case of unbalanced parallel flow	76
	arrangement for low temperature application	
6.6	Testing conditions of the thermosyphon air preheater	77
6.7	Testing conditions and related geometrical parameters of the	81
	thermosyphon heat exchanger	
6.8	Results of simulation in the case of parallel flow arrangement;	87
	inlet temperature of cold air = 30°C	
6.9	Results of simulation in the case of counter flow arrangement;	88
	inlet temperature of cold air = 30°C	
7.1	The 2 nd law efficiency in the case of balanced counter flow	98
	arrangement for low temperature application	

.

7.2	The 2 nd law efficiency in the case of balanced parallel flow	99
	arrangement for low temperature application	
7.3	The 2 nd law efficiency in the case of unbalanced counter flow	100
	arrangement for low temperature application	
7.4	The 2 nd law efficiency in the case of unbalanced parallel flow	101
	arrangement for low temperature application	
7.5	The 2 nd law efficiency in the case of parallel flow arrangement;	102
	inlet temperature of cold air = 30°C	
7.6	The 2 nd law efficiency in the case of counter flow arrangement;	103
	inlet temperature of cold air = 30°C	

LIST OF FIGURES

Figure		Page
1.1	The thermosyphon heat pipe	2
2.1	Typical gas-loaded heat pipe	6
2.2	Effect of filling ratio on critical heat flux of the thermosyphon	11
2.3	The experimental apparatus	14
2.4	Temperature distributions of ethanol-water mixtures along the	17
	thermosyphon at various conditions	
2.5	Temperature distributions of TEG-water mixtures along the	18
	thermosyphon at various conditions	
2.6	The relations between heat transfer rate of the thermosyphon heat	20
	pipe with binary mixtures and hot oil temperature at various	
	conditions	
2.7	The relation between thermal resistance of the thermosyphon heat pipe	21
	with binary mixtures and hot oil temperature at various conditions	
2.8	The relation between effectiveness of the thermosyphon heat pipe	22
	with binary mixtures and hot oil temperature at various conditions	
2.9	A comparison of boiling heat transfer coefficients inside the	24
	thermosyphon between the experimental and calculation data	
2.10	Comparisons of boiling heat transfer coefficients from	25
	the experiments and equation (2.11)	
2.11	A comparison of Nusselt number of boiling of water from	25
	the experiments and equation (2.12)	
2.12	Comparisons of condensation heat transfer coefficient	26
	from the experiments and equation (2.13)	
2.13	Comparisons of boiling heat transfer coefficients of ethanol-	27
	water mixtures from the experiments and equation (2.14)	
2.14	Comparisons of boiling heat transfer coefficients of TEG-	28

	water mixtures from the experiments and equation (2.14)	
2.15	Comparisons of condensation heat transfer coefficients of	28
	ethanol-water mixtures from the experiments and equation (2.14)	
2.16	Comparisons of condensation heat transfer coefficients of	29
	TEG-water mixtures from the experiments and equation (2.14)	
3.1	The experimental apparatus	31
3.2	CHF of thermosyphon heat pipe using TEG-water mixtures	33
3.3	A comparison of critical heat flux from the experiment and the ESDU	34
	model with various mixtures content of TEG	
3.4	A comparison of critical heat flux from the experiment and the ESDU	34
	model with various mixtures content of ethanol	
4.1	Cost saving at various area of air preheater	39
4.2	Details of the experimental apparatus	41
4.3	Top view of the apparatus	42
4.4	Side view of the apparatus	42
4.5	Thermosyphon heat pipes	43
4.6	Radial tube gas burner	43
4.7	Position of the pipes inside the heat exchanger	44
4.8	Standard nozzle for measuring the air flow rate	44
4.9	An apparatus for filling in the working fluid	45
4.10	Positions for measuring temperatures of the fluid at the inlet and the	47
	outlet ports of the test section (9 points per one section)	
5.1	Thermal resistance circuit of the thermosyphon	49
5.2	Tube arrangements in a tube bank	50
5.3	Geometrical characteristic of circular fin	52
5.4	Flow arrangement of the thermosyphon heat exchanger	56
5.5	Flow chart for calculating the heat transfer rate by using the uniform	57
	heat transfer method	
5.6	Flow chart for calculating the heat transfer rate of the counter flow	58
	heat exchanger in case of using the non-uniform heat transfer method	

.

5.7	Flow chart for calculating the heat transfer rate of the parallel flow	59
	heat exchanger in case of using the non-uniform heat transfer method	
5.8	Temperature profiles of balanced counter flow heat exchanger	62
5.9	Temperature profiles of unbalanced counter flow heat exchanger	62
5.10	Temperature profiles of balanced parallel flow heat exchanger	63
5.11	Temperature profiles of unbalanced parallel flow heat exchanger	63
5.12	Heat transfer rate at each row of the thermosyphon heat exchanger	64
5.13	Comparisons of heat transfer area calculated by uniform and	64
	non-uniform heat transfer methods	
6.1	The flow chart of the two-fluid thermosyphons in low working	69
	temperature	
6.2	Appropriate number of ethanol thermosyphon of balanced counter flow;	70
	the inlet cold air is 30°C	
6.3	Temperature profile of the balanced parallel flow	71
6.4	The comparison of heat transfer rate from the experimental results	78
	and simulations	
6.5	A flow chart presenting the calculation of the suitable mixture	82
	content of TEG-water in each row of the thermosyphon heat exchanger	
6.6	A comparison of temperature profile of parallel flow thermosyphon air	83
	preheater between using TEG-water mixtures and pure TEG	
	(no. 7 in Table 6.8)	
6.7	A comparison of temperature profile of balanced counter flow	84
	thermosyphon air preheater between using TEG-water mixtures	
	and pure TEG (no. 3 in Table 6.9)	
6.8	Comparison of temperature profile of unbalanced counter flow	85
	thermosyphon air preheater between using TEG-water mixtures	
	and pure TEG (no.18 in Table 6.9)	
7.1	Counter flow heat exchanger	89
7.2	The effect of inlet temperature of hot air and mass flow rate on	92
	the 2 nd law efficiency; water and balanced counter & parallel flows	

.

,

7.3	The effect of inlet temperature of hot air and mass flow rate on	92
	the 2 nd law efficiency; water and unbalanced counter & parallel flows	
7.4	The effect of inlet temperature of hot air and mass flow rate on	93
	the 2 nd law efficiency; ethanol and balanced counter & parallel flows	
7.5	The effect of inlet temperature of hot air and mass flow rate on	93
	the 2 nd law efficiency; ethanol and unbalanced counter & parallel flows	
7.6	The effect of inlet temperature of hot air and mass flow rate on the 2 nd	94
	law efficiency; 2-kinds and balanced counter & parallel flows	
7.7	The effect of inlet temperature of hot air and mass flow rate on	94
	the 2 nd law efficiency; 2-kinds and unbalanced counter & parallel flows	
7.8	A temperature profile of water thermosyphon at various mass flow rate	95
7.9	A comparison of 2 nd law efficiency at various kinds of working fluids	95
7.10	The 2 nd law efficiency of various kind of working fluids of balanced	96
	counter flow heat exchanger operating at high temperature	
7.11	The 2 nd law efficiency of various kind of working fluids of balanced	97
	parallel flow heat exchanger operating at high temperature	

NOMENCLATURE

Symbol		Unit
\boldsymbol{A}	area	m^2
A_{cs}	cross sectional area	m ²
Во	· Bond number	
c_c	capital cost	Baht
c_e	energy cost	Baht/J
crf	capital recovery factor	
C_{I-4}	empirical constants	
C_{om}	operating and maintenance cost	Baht/yr
C_p	specific heat	J/kgK
D	diameter	m
E	energy saving	J
f_{1-3}	parameter	
f_s	fin gap	m
f_t	fin thickness	m
g	gravitational acceleration	m/s ²
g_c	conversion factor	1 kgm/Ns ²
h	heat transfer coefficient	W/m^2K
i	interest rate	
j	Colburn factor	
k	thermal conductivity	. W/mK
K_p	parameter	
L	length	m
m	mass flow rate	kg/s
n_c	number of column of tube bank	
n_f	total number of fin	
Q	heat transfer rate	W

r	radius	m
S_{l}	longitudinal pith of tube bank	m
S_{t}	transverse pith of tube bank	m
t_{op}	operating time	s ·
T	temperature	°C
ΔT_e	temperature difference between inside surface	°C
	of evaporator tube and working fluid	
ΔT_c	temperature difference between inside surface	°C
	of condenser tube and working fluid	
ΔT_{lmtd}	log mean temperature difference	°C
x	mole fraction	
X	factor	
X_L	factor	
X_M	factor	
Y	factor	
Z	thermal resistance	K/W
Greek symbo	ls	
ε	2 nd law efficiency	
ϕ	factor	
η	efficiency	
φ	factor	
λ	latent heat	J/kg
μ	dynamic viscosity	Pas
ρ	density	kg/m³
σ	surface tension	N/m
Subscripts	-	
b	bare tube	
с	condenser section, cold air	
e	evaporator section	

f	fin, film evaporation
h	hot air
i	inside, inlet
l	liquid
0	outside, outlet
p	pool boiling
s	surface
ν	vapor
w	working fluid, water

CHAPTER 1

INTRODUCTION

1.1 State of Problems and Background

At present, development of heat exchanger for energy recovery from industrial waste heat has become an interesting topic for energy conservation programs. The thermosyphon heat pipe, one type of heat exchanger, has been used in many industrial processes because of its high advantages such as high thermal conductivity, low cost and being easy to be constructed.

The thermosyphon heat pipe shown in Figure 1.1 can be divided into three parts, evaporator, adiabatic and condenser. When heat is added to the evaporator section, the working fluid inside the heat pipe is boiled and vaporizes. The vapor carries heat from the heat source, flows to the condenser section and rejects heat to the heat sink. The working fluid condensate turns back to the evaporator section by gravity.

The thermosyphon normally uses a single component, especially water, as a working fluid, because water has a high working temperature range approximately 60-300°C [1-3] and high latent heat of vaporization. However, in some working conditions, temperature of heat source may be lower or higher than that of the normal range. As a result, the heat transfer rate of the thermosyphon heat pipe tends to decrease. In this study, an idea that implemented binary working fluids in the thermosyphon heat pipe is proposed. Both experimental and numerical approaches are performed to investigate its feasibility.

In case of lower temperature heat source (lower than 80°C), ethanol-water is proposed as a working fluid because ethanol has lower boiling point than water. Consequently it can be boiled easily and higher performance of the thermosyphon should be obtained. In case of higher temperature heat source (more than 300°C) or higher heat flux, for water, the transfer of heat may be hindered by the critical limit,

particularly flooding or dryout limit. To extend these limit, triethylene glycol (TEG)-water is proposed to be a working fluid. Because TEG has high boiling point (278°C at normal pressure), TEG in the mixture may retard the limits.

The aim of this research is to study the performance of the thermosyphon using binary working fluids, ethanol-water and TEG-water. The heat transfer model for single component is also modified to predict the heat transfer coefficients of the mixtures. Moreover, the application of binary working fluid with the thermosyphon heat exchanger is investigated to find out the suitable working fluid or mixture content of each row of the thermosyphon heat exchanger, which gives the highest heat transfer rate.

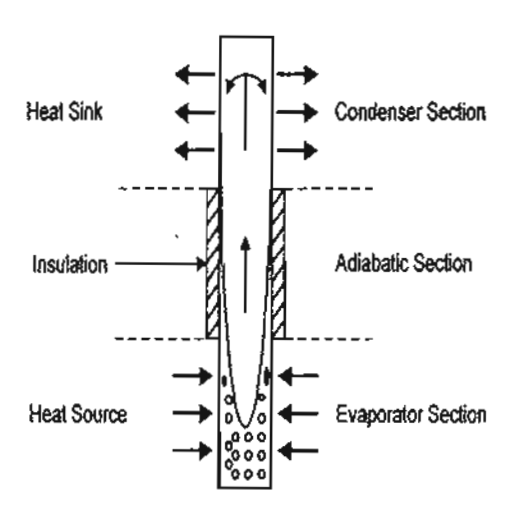


Figure 1.1 The thermosyphon heat pipe.

1.2 Research Objectives

- 1.2.1 Constructing expressions to evaluate the heat transfer coefficient of the thermosyphon heat pipe using binary working fluids.
- 1.2.2 Developing a method to calculate the thermal performance of the thermosyphon heat exchanger using binary working fluids.

1.3 Scope of Work

This research can be divided into two parts. The first part is the study of the heat transfer characteristic of the thermosyphon using ethanol-water and TEG-water as working fluids. In this part, the effect of the mixtures content, the pipe size and the working temperature will be considered. The model used to calculate the heat transfer coefficient is also modified for binary mixtures.

The second part of this research is the design of the heat pipe heat exchanger for exchanging heat between hot and cold streams of air by using the information from the first part. This part focuses on the effect of the mixture content, the heat pipe arrangement, the flow direction and the temperatures of the hot and the cold streams to the heat exchanger performance.

1.4 Methodology

- 1.4.1 Studying the thermal behavior of the thermosyphon heat pipe using ethanol-water and TEG-water mixtures.
- 1.4.2 Constructing the mathematical models to predict the boiling and condensation heat transfer coefficients of the thermosyphon using ethanol-water and TEG-water mixtures.
 - 1.4.3 Designing and constructing the thermosyphon heat exchanger.
- 1.4.4 Testing the performance of the thermosyphon heat exchanger by using pure water, ethanol and ethanol-water mixtures.
- 1.4.5 Setting the simulation program for calculating the performance of the thermosyphon heat exchanger and finding out the suitable working fluid in each row in cases of low and high working temperatures.

1.5 Expected Benefits

The information data from this research can be used to design and develop high performance thermosyphon heat exchangers by using binary working fluids at various operating temperatures.

CHAPTER 2

PERFORMANCE ANALYSIS OF THERMOSYPHON HEAT PIPE USING BINARY WORKING FLUIDS

2.1 Introduction

This chapter focuses on the of the thermosyphon heat pipe using ethanolwater and TEG-water. The parameters affecting the performance such as the pipe size, the working temperature and the mixture content have been investigated and the models for predicting the boiling and condensation heat transfer coefficients of the thermosyphon have also been carried out.

2.2 Literature Reviews

2.2.1 Boiling and Condensation of Binary Mixtures

Faghri [2] concluded the physical phenomenon of the gas-loaded heat pipe as follows:

Gas-loaded heat pipe is the most commonly used as a variable conductance heat pipe. This heat pipe used fixed amount of buffer gas to control its operating temperature, as shown in Figure 2.1. During gas-loaded heat pipe operation, the buffer gas is swept toward the condenser section by the vapor. Since the gas is non-condensable, it remains in the condenser section, forming a barrier to vapor flow and condensation. This barrier effectively eliminates convective heat transfer in the inaction portion of the condenser, thus providing a control mechanism for the heat sink conditions.

With further increase of heat flux, an increase in the vapor temperature and pressure in the thermosyphon appears. This increase in the vapor pressure compresses the non-condensable gas plug, activating more of the condenser section.

Since more of the condenser section is available for convective heat transfer, the heat transfer from the condenser increases and the condenser temperature remains constant. This control allows a gas-loaded heat pipe to operate at nearly isothermal condenser conditions with a varying evaporator input heat load. However, the amount of input heat load variation for which an isothermal condenser is maintained depends on several physical properties of the working fluid and the buffer gas, as well as the structure of the heat pipe.

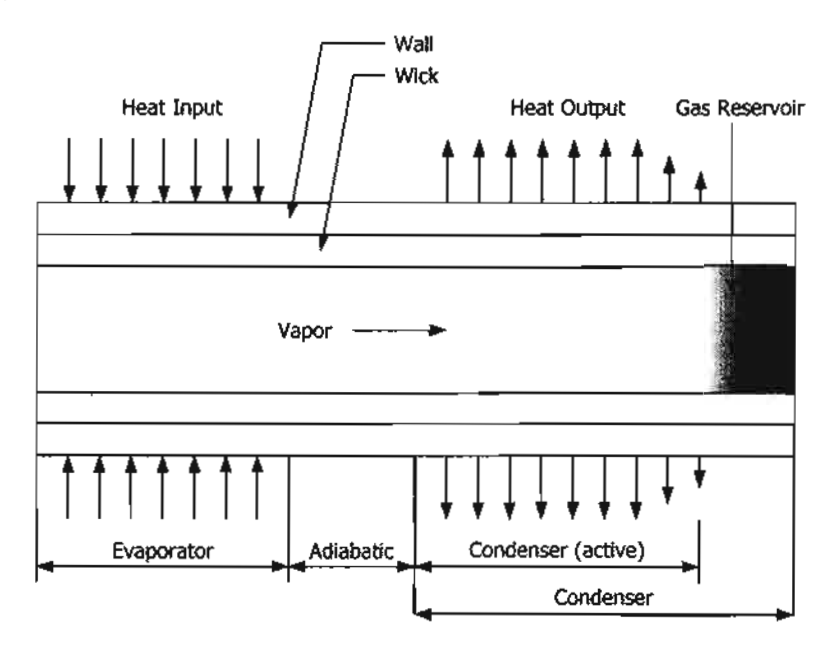


Figure 2.1 Typical gas-loaded heat pipe.

Peterson, Hijikata and Tien [4] studied the variable conductance behavior of the thermosyphon heat pipe using binary mixture as a working fluid. The refrigerant mixture R113-R11 was used as a working medium of the thermosyphon with no charge of non-condensable gas. It was found that when inputting heat to the evaporator section, more volatile component, R113, vaporizes and acts as a buffer or a non-condensable gas of the thermosyphon. Therefore, the phenomena look like a gas-loaded heat pipe. It was also found that using binary mixture could provide equal or superior variable conductance performance to gas-loaded heat pipe. The vapor

temperature and the pressure inside the thermosyphon change only slightly over wide ranges of power input.

Wei and Yuan [5] studied the thermal characteristics of the thermosyphon using methanol-water as a working fluid. With a heat input of 700-1500 W heating power to the evaporator section, it was found that the axial distributions of wall temperatures in case of binary mixture working fluids are higher than that of pure water. This result comes from the fact that the evaporation rate of methanol is higher than that of water. Therefore the average concentration of methanol at each cross sectional area increases from the evaporator end. So, the saturation temperature and the thermal properties of the mixture change along the axis of the thermosyphon. This causes the uneven distribution of wall temperature of tube. Moreover, it was found that the heat transfer coefficient increases as the methanol fraction in the thermosyphon increases, and the heat transfer coefficient reaches its maximum when the mole fraction of methanol is 0.3. If the methanol concentration continue to increase, the heat transfer coefficient declines. When the thermosyphon inclines, the heat transfer coefficient of water is better than that of binary mixture. However, there was no explanation about these phenomena.

Fox, Nagasaki, Hijikata and Peterson [6] studied the reflux condensation of binary mixtures in a two-phase thermosyphon. Hexane-pentane and hexane-R11 mixtures were used in this research work. The heat input to the evaporator section was rised from 20 to 300 W and the gas-loaded phenomenon was investigated. From the experiments, it was found that when the molecular weight of the volatile component was lower than the condensable species (hexane-pentane) the flow patterns inside the thermosyphon were generally stable and the buffer gas region can be observed. However, when the molecular weight of the volatile component was higher than the condensable species (hexane-R11), the flow inside the thermosyphon was generally unstable and no buffer gas region. However at high power input (higher than 100 W, in this research), it was found that the non-condensable gas region was compressed to zero.

Korner [7] proposed the boiling heat transfer correlation of binary mixture as

$$\frac{h}{h_{M}} = \frac{1}{1 + A_{0}(0.8 + 0.12P)(y_{1} - x_{1})},$$
 (2.1)

$$h_{kl} = x_1 h_1 + (1 - x_1) h_2,$$
 (2.2)

where

h = boiling heat transfer coefficient of binary mixtures (W/m²K)

 h_{ld} = ideal boiling heat transfer coefficient of binary mixtures (W/m²K)

x = mole fraction in liquid phase

y = mole fraction in vapor phase

P = pressure (Bar)

 A_0 = correlation constant.

Note that the correlation constant depends on the binary mixture and normally less than unity such as in the case of acetone-ethanol, A_0 equals to 0.75.

From the above research works, it can be concluded that the binary working fluid inside the thermosyphon acts as a gas-loaded heat pipe. Since the more volatile component behaves as a non-condensable gas in the thermosyphon. However, this phenomenon depends on the molecular weight of the more volatile component. If it is lower than that of condensable component, the gas-loaded heat pipe phenomenon will occur. On the other hand, if it is higher than the molecular weight of condensable component, the unstable condition of gas mixture will occur and no effect from buffer gas. This means that both components can be boiled and condensed.

2.2.2 Boiling and Condensation Heat Transfer Coefficient of the

Thermosyphon

ESDU [8] collected many data and correlations of both boiling and condensation inside the thermosyphon and proposed these new correlations in term of the thermal resistance as follows:

Boiling

$$Z_e = Z_p F + Z_f (1 - F), \qquad (2.3)$$

where

$$Z_{film} = \frac{0.235 Q^{1/3}}{{D_I}^{4/3} g^{1/3} L_e \phi_1^{4/3}} \,, \quad Z_{pool} = \frac{1}{\phi_2 g^{0.2} Q^{0.4} \left(\pi D_I L_e\right)^{0.6}} \,,$$

$$\phi_1 = \left(\frac{\lambda k_i^3 \rho_i^2}{\mu_i}\right)^{0.25}, \quad \phi_2 = 0.32 \frac{\rho_i^{0.65} k_i^{0.3} C_{pi}^{0.7}}{\rho_v^{0.25} \lambda^{0.4} \mu_i^{0.1}} \left[\frac{P_v}{P_a}\right]^{0.23}.$$

Condensation

$$Z_c = \frac{0.235Q^{1/3}}{D^{4/3}q^{1/3}L_c\phi_1^{4/3}},$$
 (2.4)

where

Z = thermal resistance (K/W)

F = filling ratio of working fluid in evaporator section (%)

Q = heat transfer rate (W)

 D_i = inside diameter of tube (m)

L = length (m)

P = pressure (Pa)

g = gravitational acceleration (9.81 m/s²)

 C_p = specific heat (J/kgK)

k = thermal conductivity (W/mK)

 λ = latent heat of vaporization (J/kg)

 μ = dynamic viscosity (Pa.s)

 ρ = density (kg/m³)

subscripts

a = absolute

c = condenser section

e = evaporator section

f = film boiling

l = liquid phase

p = pool boiling

v = vapor phase.

Although the correlation of ESDU can be used with in high operating range and in various type of working fluid, in some conditions, especially at low operating temperature, the use of ESDU correlations may give some errors. Shiraishi, Kikuchi and Yamanishi [9] found that at low operating temperature (32-60°C) equations (2.3) and (2.4) could predict the heat transfer coefficient of the thermosyphon within 70-150% of the experimental values. Hahne and Gross [10] found that at a working temperature between 37-76°C, the correlations of ESDU give a lower prediction of the heat transfer coefficient (31-76% for boiling and 46-86% for condensation).

Rohsenow [11] proposed the correlation for calculating the pool boiling heat transfer coefficient as

$$h_{p} = \frac{Q^{1-r}C_{pl}}{C_{sf}A\lambda_{l}Pr^{s}} \left(\frac{1}{A\mu_{l}\lambda_{l}} \sqrt{\frac{g_{c}\sigma_{l}}{g(\rho_{l} - \rho_{v})}} \right)^{-r}, \qquad (2.5)$$

where

 C_{sf} = liquid-surface combination coefficient

A = heat transfer area

 g_c = conversion factor (in SI unit = 1 kgm/Ns²)

 σ = surface tension (N/m).

Nusselt [12] proposed the film theory for evaluating the condensation heat transfer coefficient as

$$h_c = 0.943 \left(\frac{g\rho_I(\rho_I - \rho_V)\lambda_I k_I^3}{\mu_I \Delta T_c} \right)^{0.25}, \tag{2.6}$$

where

 ΔT_c = temperature difference between vapor and surface (°C).

Note that Nusselt equation could be used with the film evaporation inside the thermosyphon [13].

2.2.3 Suitable Filling Ratio of the Thermosyphon

Bezrodnyi and Alekseenko [14] advised the suitable liquid filled in the thermosyphon and it could be calculated by

$$V_f = 0.001 D_I (L_e + L_a + L_c),$$
 (2.7)

where

 V_f = volume of liquid fill (m³)

 L_a = length of adiabatic section (m).

However, they noted that the proper filling ratio should be within 40-60% of evaporator volume.

Shiraishi, Yoneya and Yabe [15] tried to find the relation between critical heat flux and liquid fill of the thermosyphon and found that when the filling ratio was more than 20%, there was no effect on the critical heat flux and the results were shown in Figure 2.2.

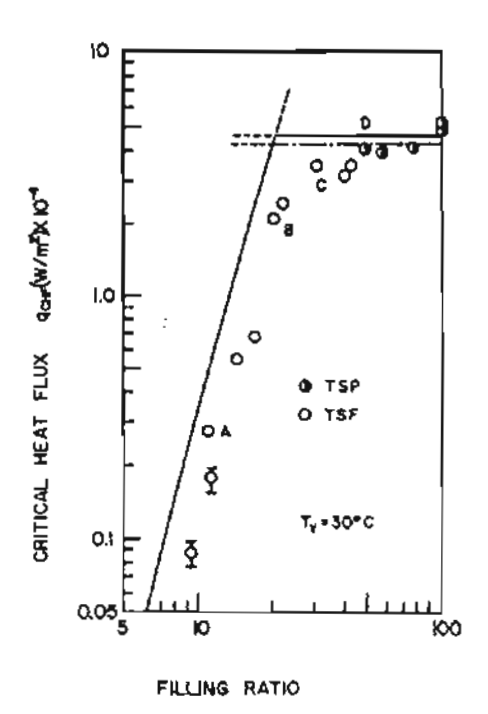


Figure 2.2 Effect of filling ratio on critical heat flux of the thermosyphon. [15]

From the above reviews, it is found that the suitable filling ratio should be 40-60%. Therefore, in this research, 50% of filling ratio is selected as a volume of liquid fill inside the thermosyphon.

2.3 Experimental Set-up

2.3.1 Working Fluid Selection

The concept of this research is to extend the limit of using water as working fluid at a lower or a higher temperature application by adding some lower boiling point component in case of lower temperature and higher boiling point component in case of higher temperature. To relief the effect of buffer gas inside the thermosyphon like a gas-loaded heat pipe because it will reduce the area of the condenser section which results in low heat transfer, the suitable addition working fluid should be selected.

In case of low operating temperature, normally water is selected as a working fluid because of its high latent heat of vaporization. However, at lower operating temperature, water is difficult to boil, therefore, lower boiling point working fluids should be selected for mixing with water to improve the performance. Ethanol, methanol and acetone are common working fluids, which have low boiling point. However, for acetone, it is found that when mixing with water there is a chemical reaction and some colloid occurs. In case of methanol-water mixture, it is found that the effect of buffer gas will occur [5] and it is not good to use this kind of working fluid. In case of ethanol, it can mix with water very well and the molecular weight is higher than water and it has no buffer gas effect. Therefore, in this research, ethanol-water mixture is chosen as the working fluid for low temperature applications.

In case of high operating temperature or high heat flux, the flooding limit of the working fluid inside the thermosyphon always occurs. From the previous work [16], it is found that using TEG-water mixture can extend this limit. However there is no enough data about this phenomenon. So, TEG-water mixture is selected as a

working fluid in this experiment for high heat flux or high operating temperature application.

2.3.2 Experimental Apparatus and Test Procedure

Figure 2.3 shows the schematic diagram of the experimental apparatus. It consists of a thermosyphon heat pipe, a heat source and a heat sink and a constant head tank. In this experiment, 3 diameter sizes of the thermosyphon, 25.40,19.05 and 12.70 mm with 2 mm thickness have been tested. All of the pipes are made of stainless steel 304. The total length is 100 cm, of which 40 cm is for the evaporator, 40 cm is for the condenser and 20 cm. is for the adiabatic section.

The heat source is a hot oil bath and the temperature of the oil is controlled by a temperature controller. The heat sink is a water jacket with water flowing in and out of the jacket to absorb heat at the condenser section. The inlet temperature of the cooling water is equal to the ambient temperature (around 27-30°C). The flow rate of the cooling water is controlled by a constant head tank.

Seven points of K type thermocouples are attached to the outer surface of the thermosyphon at 5, 20, 35, 50, 65, 80 and 95 cm from the evaporator end. Moreover, for the biggest size of the tested thermosyphon, seven thermocouples are inserted into the pipe to measure the inside temperature and they are located at the same distance as the surface measurement. The temperatures of the hot oil, the inlet and the outlet temperatures of the cooling water, the pressure inside the thermosyphon and the flowrate of the cooling water are also recorded under steady-state conditions.

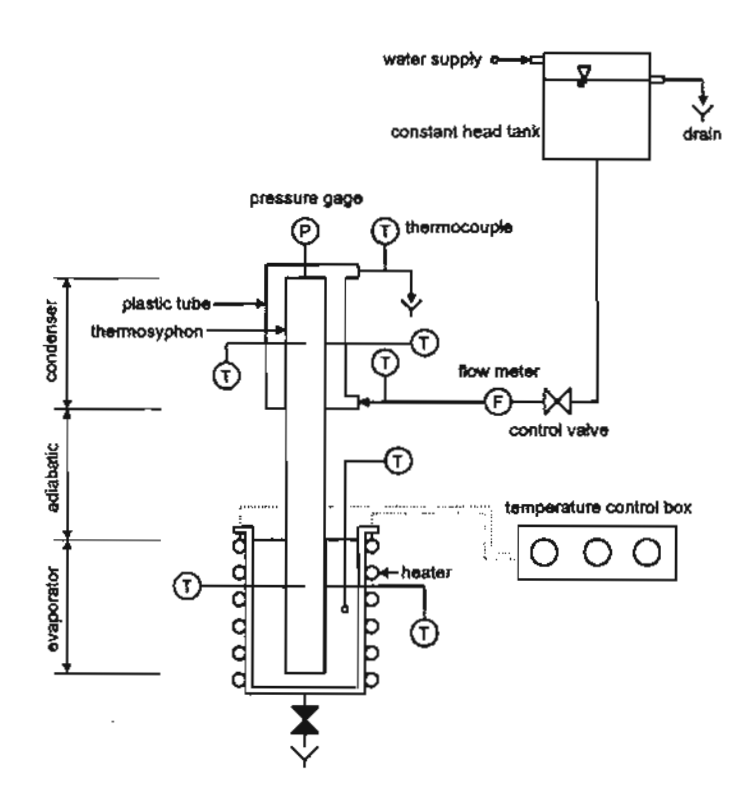


Figure 2.3 The experimental apparatus.

Ethanol-water and TEG-water at 0, 25, 50, 75 and 100% by volume of higher volatile component are used as working fluids. The filling ratio of all tests is 50% of the evaporator section's volume. The temperature of hot oil is controlled within a range of 40 to 225°C and the flowrate of the cooling water is around 6-9 g/s. The temperature and the pressure of each point are measured under steady state conditions.

2.4 Heat Transfer Analysis

In this research, the relation of heat transfer rate, thermal resistance and effectiveness at various hot oil temperatures are calculated as follows:

$$Q = \dot{m}_w C_{\rho w} (T_{wo} - T_{wl}), \qquad (2.8)$$

where

 T_{wi} = inlet temperature of cooling water (°C)

 T_{wo} = outlet temperatures of the cooling water (°C).

The thermal resistance, Z, of the thermosyphon could be calculated from

$$Z = \frac{T_{se,ave} - T_{sc,ave}}{Q}, \qquad (2.9)$$

where

 $T_{se,ave}$ = average surface temperature of evaporator section (°C)

 $T_{sc,ave}$ = average surface temperatures of condenser section (°C).

The effectiveness of the thermosyphon could also be estimated from

$$Effectiveness = \frac{T_{wo} - T_{wl}}{T_{oll} - T_{wl}}.$$
 (2.10)

The heat transfer model of heat transfer coefficient of pure working fluids has been correlated. Pool boiling equation of Rohsenow [11] is modified to predict the boiling heat transfer coefficient inside the heat pipe. The equation is

$$h_{e} = \frac{C_{1}}{\Delta T_{e} A} \left[\left(\frac{\Delta T_{e}}{B} \right)^{3} \right]^{c_{2}}, \qquad (2.11)$$

$$A = \frac{1}{\mu_{I} \lambda_{I}} \sqrt{\frac{g_{c} \sigma_{I}}{g(\rho_{I} - \rho_{v})}},$$

$$B = \frac{\lambda_{I} \mu_{I}}{k_{I}},$$

where

 ΔT_e = the temperature difference between inside and surface at the evaporator section (°C)

 $C_1, C_2 =$ correlation constants.

Note that in case of water at low operating temperature, water is difficult to boil and nucleate boiling does not occur. Normally it has only the evaporation of the working fluid at the water surface. So in this case the other form of Rohsenow equation [4] is modified to predict the boiling heat transfer coefficient of the thermosyphon as follows:

$$Nu = C_3 Re^{C_4} Pr^{9.4}, (2.12)$$

where

$$Nu = \frac{h_b}{k_I} \left[\frac{\sigma}{g(\rho_I - \rho_g)} \right]^{1/2},$$

$$Re = \frac{q}{\lambda_I \rho_I} \left[\frac{\sigma}{g(\rho_I - \rho_g)} \right]^{1/2} \frac{\rho_I}{\mu_I},$$

$$Pr = \frac{C_\rho \mu_I}{k_I},$$

where

Nu = Nusselt number

Re = Reynolds number

Pr = Prandtl number

 C_{3} , C_{4} = correlation constants.

At the condenser section, Nusselt's equation of condensation [12] is used to predict the heat transfer coefficient of the condenser section. Nusselt's equation is

$$h_c = C_5 \left(\frac{\rho_f^2 g \lambda_f k_f^3}{\mu_f L_c \Delta T_c} \right)^{C_6}, \tag{2.13}$$

where

 $C_5, C_6 =$ correlation constants.

For binary mixture, a method to evaluate the mixture heat transfer coefficient from each component [7] has been proposed as:

$$h_m = x_1 h_1 + (1 - x_1) h_2,$$
 (2.14)

where

 h_m = heat transfer coefficient of the mixture (W/m²K)

 x_1 = mole fraction of component 1.

2.5 Results and Discussion

2.5.1 Temperature Distributions Inside the Thermosyphon

The temperature distributions inside the thermosyphon are shown in Figures 2.4-2.5 for ethanol-water and TEG-water respectively.

In Figure 2.4 it is found that the temperature difference of the evaporator and the condenser sections at low temperature heat source (60°C) depend on the amount of ethanol in water. At this heat source temperature, low amount of water could be boiled, so heat transfer is deteriorated, which causes high temperature difference between the evaporator and the condenser sections. At higher heat source temperature (150°C) both components in the binary mixtures can be boiled and heat transfer rates are high, so the temperature distributions of the fluids inside the thermosyphon are nearly uniform.

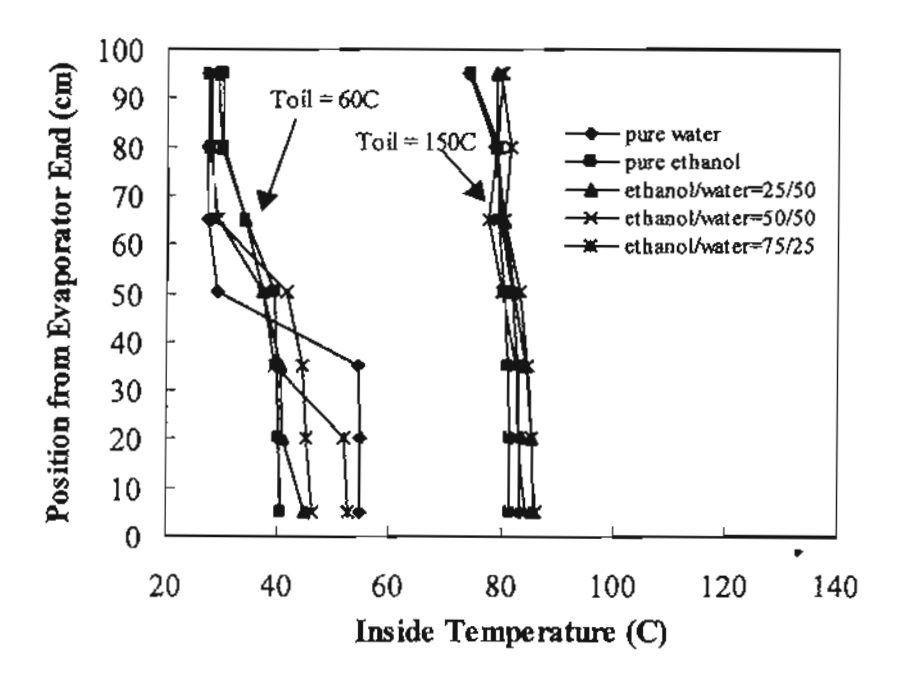


Figure 2.4 Temperature distributions of ethanol-water mixtures along the thermosyphon at various conditions.

The temperature distributions of TEG-water are shown in Figure 2.5. Since TEG has a very high boiling point (278°C). So even the heat source temperature is 150 °C, pure TEG is difficult to be boiled. Thus the heat transfer rate of pure TEG is very low and high temperature difference of the evaporator and the condenser sections is obtained. But when water is mixed with the TEG, the portion of water could be boiled and it brings about better heat transfer.

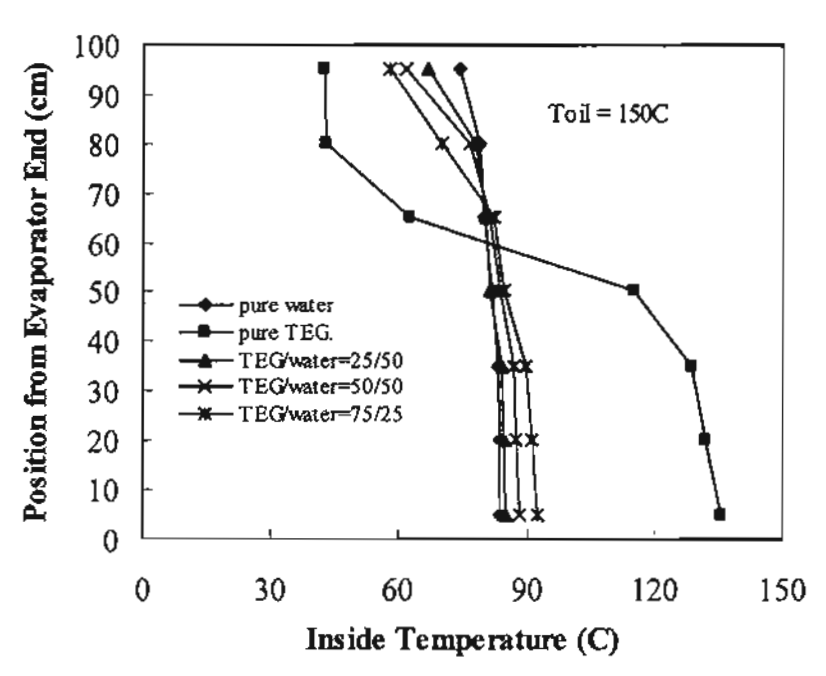


Figure 2.5 Temperature distributions of TEG-water mixtures along the thermosyphon at various conditions.

2.5.2 Heat Transfer Rate

The heat transfer rates at various hot oil temperatures are shown in Figures 2.6 a-f. In case of ethanol-water mixtures (Figures 2.6 a-c), it is found that, at low hot oil temperature, the heat transfer rates of ethanol-water mixtures are higher than pure water and close to pure ethanol. But when the hot oil temperature increases, the heat transfer rate for pure water increases more rapidly than those of the mixtures and it overcomes the mixtures at high temperature. This phenomenon occur because at a low temperature, ethanol can be boiled more easily than water and more heat transfer

rate is obtained. But at a higher temperature, both ethanol and water can be boiled and the latent heat of vaporization of water is higher than that of ethanol. Therefore, at this condition the thermosyphon with pure water can transfer more heat than that with ethanol or mixtures of water and ethanol.

Flooding of working fluid in a small size of the thermosyphon (12.70 mm diameter) has been observed in the experiment. The heat transfer rate drops drastically and the result is shown in Figure 2.6 a. This phenomenon always occurs when using a small size of thermosyphon with high temperature [3]. The critical heat flux due to the flooding limit varies with the content of water in the mixtures.

In case of TEG-water mixture (Figures 2.6 d-f), it is found that the heat transfer rate of the thermosyphon varies according to the content of TEG which is more volatile component in the mixture. Lower amount of TEG content results in higher heat transfer rate. From Figure 2.6 d, it could be found that the fluid flooding does not occur even the temperature is high. With a small amount of TEG (25%) mixed with water, the heat transfer rate is nearly the same as that mixed with pure water.

2.5.3 Thermal Resistance

The relation between the thermal resistance calculated from equation (2.15) and the hot oil temperature is shown in Figures 2.7 a-f.

At low heat source temperature, the resistance is high since low amount of vapor is generated. As the temperature is increased, more amount of vapor is obtained and heat could be transferred easily. As a result, the resistance drops drastically.

Similar to Figure 2.6, lower resistance is obtained with high fraction of more volatile component in the binary mixtures. In case of ethanol-water mixture, at high temperature when flooding occurs, the resistance increases again.

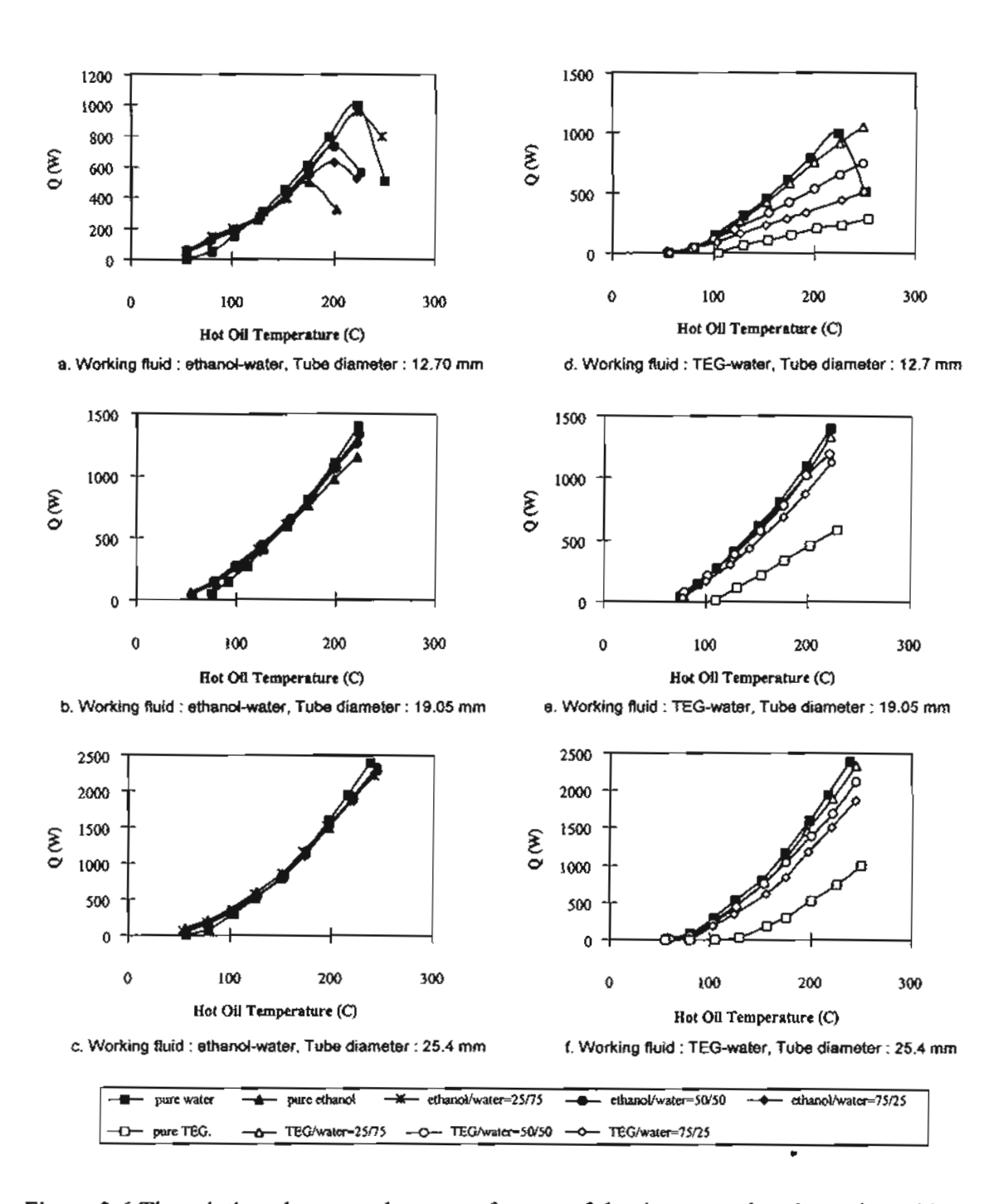


Figure 2.6 The relations between heat transfer rate of the thermosyphon heat pipe with binary mixtures and hot oil temperature at various conditions.

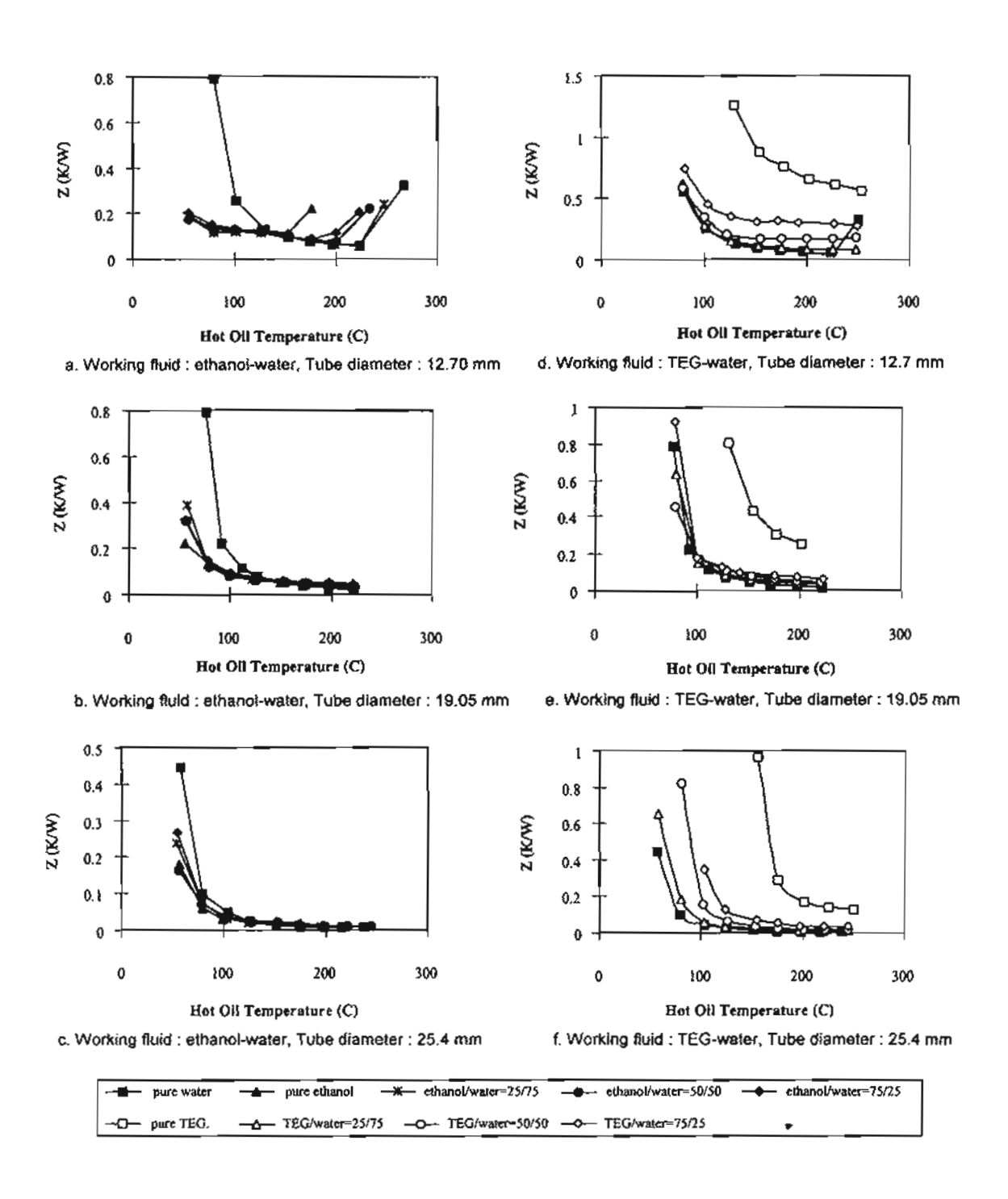


Figure 2.7 The relation between thermal resistance of the thermosyphon heat pipe with binary mixtures and hot oil temperature at various conditions.

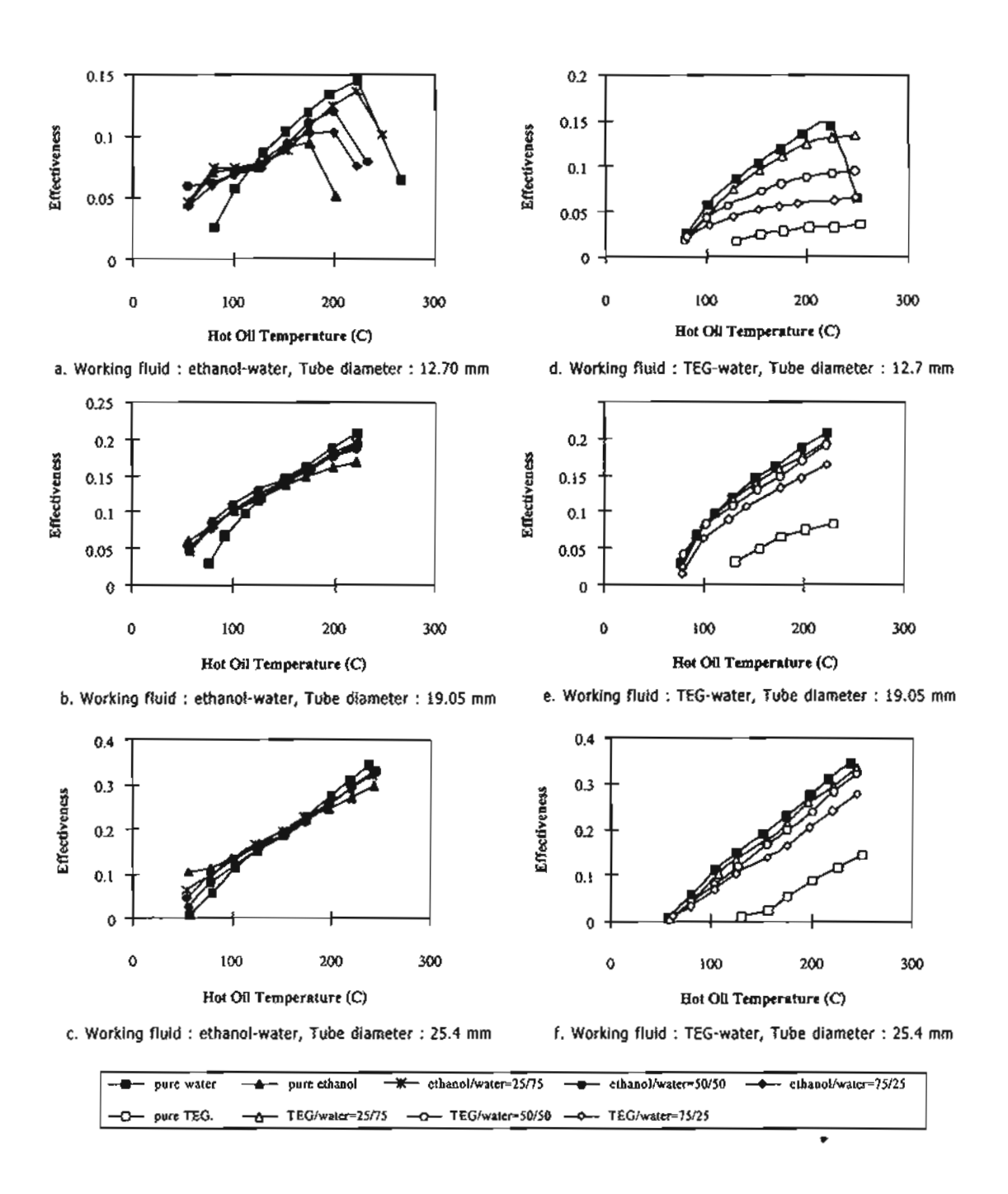


Figure 2.8 The relation between effectiveness of the thermosyphon heat pipe with binary mixtures and hot oil temperature at various conditions.

2.5.4 Effectiveness

The effectivenesses of the thermosyphon are shown in Figure 2.8. In case of ethanol-water mixture, at low temperature heat source, pure water has lower effectiveness than ethanol. However, with further increase of temperature, the effectiveness of pure water is better than those of mixture because of its high latent heat. In case of TEG-water, lower fraction of TEG in the mixture gives higher effectiveness of the thermosyphon.

Similar to Figures 2.6 and 2.7, when flooding occurs, the effectiveness of the thermosyphon drops rapidly. From Figure 2.8 d, it is found that with small fraction of TEG (25%) the critical limit could be extended.

2.5.5 Heat Transfer Model of Pure Working Fluid

Figures 2.9 a and b show the comparison of Nusselt number of boiling of water and ethanol at various temperature of working fluid. For water having a temperature of working fluid lower than 55°C, the Nusselt number drops drastically with the reduction of working fluid temperature. However, when the temperature is over 55°C the Nusselt number is nearly constant since the nucleate boiling of water has occurred. In case of ethanol, it is found that the Nusselt number is nearly constant for all temperatures in the range of 30-120°C since ethanol can be boiled easily. As a result, in case of water, it is good to separate the model into two parts; namely the inside temperature lower than 55°C and the temperature above 55°C.

For the temperature over 55°C, Rohsenow's equation for boiling from equation (2.11) is used to calculate the boiling heat transfer coefficient of the pure working fluid inside the pipe. The factors C_1 and C_2 in equation (2.11) can be found based on experimental data which are tabulated in Table 2.1.

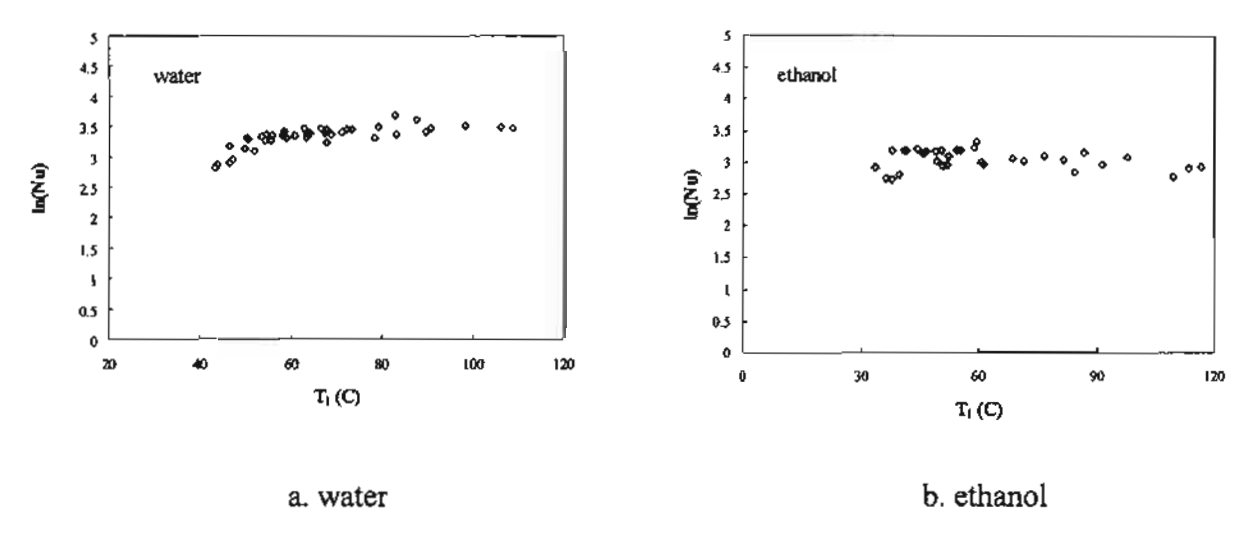


Figure 2.9 A comparison of boiling heat transfer coefficients inside the thermosyphon between the experimental and calculation data.

Table 2.1 Factors C_1 and C_2 from the experiments.

working fluid	C_1	C_2		
Water	18.688	0.3572		
Ethanol	17.625	0.3300		
TEG	20.565	0.3662		

Figure 2.10 shows the results of the heat transfer coefficients of the pure working fluids; water, TEG and ethanol calculated from Rohsenow's equation compared with those of the experimental data.

For the temperature lower than 55°C, Rohsenow's equation of boiling from equation (2.12) is used to calculate the boiling heat transfer coefficient of the pure working fluid inside the pipe. Figure 2.11 shows the comparisons between boiling heat transfer coefficient of water from the experiments and equation (2.12). The factors C_3 and C_4 of water in equation (2.12) can be found from the experimental data which are shown in Table 2.2.

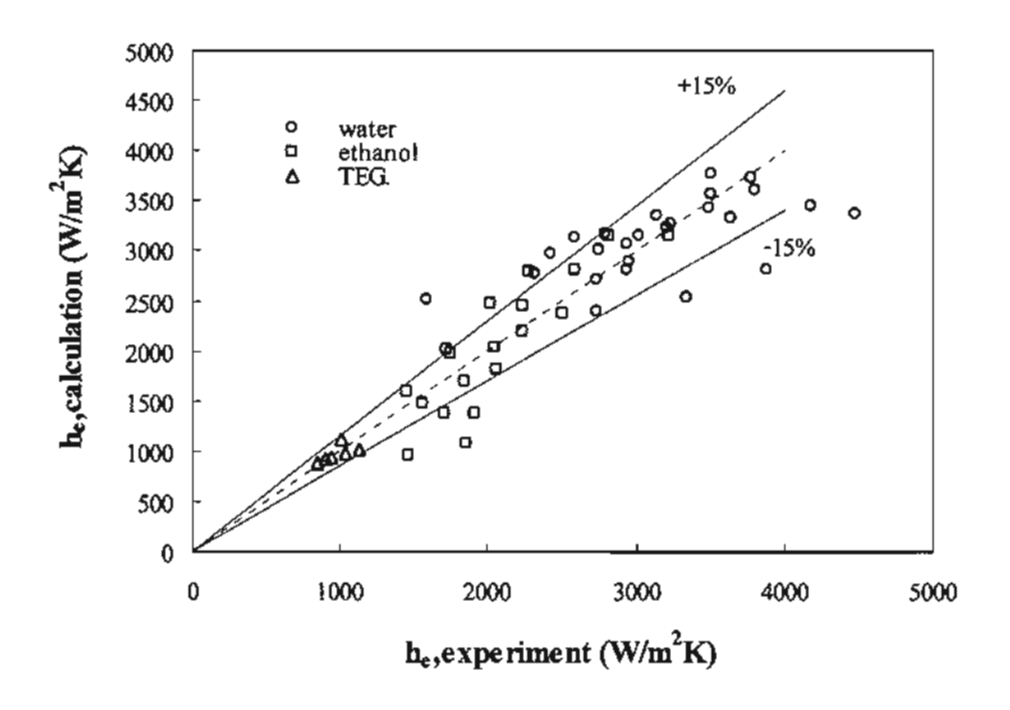


Figure 2.10 Comparisons of boiling heat transfer coefficients from the experiments and equation (2.11).

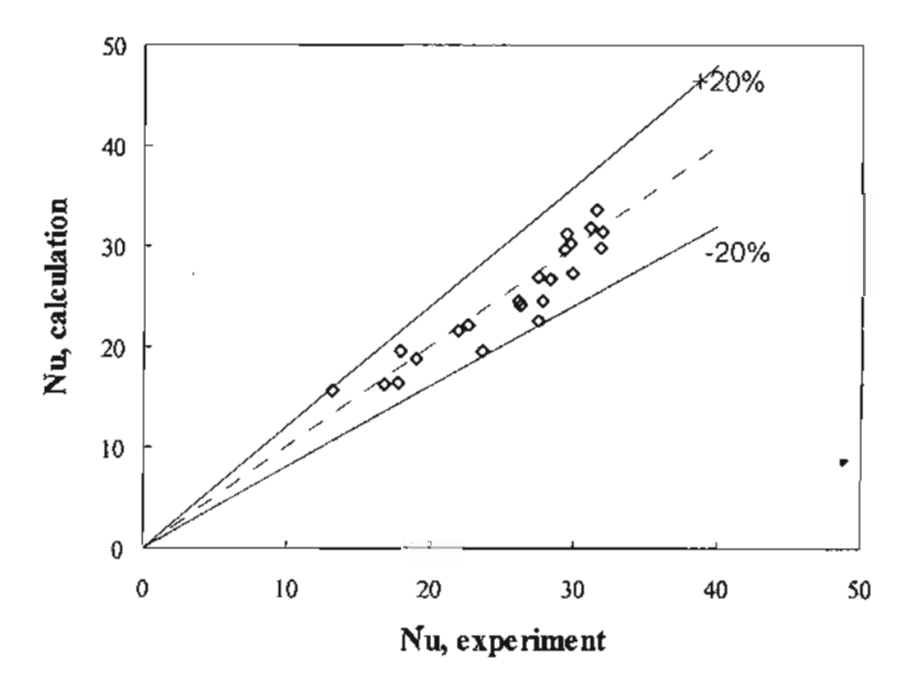


Figure 2.11 A comparison of boiling heat transfer coefficients of water from the experiments and equation (2.12).

Table 2.2 The correlation coefficient C_3 and C_4

Working Fluid	C ₃	C ₄		
Water	41.27	0.37		

At the condenser section, Nusselt's equation is used to correlate the condensation heat transfer coefficient inside the thermosyphon. The factors C_5 and C_6 in equation (2.13) can be found from our experiments and are shown in Table 2.3. The comparison of the calculated condensation heat transfer coefficients from equation (2.13) with those of the experiments are shown in Figure 2.12.

Table 2.3 Factors C_5 and C_6 from the experiments.

working fluid	C ₅	C ₆		
Water	0.943	0.233		
Ethanol	0.930	0.260		
TEG	0.943	0.180		

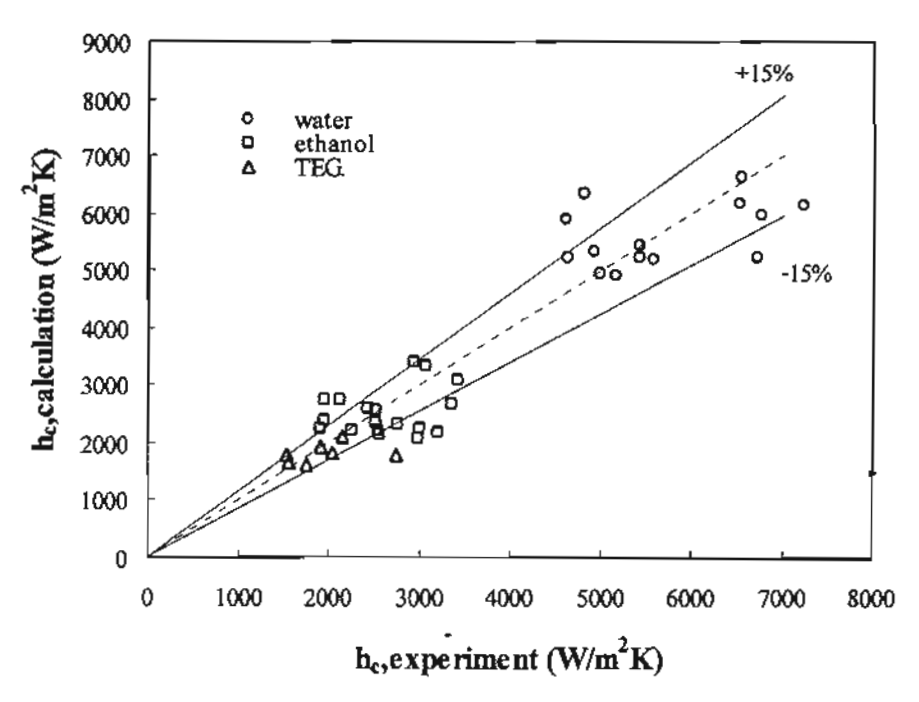


Figure 2.12 Comparisons of condensation heat transfer coefficients from the experiments and equation (2.13).

2.5.6 Heat Transfer Model of Binary Working Fluids

In this research, the weighted average of heat transfer coefficient of each component from equation (2.14) is used to predict the heat transfer coefficients from the experiments. The results are compared with those obtained from the experiments and are shown in Figures 2.13-2.16 for boiling and condensation at the evaporator and the condenser, respectively.

From the experiment, it is found that, the heat transfer coefficient of the binary mixture calculated from equation (2.14) could predict the experimental results precisely. Even through this equation is in the form of ideal heat transfer coefficient of binary mixture explained by Korner equation [7] (equation (2.1)), the normally factor A_0 and (y_1-x_1) are less than unity and in case of thermosyphon, the pressure inside the tube is very low (lower than ambient pressure). Therefore, the term $A_0(0.8+0.12P)(y_1-x_1)$ is very low. Consequently, it can be estimated that the heat transfer coefficient of binary mixture is approximately equal to that of the ideal case. Thus equation (2.14) can be used to predict the heat transfer coefficient very well.

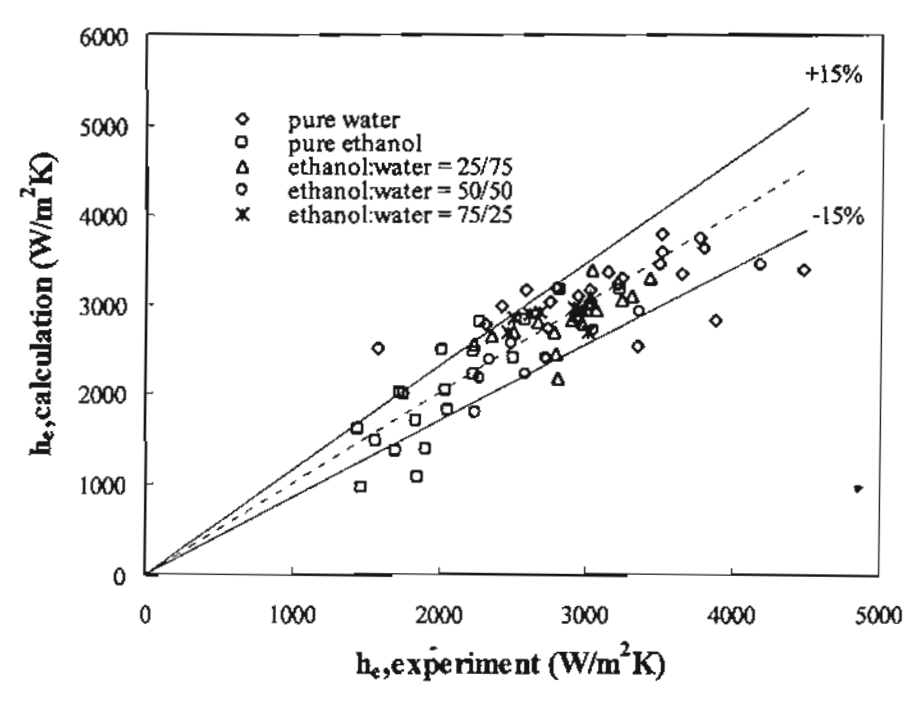


Figure 2.13 Comparisons of boiling heat transfer coefficients of ethanolwater mixtures from the experiments and equation (2.14).

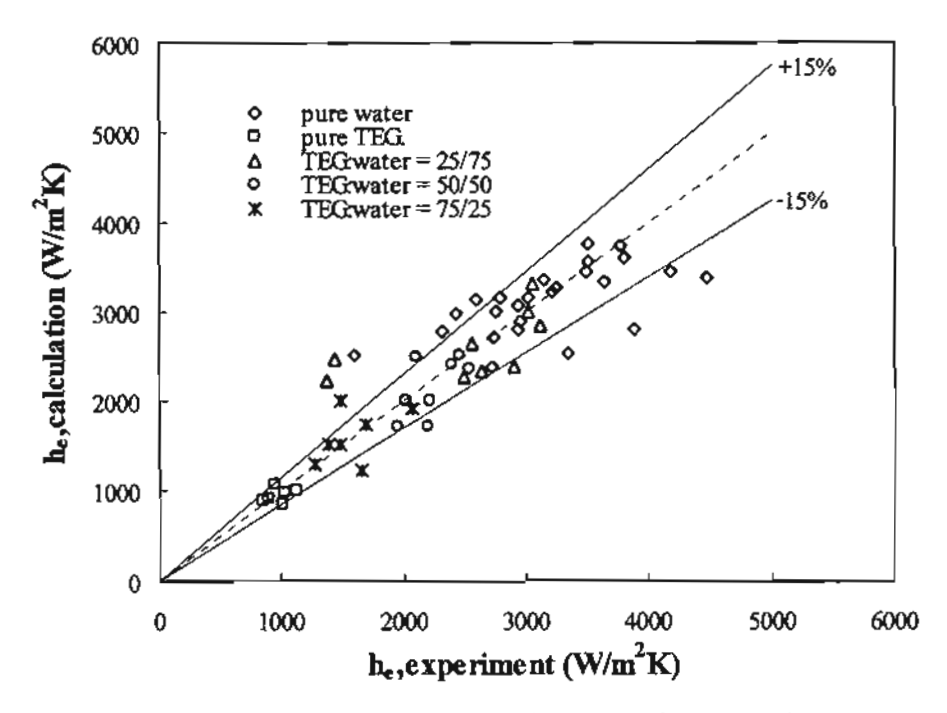


Figure 2.14 Comparisons of boiling heat transfer coefficients of TEGwater mixtures from the experiments and equation (2.14).

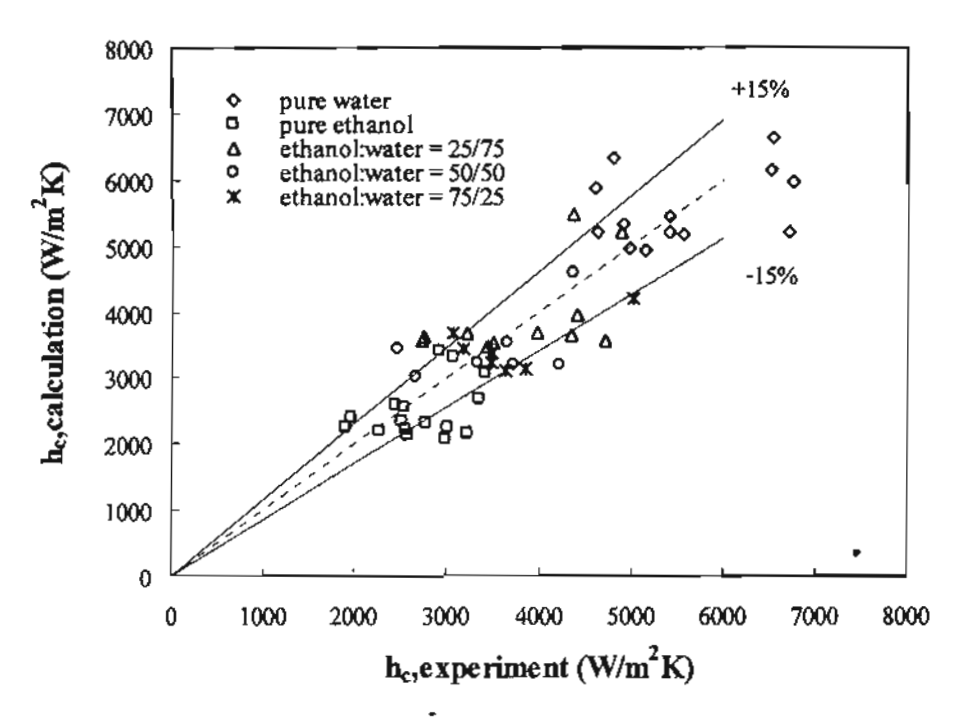


Figure 2.15 Comparisons of condensation heat transfer coefficients of ethanolwater mixtures from the experiments and equation (2.14).

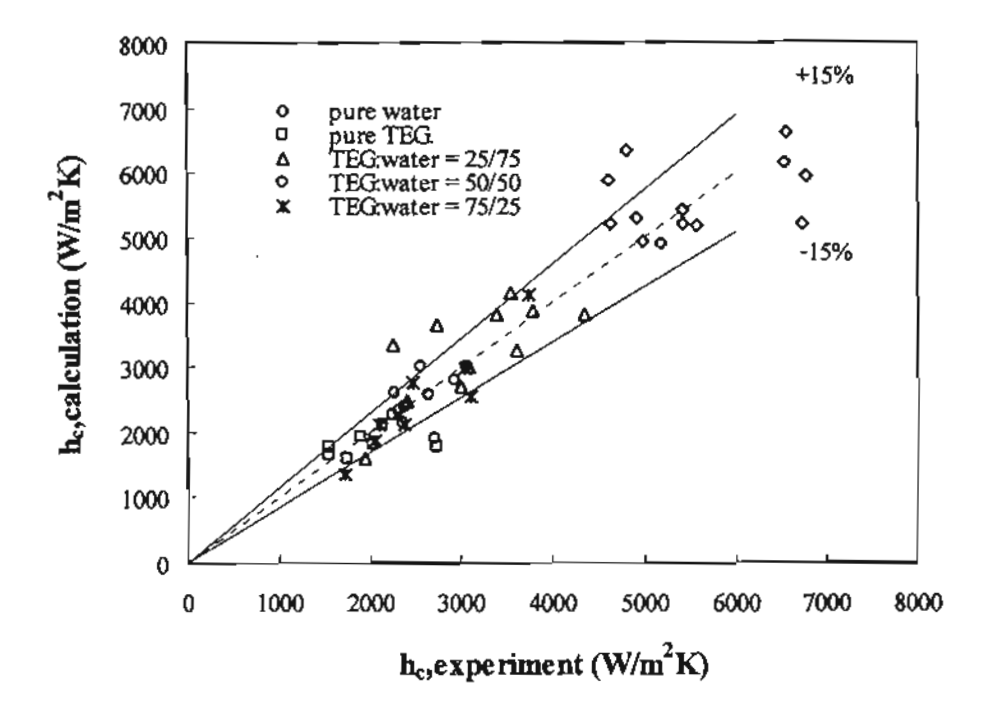


Figure 2.16 Comparisons of condensation heat transfer coefficients of TEGwater mixtures from the experiments and equation (2.14).

2.6 Conclusion

There is a high potential to improve performance of a thermosyphon heat pipe by using binary mixtures. Ethanol-water mixture gives higher heat transfer rate than water at a low temperature heat source, however lower than that of pure ethanol. In case of TEG-water mixture, the heat transfer rate of the thermosyphon decreases depending on the content of TEG in the mixture. It is found that a small amount of TEG in the mixture (25%) can increase the critical heat flux due to the flooding limit of the small size of the thermosyphon while the heat transfer rate is reduced slightly. •

The boiling equation of Rohsenow and the condensation equation of Nusselt could be used to predict the heat transfer coefficients of the boiling and the condensation inside the thermosyphon. In case of the binary mixtures, the weighted average of the heat transfer coefficient of each component can be used to predict the total heat transfer coefficient.

CHAPTER 3

FLOODING LIMIT EXTENSION OF THERMOSYPHON HEAT PIPE

3.1 Introduction

From the previous chapter, it is found that adding a small amount of TEG can extend the flooding limit of the small size thermosyphon. This chapter reports in details about this phenomenon in order to find out the effect of mixture content of TEG and the working temperature on the critical heat flux (CHF) due to the flooding limit and also develop the correlation to predict this effect.

3.2 The Experimental Set-up

The CHF due to flooding limit of a TEG-water thermosyphon has been investigated and Figure 3.1 shows a schematic diagram of the experimental apparatus. A 9.5 mm diameter copper tube with 1 mm thickness has been used as a thermosyphon. The length of evaporator, adiabatic and condenser sections are 40, 20 and 40 cm respectively. Four K-type thermocouples are attached at the outer surface of the tube along the length of the evaporator section and the other four are also attached at the condenser section for measuring the surface temperature. The pressure gage is mounted on the top part of the tube for measuring inside pressure. A hot paraffin oil bath with an electric heater and a temperature control box is used as the heat source of the evaporator section. Air bubbles are also injected to paraffin oil to make a uniform temperature. The condenser section is inserted into the cooling jacket. The mass flowrate of cooling water is controlled by a constant head tank and the water flows through the jacket to absorb heat from the condenser section. The inlet and the outlet temperatures of cooling water

are measured by a set of thermocouples and a flow meter is used to measure the mass flow rate. These values are used to calculate the heat transfer rate of the thermosyphon.

In this study, the temperature of hot paraffin oil is controlled between 90 - 200°C and the temperature of the cooling water is kept constant at 30°C and the mass flow rate is 0.0054 kg/s. The working fluid inside the thermosyphon is TEG-water mixture at 0, 25, 50, 75 and 100% by volume of TEG. The filling ratio is 50% of the evaporator volume. The experiments have been carried out under steady-state conditions.

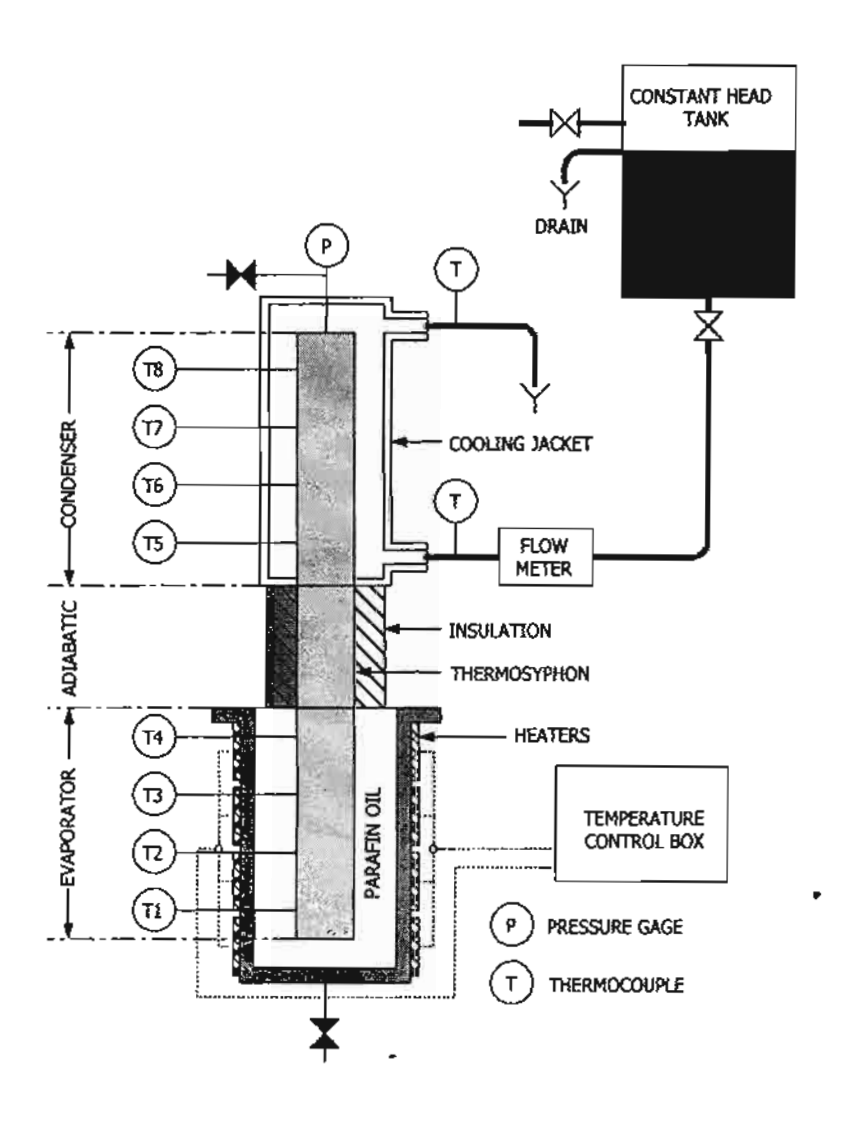


Figure 3.1 The experimental apparatus.

3.3 Theoretical Background

ESDU [8] proposed a correlation to calculate the critical heat flux due to flooding limit and is in the form of

$$Q_{max} = f_1 f_2 f_3 \lambda_I A_{cs} (g \sigma_I (\rho_I - \rho_V))^{0.25} \rho_V^{0.5}, \qquad (3.1)$$

where

 A_{cs} = cross-sectional area of the thermosyphon (m²).

The factor f_i is the function of Bond number (Bo) and it can be evaluated from

$$f_1 = -0.0331Bo^2 + 0.8161Bo + 3.2134$$
, (3.2)

where

$$Bo = D_i \left(\frac{g(\rho_I - \rho_V)}{\sigma_I} \right)^{0.5}. \tag{3.3}$$

The factor f_2 is a function of the dimensionless pressure parameter (K_p) which is defined as

$$K_{\rho} = \frac{P_{\nu}}{\left(g(\rho_{I} - \rho_{\nu})\sigma_{I}\right)^{0.5}} \tag{3.4}$$

and

$$f_2 = K_p^{-0.17}$$
 if $K_p \le 40000$

$$f_2 = 0.165$$
 if $K_p > 40000$.

The function f_3 is unity if the pipe is in vertical direction.

3.4 Results and Discussion

Figure 3.2 shows the critical heat flux of the thermosyphon heat pipe having various contents of TEG-water mixture. It is found that using TEG-water can extend CHF due to flooding limit and this limit is proportional to the content of TEG in the mixture. The heat transfer rate of the thermosyphon using pure TEG is the lowest compared to those of pure water and the binary mixture because of a very low latent heat of pure TEG and its high normal boiling point (278°C at normal pressure for TEG).

Figure 3.3 shows the comparison of the experimental results CHF with those calculated from the ESDU correlation. Both results agree quite well. Note that the properties of the binary mixture can be evaluated from the methods in references [17-22].

Figure 3.4 also shows the comparison of the experimental CHF from the previous chapter with that calculated from ESDU correlation in the case of ethanol-water mixture. It is found that ESDU correlation also agrees well with the experiments both pure fluid and binary mixtures.

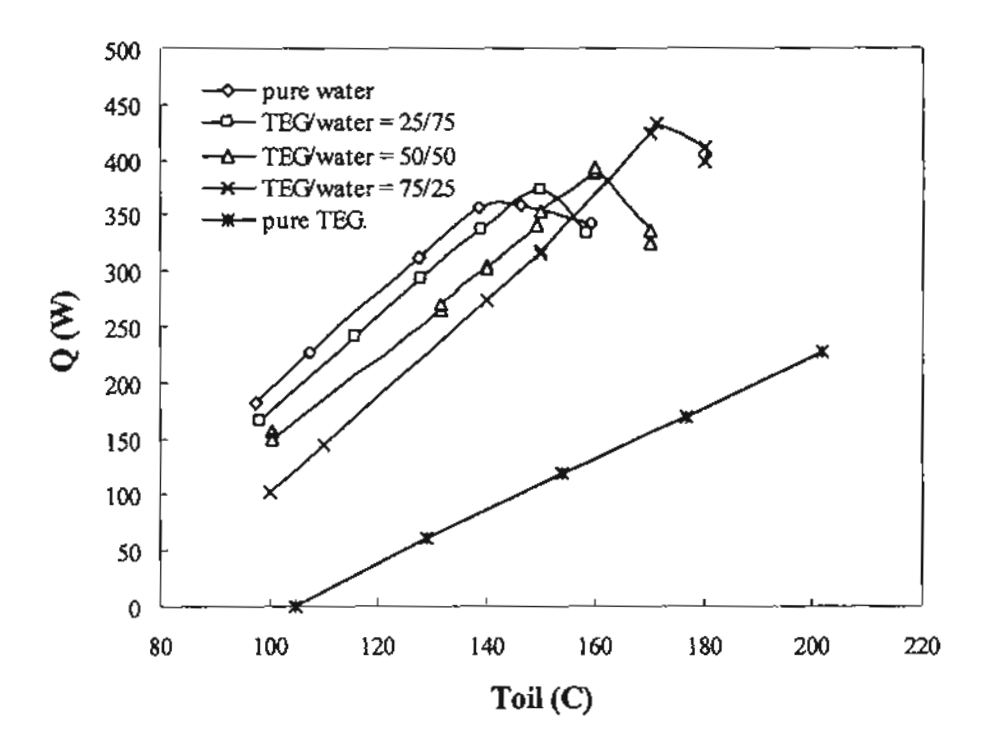


Figure 3.2 CHF of thermosyphon heat pipe using TEG-water mixtures.

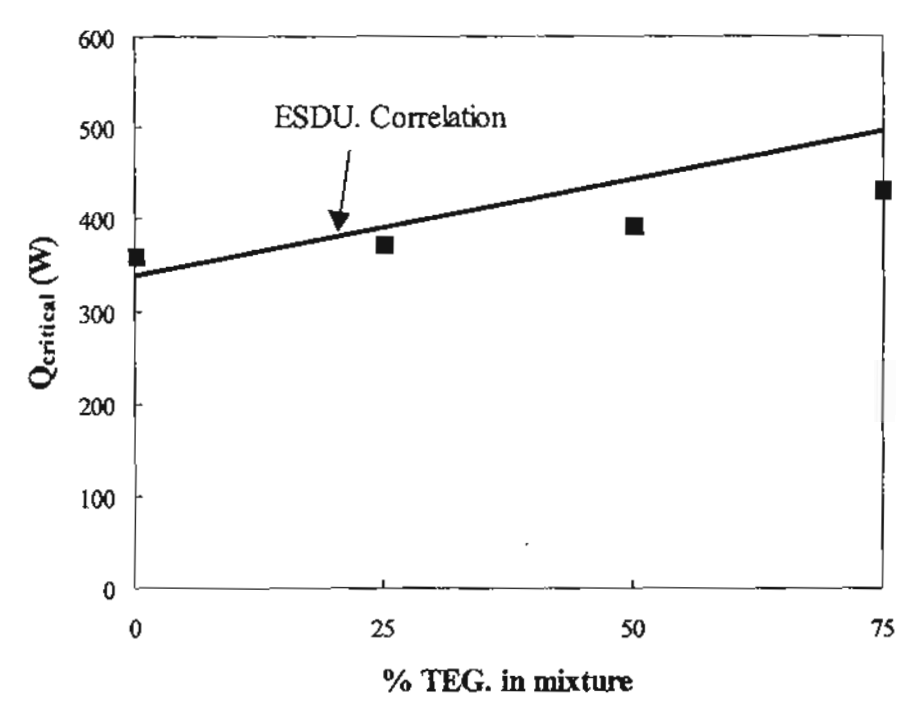


Figure 3.3 A comparison of critical heat flux from the experiment and the ESDU model with various mixtures content of TEG.

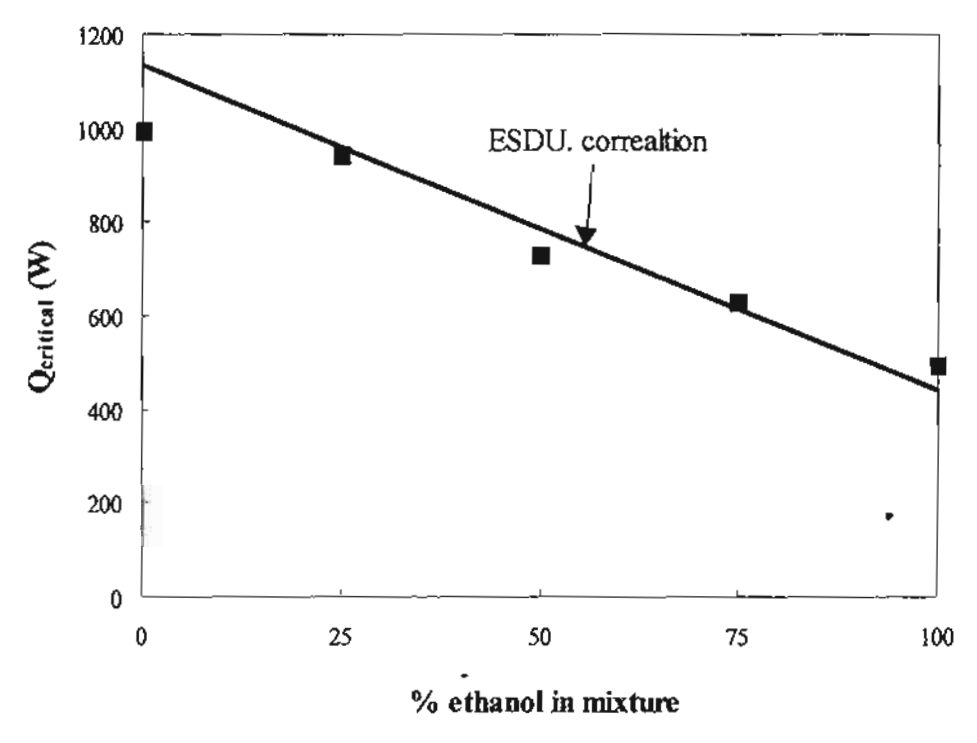


Figure 3.4 A comparison of critical heat flux from the experiment and the ESDU model with various mixtures content of ethanol.

3.5 Conclusion

A small portion of TEG in water can extend flooding limit of the thermosyphon. The CHF varies depending on the amount of TEG in the mixture. As the amount of TEG increases, the CHF increases, but, the performance of the thermosyphon decreases. ESDU correlation could be used to calculate CHF due to flooding limit. The results agree well with the experiment data not only for TEG-water mixture but also for ethanol-water mixture.

CHAPTER 4

DESIGN AND CONSTRUCTION OF THERMOSYPHON HEAT EXCHANGER

4.1 Introduction

In this chapter, the design and construction of thermosyphon heat exchanger exchanging heat between the hot and the cold streams of air have been carried out. The conditions of waste heat from the 1 ton package boiler have been considered as the case study for design.

4.2 Literature Reviews

Wadowski, Akbazadeh and Johnson [23] studied the performance of an air-to-air thermosyphon heat exchanger using R22 as the working fluid. Three, six, nine and twelve rows of the thermosyphon were tested under equal evaporator and condenser sections face velocities ranging from 0.5-2.5 m/s. The inlet temperature difference between the hot and the cold streams was increased from 5 to 60 °C where the inlet temperature of hot air did not exceed 70°C. It was found that the effectiveness of the thermosyphon heat exchanger ranging from 30-70% depends on the number of tube rows and the face air velocity. The effectiveness increases with the number of the tube rows, however its decreases with the increases of face air velocity.

Terdtoon, Chaitep, Soponpis and Groll [24] designed and constructed a thermosyphon economizer for a local package boiler in northern Thailand. The economizer recovers the waste heat from a 1 ton/hr package boiler in a local factory. The economizer itself dimensioned 1.2 m × 1.5 m × 1.5 m, with 78 stainless steel-water thermosyphons in a 7 row × 12 column arrangement. The diameter of each thermosyphon was 25.7 mm with evaporator, adiabatic and condenser sections of 0.7, 0.05 and 0.25 m respectively. Flue gas at a high temperature of 280°C and a velocity of

4.5 m/s passed through the evaporator section with a face area of 0.7×1.2 m. The economizer was installed at the chimney of the package boiler. A test run was conducted to determine the thermal characteristics, e.g. the heat transfer rate, the thermal resistance, the effectiveness, and the rate of energy saving. It was found that the thermal effectiveness of the economizer is 0.58 and the energy saving was acceptable.

Dube, Saucius, Akbazadeh and Devis [25] compared the performance of a thermosyphon heat exchanger using copper finned tube and steel finned tube. The tube diameter was 15.88 mm with 2 mm thickness. There were 6 rows and 4 column in a staggered array. The evaporator, adiabatic and condenser sections length were 304.8, 150 and 304.8 mm respectively with 328 fin/inch of aluminum circular fin. Water was chosen as a working fluid with 60% filling ratio of the evaporator section. From the experiment, it was found that the effectiveness of the copper tube was approximately 10% higher than that of steel tube. The effectiveness was around 55.5% for copper tube and 45% for steel tube. It was also found that increase of the face velocity decreased the effectiveness of the heat exchanger.

Hsieh and Huang [26] studied the effect of tube arrangement and flow pattern of a thermosyphon heat exchanger. It was found that staggered arrangement gave higher heat transfer rate than that of in-line arrangement, however, this process caused higher pressure drops. Counter flow direction also gave higher performance than that of parallel flow. The flow pattern gave more effect than the tube arrangement.

4.3 <u>Design of Thermosyphon Heat Exchanger</u>

4.3.1 Suitable Size of Thermosyphon Heat Exchanger

In this research, the thermosyphon heat exchanger is designed for recovering waste heat from exhaust gas of package steam boiler capacity of 1 ton/hr, which is normally used in hotel or hospital.

Wuttijumnong [27] made energy audit of a package steam boiler with 1 ton/hr capacity and the information data were as follows:

Type of boiler

Package boiler, 3 fire paths

Capacity (measured) 0.166 ton/hr (steam)

Dimensions 1.25 m in diameter and 2.25 m length

Company York Shipley

Exhaust gas temp. (average) 231.31 °C

Air inlet temp. (average) 30 °C

Air flow rate 700 m³/hr

The above data is used for design the suitable size of thermosyphon air preheater based on the energy recovery and economic analysis. The cost saving when using the thermosyphon air preheater with the package steam boiler can be calculated from

$$C_t = t_{op} \times c_e \times E - crf \times c_c - C_{om}, \tag{4.1}$$

where

 C_t = cost saving in one year (Baht/yr)

 c_e = energy cost (Baht/J)

 C_{am} = operating and maintenace cost (Baht/yr)

 c_c = capital cost (Baht)

 t_{op} = operating time (s)

crf = capital recovery factor

E = energy saving (J).

The operating time in one year is equal to 6,912,000 s (8 hr/day and 240 day/yr). The operating and maintenance cost is assumed to be 10% of capital cost in 1 Yr. Energy cost is equal to 2.49x10⁻⁷ Baht/J (based on diesel oil price and heating value). Capital recovery factor can be calculated from

$$crf = \frac{i(1+i)^n}{(1+i)^n-1},$$
 (4.2)

where

i = interest rate

n = life time (yr).

If assuming i equals 10% and 10 year life time, crf value is equal to 0.1627, C_c is the function of area of heat exchanger and from the materials price and labor cost (30% of material cost), the capital investment can be calculated from

$$c_c = 2096.77A + 30000, \tag{4.3}$$

where

A = Area of air preheater (m^2) .

Consequently equation 1 can be written as

$$C_t = 1.723E - 375.26A - 6979.83$$
. (4.4)

From equation 4.4, the computer programming was written to solve the suitable area of the thermosyphon air preheater. The energy recovery in this equation is also the function of the area. Figure 4.1 shows the relation between area of the air preheater and cost saving in one year, it is found that the suitable size of the thermosyphon air preheater is approximately 30 m² (when using the condition of package steam boiler)

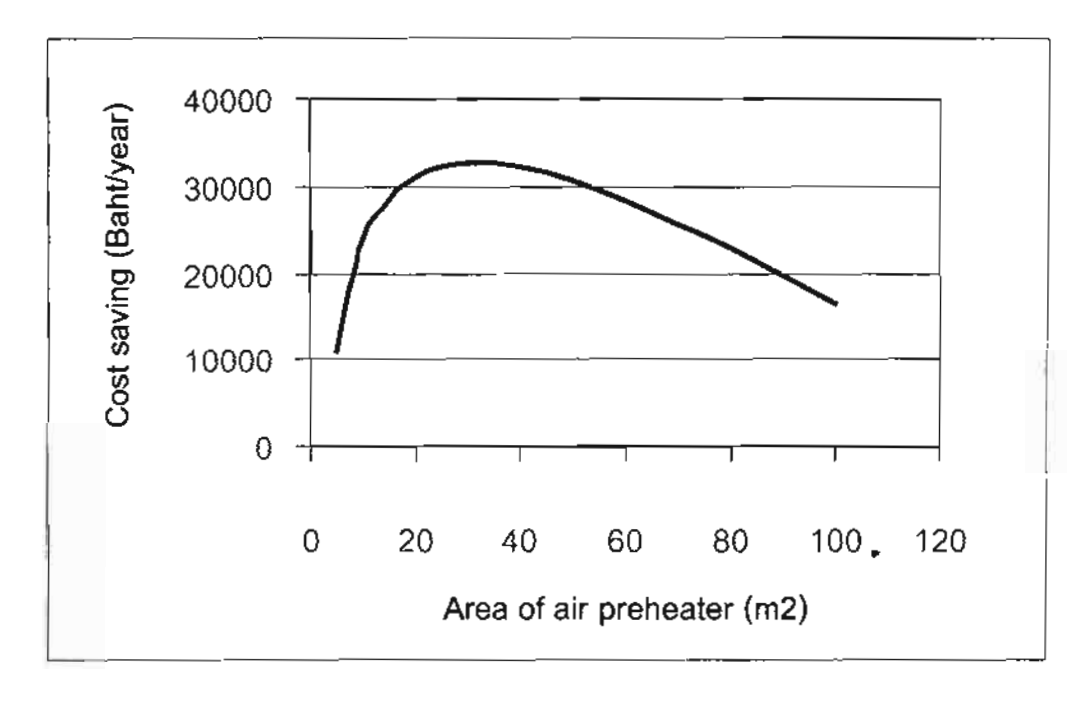


Figure 4.1 Cost saving at various area of air preheater.

Therefore, in this research, 30 m² area of the thermosyphon air preheater is used for constructing the test model. This size also covers the test conditions of the experiments.

4.3.2 Details of the Thermosyphon Heat Exchanger

From the previous section, 30 m² area of thermosyphon air preheater had been constructed as the experimental apparatus and the details are as follows:

4.3.2.1 Thermosyphon heat pipe

Material	Stainless steel 304			
Outside diameter	0.027 m			
Wall thickness	0.002 m			
Evaporator length	0.4 m			
Condenser length	0.4 m			
Adiabatic length	0.13 m			

4.3.2.2 Fin

Туре	Spiral finned
Туре	Spiral finned

Material Stainless Steel 304

Fin height 0.01 m
Fin thickness 0.0004 m

Number of fin in 1 inch (25.4 mm) 10

4.3.2.3 Pipes arrangement

Number of rows	7

Number of pipes in each row 7

Arrangement Staggered array

Transverse pitch 0.053 m

Diagonal pitch 0.053 m

4.3.2.4 Hot air system

Radial tube gas burner 100 kW

Air blower 2 hp

Length of hot gas duct 4 m

4.3.2.5 Cold air system

Air blower 2 hp
Length of cold gas duct 3 m

Figures 4.2-4.6 show the details of the apparatus. Figure 4.2 shows the counter flow arrangement, however, this unit can be changed to the parallel flow arrangement.

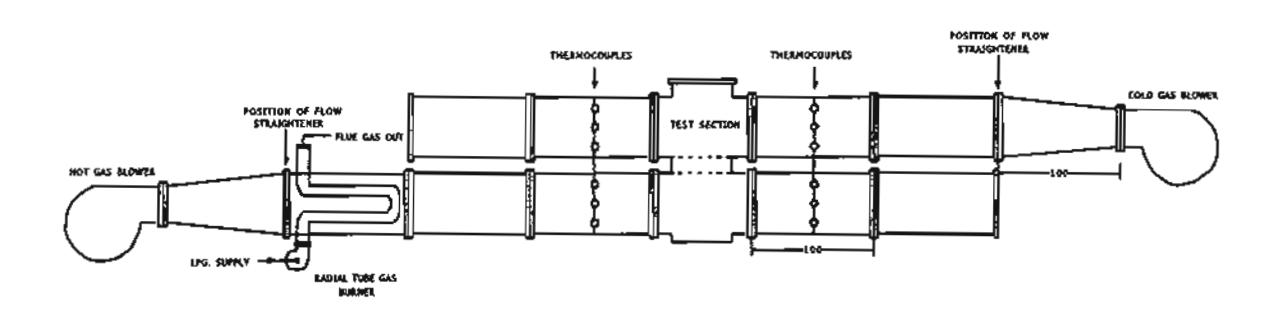


Figure 4.2 Details of the experimental apparatus.



Figure 4.3 Top view of the apparatus.

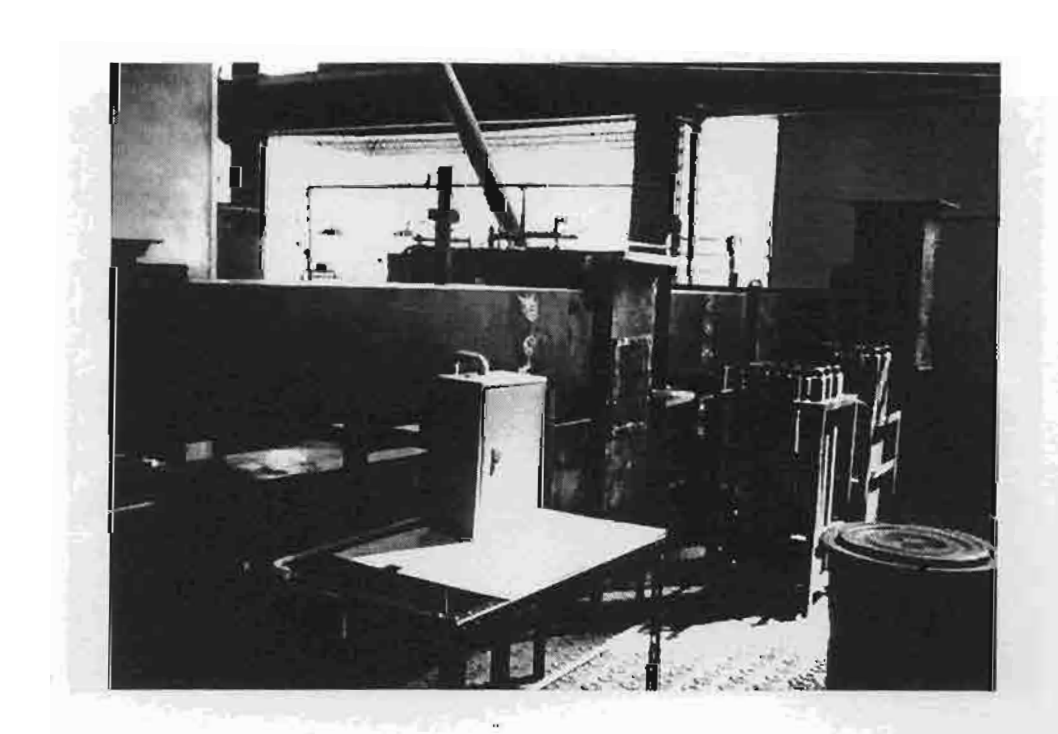


Figure 4.4 Side view of the apparatus.

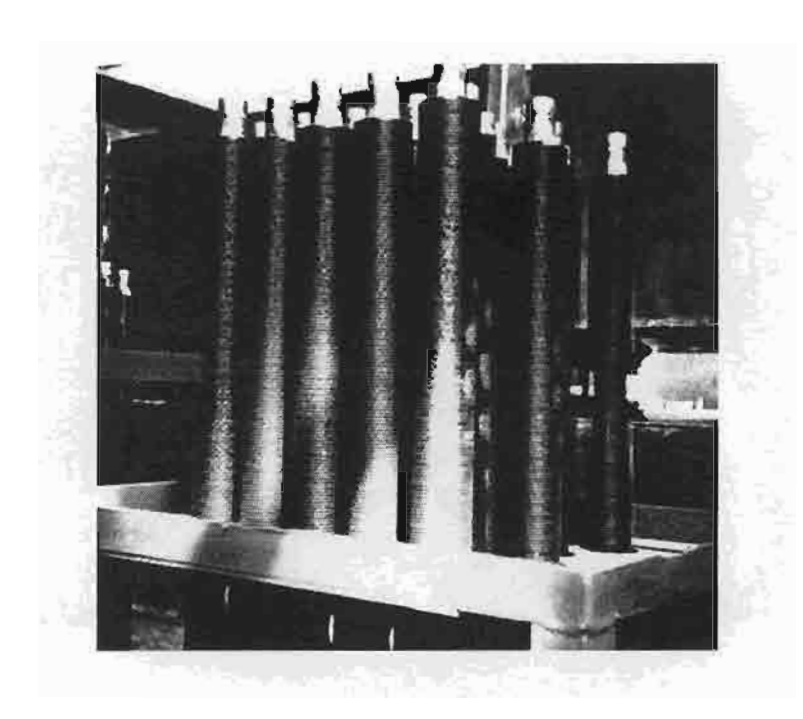


Figure 4.5 Thermosyphon heat pipes.

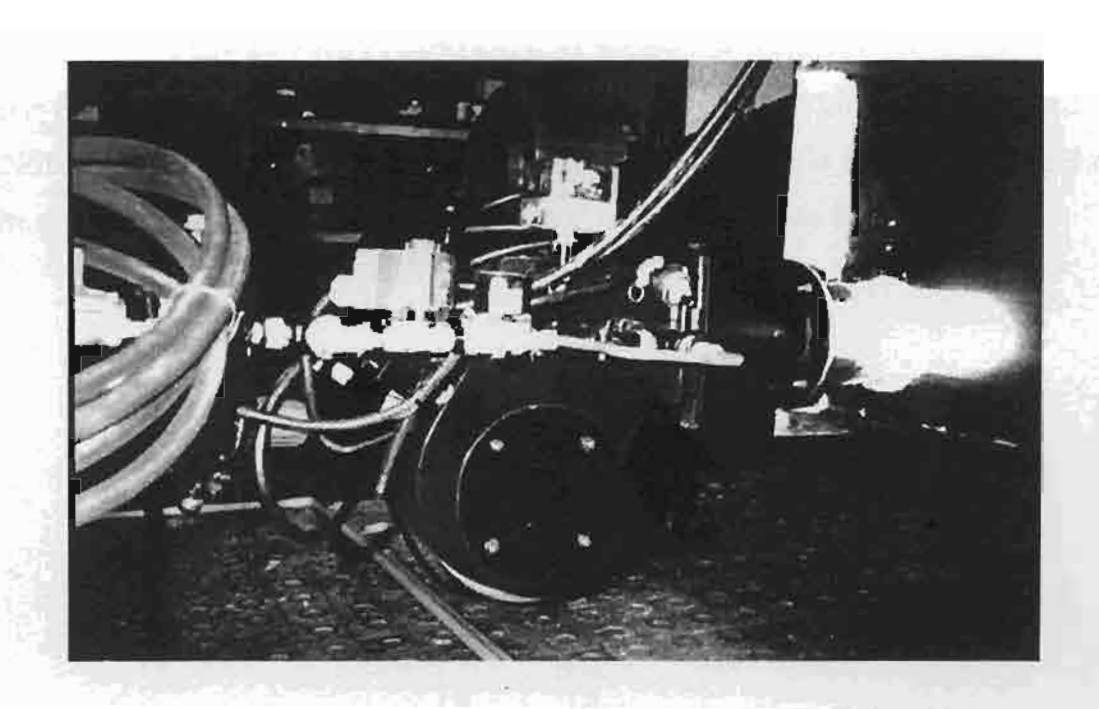


Figure 4.6 Radial tube gas burner.

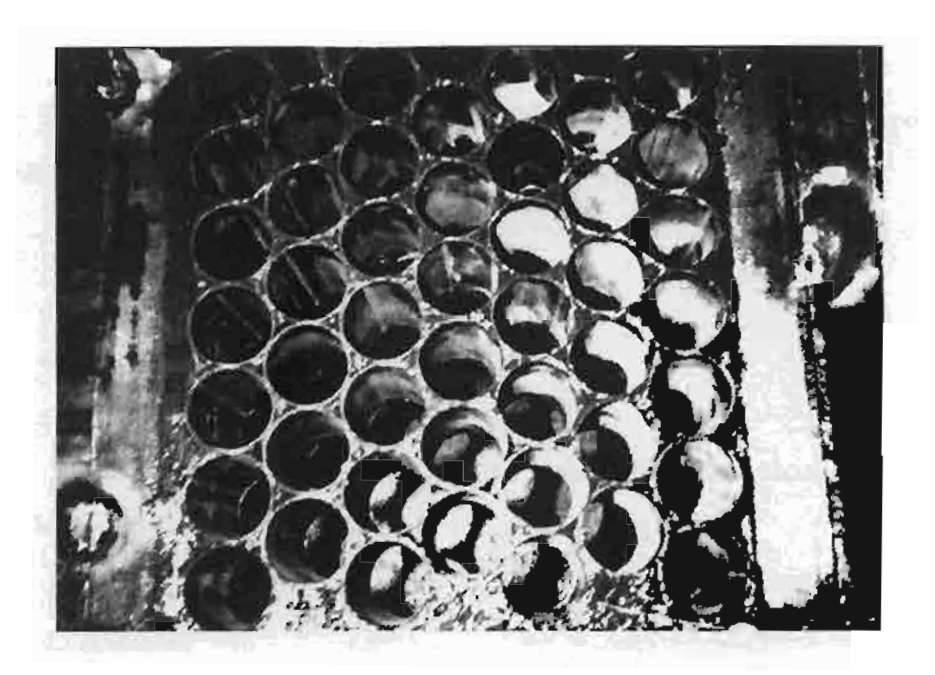


Figure 4.7 Position of the pipes inside the heat exchanger.

4.3.3 Nozzle Box

The 12.7 cm (5 inch) standard nozzle has been used for measuring the mass flow rate of the hot and the cold air streams. This method follows the standard of ANSI/ASHRAE 41.2-1987 [28]. The shape of the nozzle box is shown in Figure 4.8. The nozzle boxes are connected to the inlet port of the hot and the cold air blowers.

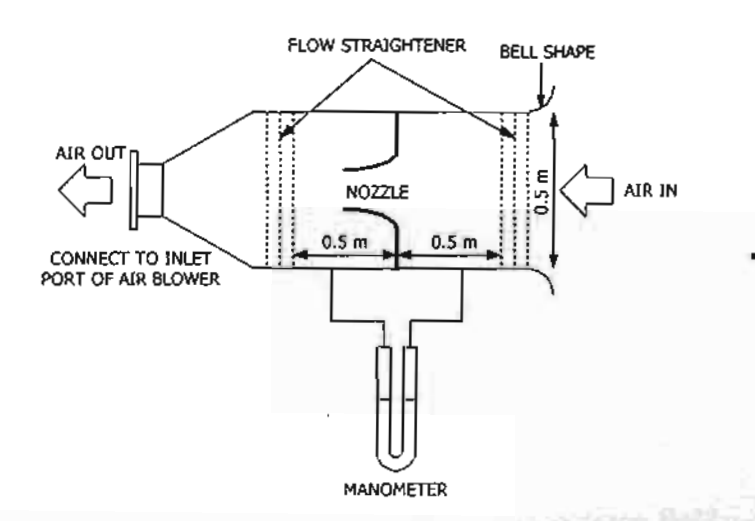


Figure 4.8 Standard nozzle for measuring the air flow rate.

The air flow rate could be controlled by adjusting the blower speed by a frequency inverter. The mass flow rate could be calculated from a measured pressure drop across the nozzle as

$$\dot{m} = 0.01576 \rho_a \sqrt{\Delta P} \tag{4.5}$$

where

 \dot{m} = mass flow rate of air (kg/s)

 ΔP = pressure drop across nozzle (Pa)

Note that Equation (4.5) is not a general form for calculating the mass flow rate. It agrees well with the nozzle in this experiment.

4.4 Testing Procedure

4.4.1 The Thermosyphon Heat Pipe

The procedures for filling the working fluid in the thermosyphon heat pipe shown in Figure 4.8 are as follow:

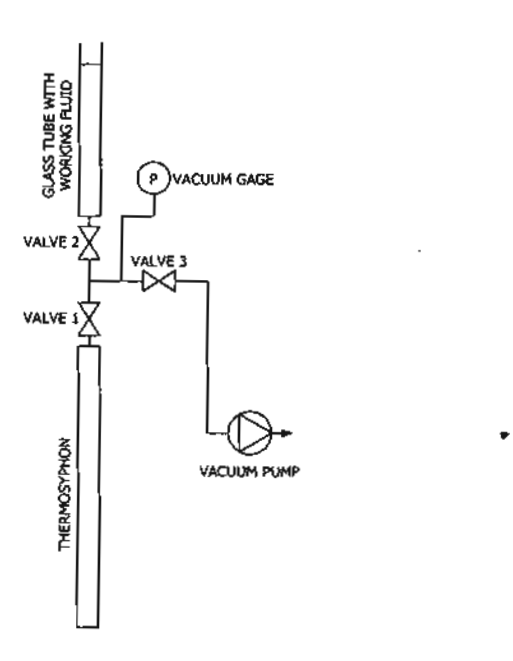


Figure 4.9 An apparatus for filling in the working fluid.

- 4.4.1.1 Clean the thermosyphon tube with acetone and water and then dry it.
- 4.4.1.2 Fit the charging valve 1 at the top of the thermosyphon tube and make sure that there is no leakage.
- 4.4.1.3 Connect the thermosyphon heat pipe to a glass tube filled with working fluid and a vacuum pump by using valves 2 and 3.
- 4.4.1.4 Close valve 2 and open valves 1 and 3, then turn on the vacuum pump to evacuate the tube until the pressure is zero (absolute pressure).
- 4.4.1.5 Close valve 3 and open valve 2, then release the working fluid from the glass tube to the thermosyphon and measure the volume of the working fluid by using the scale on the glass tube until it reaches a set value.
- 4.4.1.6 Close valve 1 and disconnect the glass tube and the vacuum pump.
 - 4.4.1.7 Repeat step 1-6 for the new tubes.

4.4.2 Test of Thermosyphon Heat Exchanger

The assembled thermosyphons are allocated in the test section and the following steps are the testing procedures of the thermosyphon heat exchanger.

- 4.4.2.1 Set the temperature of the hot air on the control panel of the gas burner.
- 4.4.2.2 Turn on the hot and the cold air blowers and adjust the mass flow rate of air by using the inverters.
- 4.4.2.3 Turn on the gas burner and the temperature of hot air will be increased to the set point.
- 4.4.2.4 Wait until the system reaches the steady state condition and then measure the inlet and the outlet temperatures of the hot and the cold air streams at the test section. The positions of the temperatures at the inlet and the outlet ports are shown in Figure 4.9.
- 4.4.2.5 Use the mass flow rate and the temperature of the hot and the cold streams to calculate the heat transfer rate of the heat exchanger.

4.4.2.6 When finishing the experiment, turn off the gas burner and wait until the temperature of the hot gas decreases to the ambient and then turn off the hot and the cold air blowers.

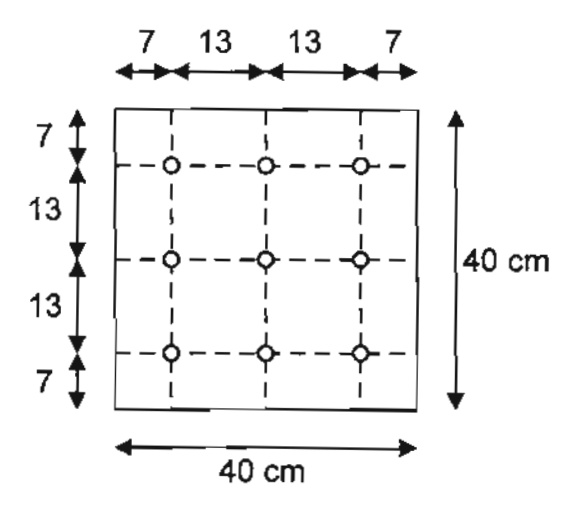


Figure 4.10 Positions for measuring temperatures of the fluid at the inlet and the outlet ports of the test section (9 points per one section).

•

CHAPTER 5

SIMULATION PROGRAM OF THE THERMOSYPHON HEAT EXCHANGER

5.1 Introduction

In this chapter, a simulation program for calculating the performance of gasto-gas thermosyphon heat exchanger has been developed. The dimensions of the thermosyphon heat exchanger, the conditions of the hot and the cold streams are the input parameters of the program.

5.2 Theoretical Background

Figure 5.1 shows the thermal resistance circuit of the thermosyphon. In this research, the pressure drop inside the thermosyphon and the axial conduction along the pipe wall are assumed negligible. Evaluation of individual thermal resistance is described as follows:

5.2.1 Air-side Thermal Resistances

The external air-side thermal resistances of the evaporator (Z_{eo}) and the condenser (Z_{co}) section can be calculated from

$$Z_{eo} = \frac{1}{h_{eo}A_{eo}}, \tag{5.1}$$

$$Z_{co} = \frac{1}{h_{co}A_{co}}, \qquad (5.2)$$

where

 h_{eo} = external air-side heat transfer coefficient of evaporator section (W/m²K)

 h_{co} = external air-side heat transfer coefficient of

condenser section (W/m2K).

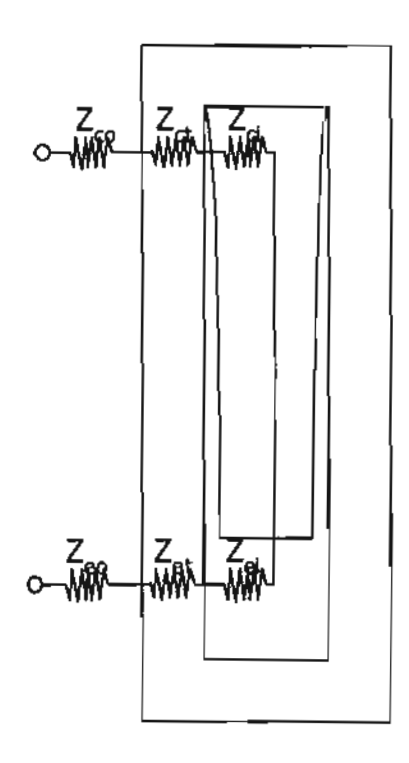


Figure 5.1 Thermal resistance circuit of the thermosyphon.

The external air-side heat transfer coefficient depends on the arrangement of the thermosyphon and also on the shape of finned tube. The correlations for calculating this values are as follows:

5.2.1.1 Bare Tube

For the flow across a bank of bare tubes shown in Figure 5.2, Zhukauskas [29] has proposed a correlation for calculating the air-side heat transfer coefficient as

$$Nu = C Re_D^m Pr^{0.36}, \qquad (5.3)$$

where

Nu = Nusselt number

 $Re_D =$ maximum Reynolds number

Pr = Prandtl number

 $C_{i,m}$ = correlation constants.

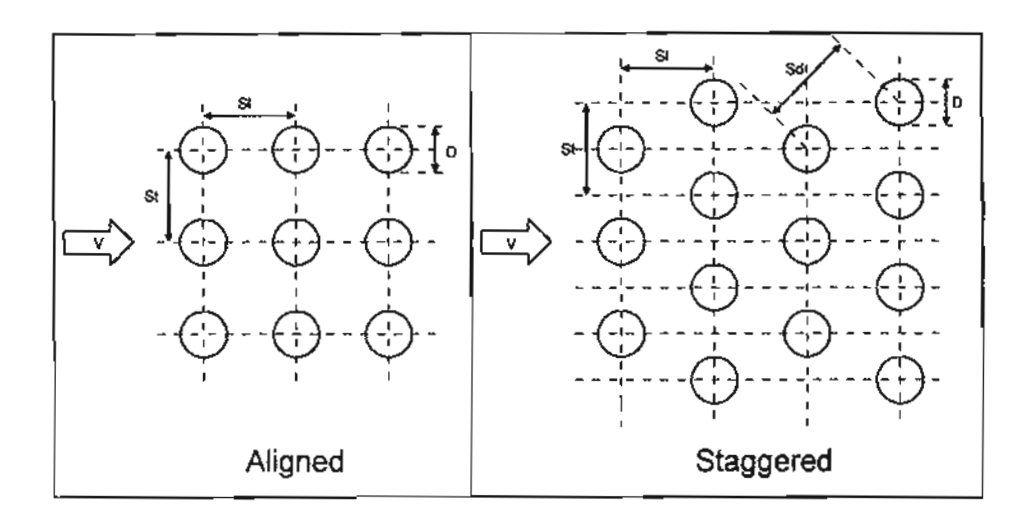


Figure 5.2 Tube arrangements in a tube bank.

Note that, ReD in this case can be calculated from

$$Re_D = \frac{\rho V_{max} D}{\mu}.$$
 (5.4)

For aligned arrangement, the maximum velocity can be calculated from

$$V_{max} = \frac{S_t}{S_t - D} V, \qquad (5.5)$$

where

 S_t = transverse pith of tube bank (m)

V =face velocity of air (m/s).

For staggered arrangement, the maximum velocity is the highest value of maximum velocity calculated from Equations (5.5) and (5.6) as

$$V_{max} = \frac{S_t}{2(S_d - D)} V, \qquad (5.6)$$

where

 S_d = diagonal pith of tube bank (m).

Correlation constants, C and m for tube bank in cross flow at various ranges of Reynolds number are shown in Table 5.1.

Table 5.1 Zhukauskas constants for tube bank in cross flow [29].

Configulation	Configulation Re _D		m		
Aligned	10-10 ²	0.80	0.40		
Staggered	10-10 ²	0.90	0.40		
Aligned	10 ² -10 ³	Approximate as a sin	ingle (isolated) cylinder		
Staggered	10 ² -10 ³	Approximate as a single (isolated) cylin			
Aligned $S_l/S_l < 0.7$	10 ³ -2×10 ⁵	0.27	0.63		
Staggered $S_i/S_i < 2$	10 ³ -2×10 ⁵	$0.35(S_{l}/S_{l})^{1/5}$	0.60		
Staggered $S_l/S_l > 2$	10 ³ -2×10 ⁵	0.40			
Aligned	igned 2×10 ⁵ -2×10 ⁶		0.84		
Staggered 2×10 ⁵ -2×10 ⁶		0.022	0.84		

Note that, at the low number of tube row, the value in Equation (5.3) should be multiplied by a correction factor given in Table 5.2.

Number of rows	1	2	3	4	5	7	10	13	16
Aligned	0.70	0.80	0.86	0.90	0.92	0.95	0.97	0.98	0.99

Table 5.2 Correction factor of Equation (5.3) at low number of tube rows [29].

5.2.1.2 Circular Finned

The shape of circular finned tube is shown in Figure 5.3. For circular finned tube having staggered array, Hewitt, Shires and Bott [30] proposed the following correlations as:

0.89

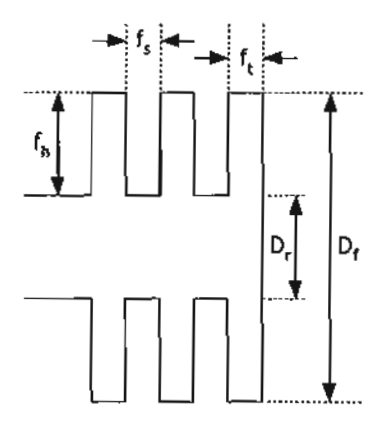


Figure 5.3 Geometrical characteristic of circular fin.

$$Nu = 0.242 Re^{0.658} \left(\frac{f_s}{f_h}\right)^{0.297} \left(\frac{S_t}{S_t}\right)^{-0.091} Pr^{0.333}, \quad (5.7)$$

where

Staggered

 S_l = longitudinal pith of the staggered array (m)

 $f_s = fin gap (m)$

 f_h = fin height (m).

For aligned arrangement Hewitt et al. [29] also proposed the following equation:

$$Nu = 0.30 Re^{0.625} \left(\frac{A}{A_t}\right)^{-0.375} Pr^{0.333}, \qquad (5.8)$$

where

A = total surface area of finned tube (m^2)

 A_t = total tube surface area (without fin) (m²).

The Reynolds number in these cases can be calculated from the maximum velocity based on the minimum flow area as follows:

$$R_{\bullet,max} = \frac{\dot{m}}{S_{min}\rho}, \tag{5.9}$$

aligned

$$S_{min} = NL \left(S_t - D_r - \frac{2f_t f_h}{f_t + f_s} \right), \tag{5.10}$$

staggered

$$S_{min} = 2NL \left(S_d - D_r - \frac{2f_t f_h}{f_t + f_s} \right), \tag{5.11}$$

where

 \dot{m} = mass flow rate of air (kg/s)

 S_{min} = minimum flow area (m²)

N = number of tube in row

L = length of tube (m)

 D_r = diameter of bare tube (m)

 f_t = fin thickness (m)

Related information for calculating the total fin surface area A_f , the total bare tube surface A_b , in each row of tube bank and the fin efficiency η_f of tube bank are given as:

$$A_{f} = \frac{NL\pi}{f_{s} + f_{t}} \left(0.5 \left(D_{f}^{2} - D_{r}^{2} \right) + D_{f} f_{t} + D_{r} f_{s} \right), \tag{5.12}$$

$$A_b = \frac{NL\pi}{f_s + f_t} (D_r f_s), \tag{5.13}$$

$$\eta_f = \frac{\tanh\left(\sqrt{2h_o / f_t k_f} \times \varphi\right)}{\sqrt{2h_o / f_t k_f} \times \varphi},\tag{5.14}$$

$$\varphi = \frac{D_r}{2} \left(\frac{D_r}{D_r} - 1 \right) \left(1 + 0.35 \ln \frac{D_r}{D_r} \right), \tag{5.15}$$

where

 D_f = diameter of fin (m)

 k_f = thermal conductivity of fin (W/mK).

Note that the fin efficiency η_f is computed from Schmidt's approximation [31].

5.2.1.3 Plain Plate Finned

For plain plate finned tube having staggered array, Webb [32] proposed a following correlation as

$$j = 0.14 Re^{-0.328} \left(\frac{S_t}{S_I}\right)^{-0.502} \left(\frac{f_s}{D_o}\right)^{0.031}, \tag{5.16}$$

$$j = \frac{h_o}{\rho V_{max} C \rho_I} P r^{2/3} \qquad . \tag{5.17}$$

where

j = Colburn factor

Related information for calculating the total fin surface area A_{f} , the total bare tube surface A_{b} , in each row of tube bank and the fin efficiency η_{f} are given as:

$$A_f = 2n_f \left((N + 0.5)S_t S_t - 0.25\pi N D_o^2 \right), \tag{5.18}$$

$$A_b = \left(\frac{\pi N L}{f_s + f_t}\right) D_o f_s , \qquad (5.19)$$

$$\eta_f = \frac{\tanh(\sqrt{2h_o / f_t k_f} \times \varphi)}{\sqrt{2h_o / f_t k_f} \times \varphi},$$
(5.20)

$$\varphi = (\phi - 1)(1 + 0.35 \ln \phi) \qquad , \tag{5.21}$$

$$\phi = 12.7 \frac{X_M}{r} \left(\frac{X_L}{X_M} - 0.3 \right)^{1/2}, \tag{5.22}$$

$$X_L = 0.5\sqrt{\frac{S_t/2}{2}^2 + S_I^2}$$
, (5.23)

$$X_M = 0.5S_t, \tag{5.24}$$

where

 n_f = number of fins.

The fin efficiency η_f is computed from Schmidt's approximation [31]. The total heat transfer surface area for all cases of finned tube (circular and plate fin) can be calculated from

$$A = \eta_f A_f + A_b. \tag{5.25}$$

5.2.2 Wall Resistances

The wall resistances in the evaporator and the condenser sections can be calculated from

$$Z_{et} = \frac{\ln(r_o / r_i)}{2\pi k_t L_e}, \tag{5.26}$$

$$Z_{ct} = \frac{\ln(r_o / r_i)}{2\pi k_t L_c}.$$
 (5.27)

5.2.3 Tube-side Thermal Resistances

The boiling and condensation resistances in the evaporator (Z_{ei}) and condenser section (Z_{ci}) can be calculated from

$$Z_{ei} = \frac{1}{h_{ei}A_{ei}}, \qquad (5.28)$$

$$Z_{ci} = \frac{1}{h_{ci}A_{ci}}, \qquad (5.29)$$

where

 h_{ei} = boiling heat transfer coefficient inside thermosyphon (W/m^2K)

 h_{ci} = condensation heat transfer coefficient inside thermosyphon (W/m²K).

The boiling and the condensation heat transfer coefficients can be evaluated from the correlations in Chapter 2.

5.2.4 Overall Thermal Resistances

The overall thermal resistance of the thermosyphon air preheater can be calculated from

$$\frac{1}{(UA)_{total}} = Z_{eo} + Z_{et} + Z_{et} + Z_{ct} + Z_{ct} + Z_{co}, \qquad (5.30)$$

where (UA)total is the overall thermal resistance of the thermosyphon air preheater.

The overall heat transfer rate of the thermosyphon air preheater from Figure 5.4 for parallel flow and counter flow arrangements can be evaluated as

$$Q_{total} = (UA)_{total} \Delta T_{lmtd},$$

$$= m_h C_{ph} (T_{hi} - T_{ho}),$$

$$= m_c C_{pc} (T_{co} - T_{ci}).$$
(5.31)

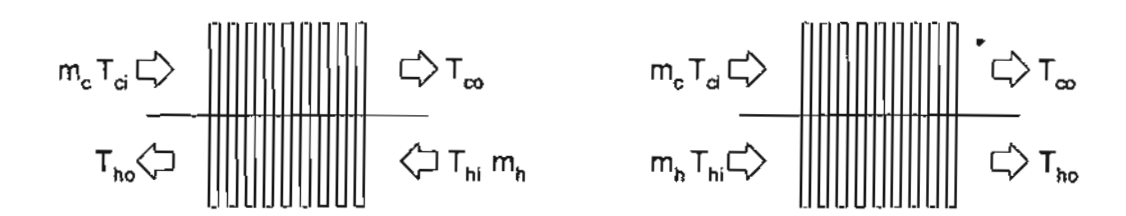
The Temperature difference, ΔT_{lmtd} , could be calculated from;

for parallel flow

$$\Delta T_{Imtd} = \frac{\left(T_{hI} - T_{cI}\right) - \left(T_{ho} - T_{co}\right)}{In \left[\frac{T_{hI} - T_{cI}}{T_{ho} - T_{co}}\right]},$$
(5.32)

for counter flow

$$\Delta T_{lintid} = \frac{\left(T_{hl} - T_{co}\right) - \left(T_{ho} - T_{cl}\right)}{ln\left[\frac{T_{hl} - T_{co}}{T_{ho} - T_{cl}}\right]}.$$
(5.33)



- a. Counter flow heat exchanger.
- b. Parallel flow heat exchanger.

Figure 5.4 Flow arrangement of the thermosyphon heat exchanger.

5.3 Simulation Program for Single Working Fluid

In this research, the new method for simulating the heat transfer rate of the thermosyphon heat exchanger has been carried out. The conventional method is that proposed by ESDU [8] by assuming the same overall heat transfer coefficient of each thermosyphon heat pipe in the heat exchanger then the heat transfer in each row has the same value. In practice, this value varies along the path of fluid flow in the heat exchanger. In this work, the heat exchange varies row by row depending on the conditions of the hot and the cold streams at the local tube row. Figure 5.5 shows the flow chart for calculating the heat transfer rate of the thermosyphon heat exchanger based on the method of ESDU and hereafter, it is called a uniform heat transfer method.

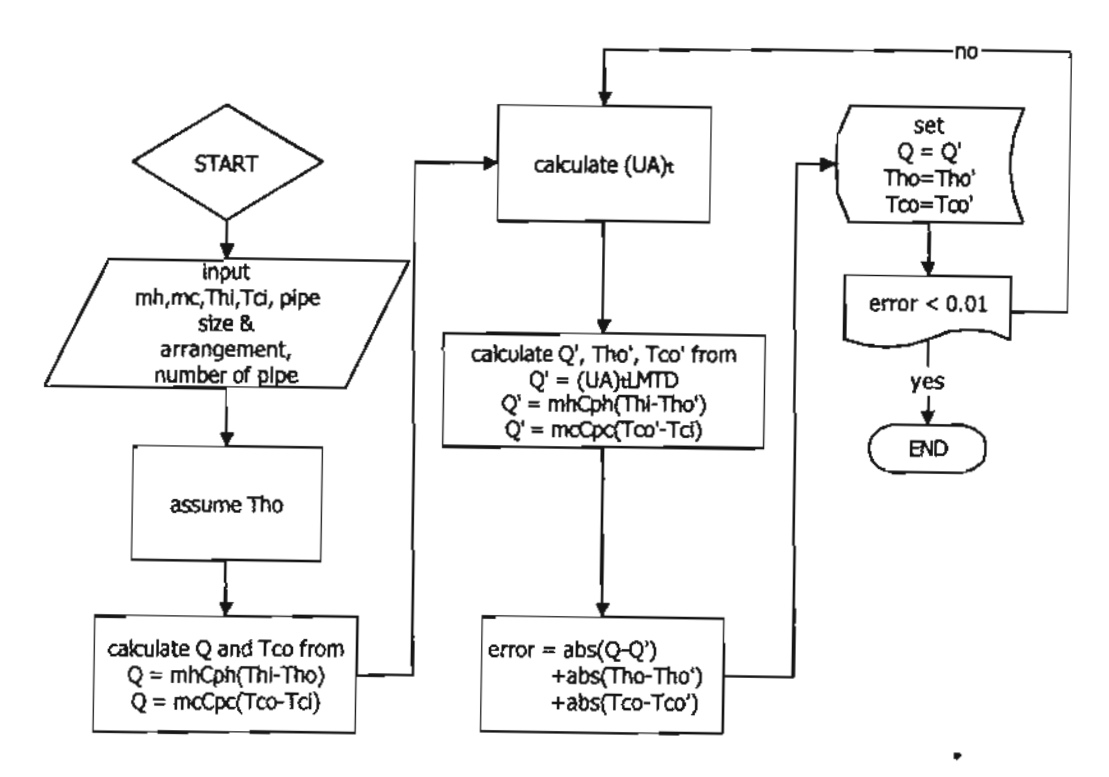
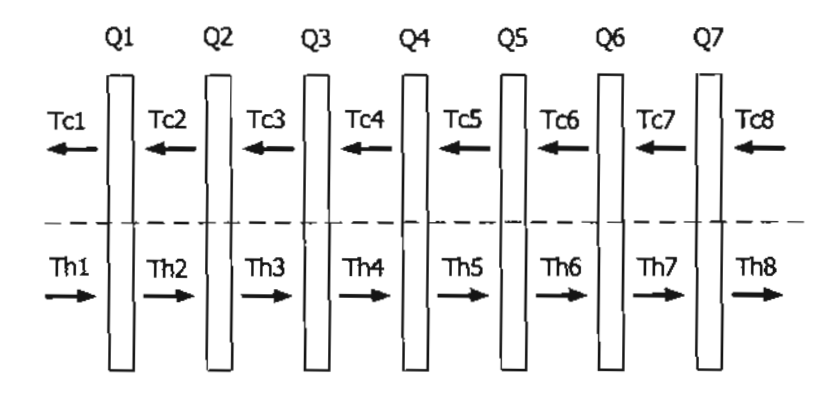
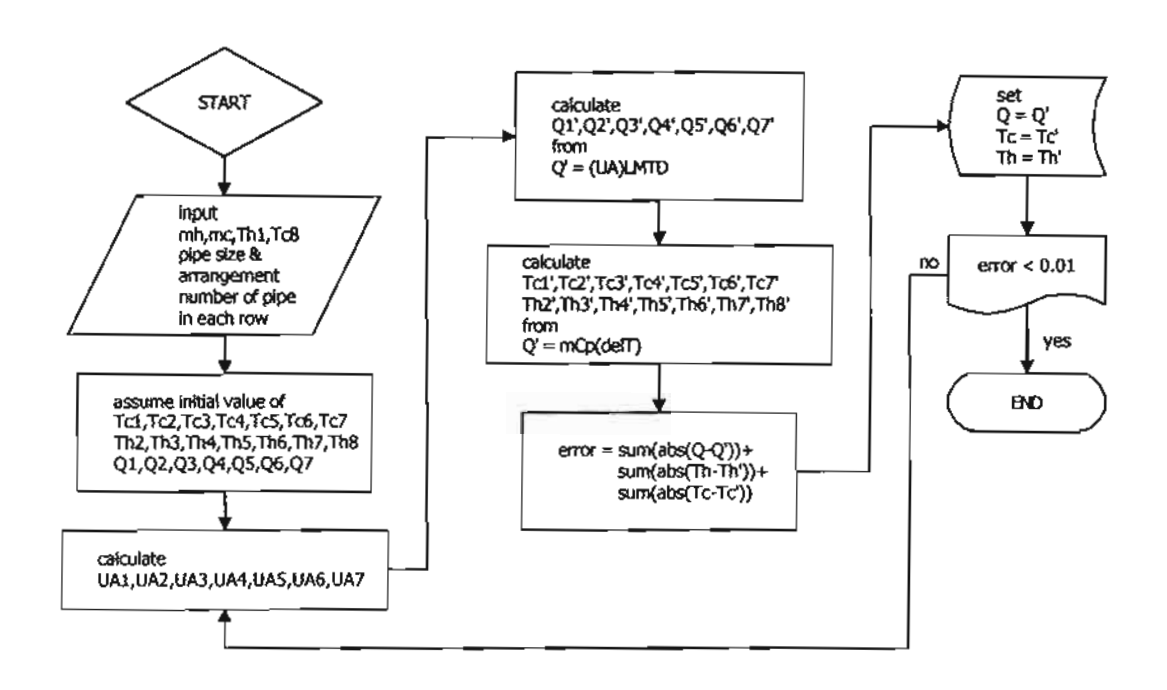


Figure 5.5 Flow chart for calculating the heat transfer rate by using the uniform heat transfer method.

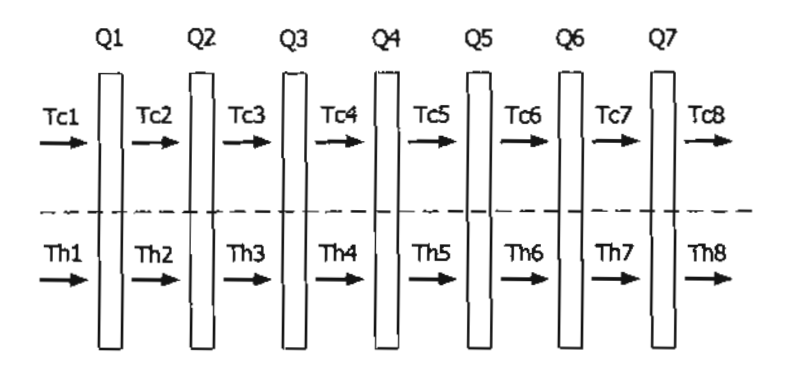


a. Flow direction and temperature profile in each part of counter flow heat exchanger.

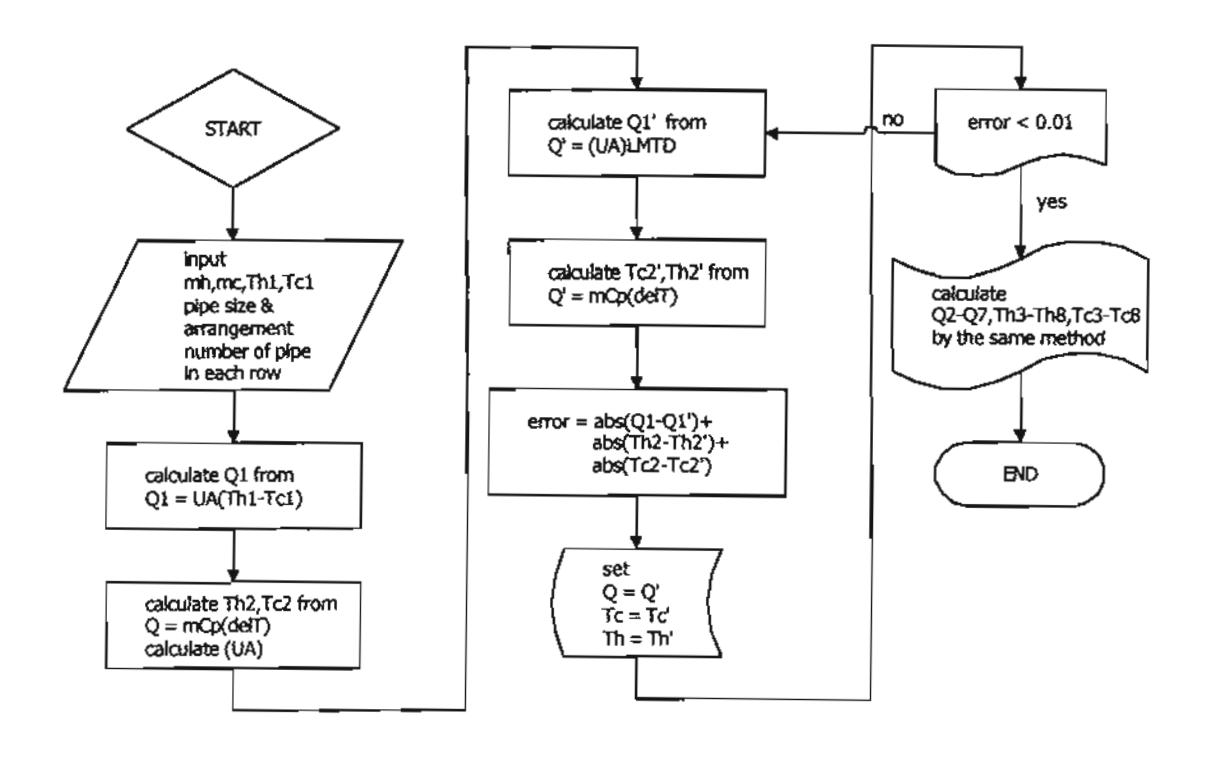


b. Flow chart for calculating the heat transfer rate.

Figure 5.6 Flow chart for calculating the heat transfer rate of the counter flow heat exchanger in case of using the non-uniform heat transfer method.



a. Flow direction and temperature profile in each part of parallel flow heat exchanger.



b. Flow chart for calculating the heat transfer rate.

Figure 5.7 Flow chart for calculating the heat transfer rate of the parallel flow heat exchanger in case of using the non-uniform heat transfer method.

In this flow chart, the heat exchanger size, the flow arrangement, the number of pipe and also the inlet temperature and the mass flow rate of the hot and the cold streams are input parameters. The next stage is assuming the value of the temperature T_{ho} and calculating the values of heat transfer rate, Q, and T_{co} . Then, calculating the heat transfer coefficient-area, UA, by iteration. Re-calculating all values again and comparing them with the previous results until the error is in the limit are conducted. So, the required values of the heat transfer rate Q, the temperatures T_{ho} and T_{co} is finally obtained.

For the new method developed in this research, namely, non-uniform heat transfer rate method, the heat transfer rate in each row is not constant. Figures 5.6 and 5.7 show the flow charts for presenting the calculation of the heat transfer rates by using the non-uniform heat transfer rate method in case of counter and parallel flows, respectively.

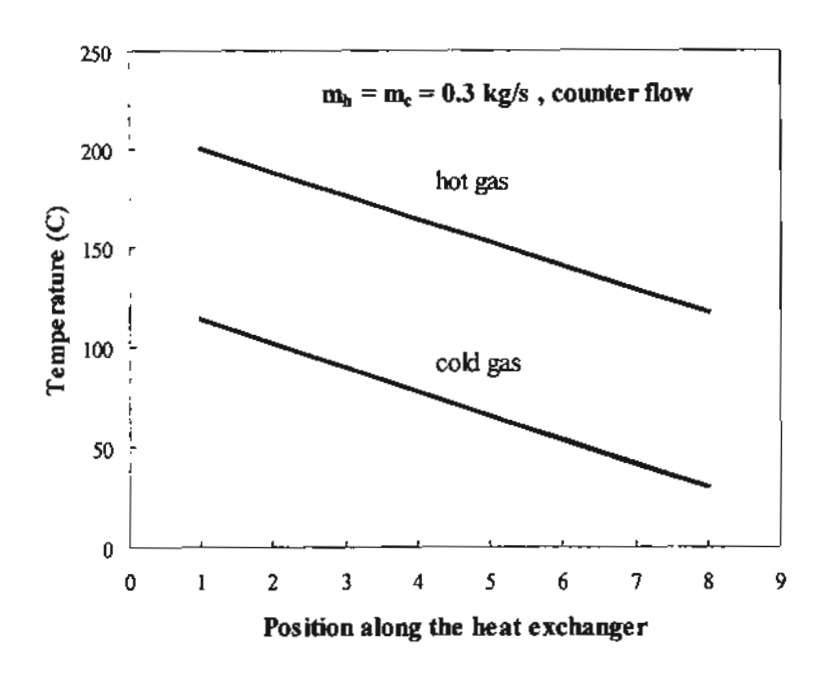
Note that, the thermosyphon heat exchanger has seven rows and the unit has the same size as the constructed testing apparatus in Chapter 4. For counter flow in Figure 5.6, firstly input all of working conditions and also dimensions of the heat exchanger then assume values of the inlet and the outlet temperatures of the hot and the cold streams and also the heat transfer rate in each row. By using trial and error technique, the real value of the temperatures and the heat transfer rate of each row should be obtained. For the parallel flow in Figure 5.7, starting with row 1 by assuming the value of Q and with the trial and error technique, the real value of the outlet temperature of the hot and the cold air streams is known, and eventually the heat transfer rate are obtained. Next starting with row 2 by using the same method until the last row is finished.

Performance analyses of a thermosyphon heat exchanger calculated by the non-uniform and uniform transfer methods have been carried out. The conditions of the heat exchanger are shown in Table 5.3. All dimensions and the relevant arrangements of the thermosyphon heat exchanger are the same as those cited in Chapter 4.

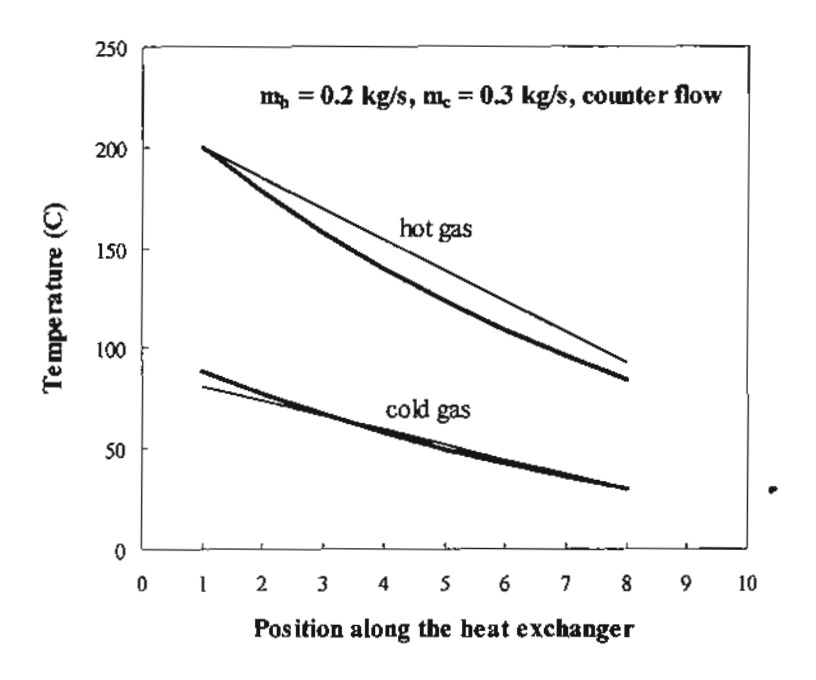
Table 5.3 Testing conditions of the simulation programs for calculate the performance of thermosyphon heat exchanger.

Item	Value
Inlet temperature of hot air	200°C
Inlet temperature of cold air	30°C
Mass flow rate of hot and cold air	0.1-0.6 kg/s
Working fluid	water
Flow pattern	counter and parallel flow

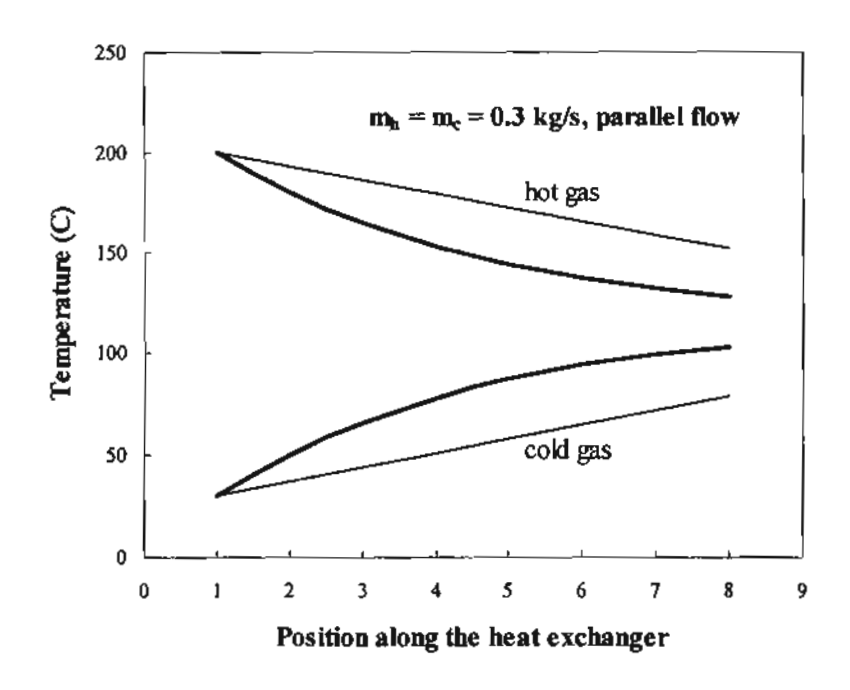
Figures 5.8-5.11 show the temperature profiles of the hot and the cold streams calculated by the uniform and the non-uniform heat transfer methods at various conditions. In Figure 5.8 the hot and the cold air have the same mass flow rates with a counter flow arrangement (balanced counter flow). In this case it is found that both calculation methods give the same result. In Figures 5.9-5.11, it is found that the uniform heat transfer method gives more error especially for parallel flow. It could be concluded that the uniform heat transfer method may be more appropriate for calculating the performance in case of balanced counter flow. In this case the temperature difference between the hot and the cold streams is nearly constant along the heat exchanger and the heat transfer coefficient is also nearly constant, consequently the heat transfer rate of the thermosyphon in each row is equal and the result agrees well with the conventional method. For the other cases, the temperature difference between the hot and the cold streams are not constant, therefore, the heat transfer rate of each row is not uniform and using the uniform heat transfer method will give an error especially in case of parallel flow where big temperature difference is achieved.



_____ uniform heat transfer _____ non-uniform heat transfer Figure 5.8 Temperature profiles of balanced counter flow heat exchanger.

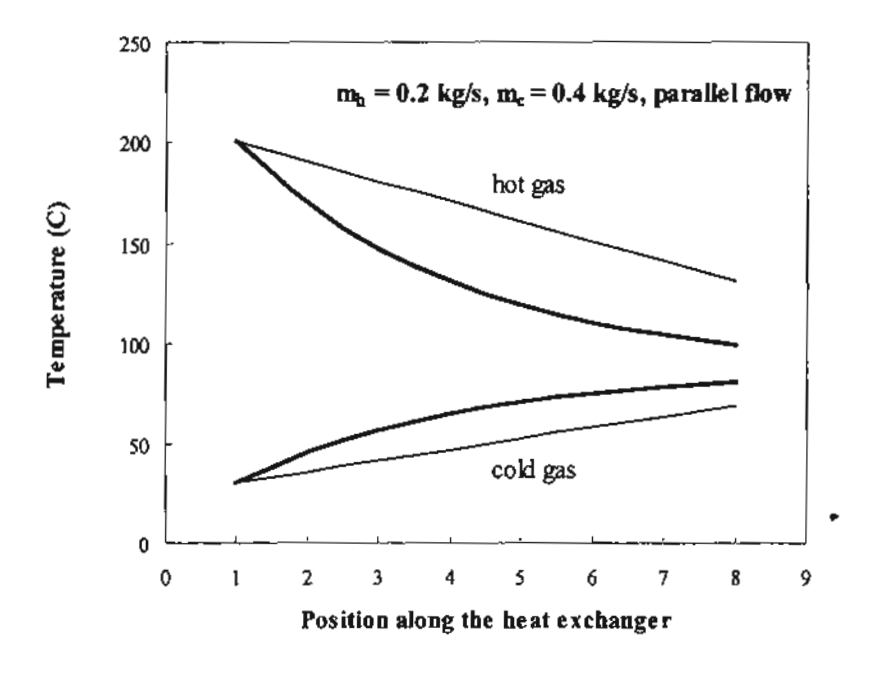


uniform heat transfer ———— non-uniform heat transfer Figure 5.9 Temperature profiles of unbalanced counter flow heat exchanger.



uniform heat transfer ______non-uniform heat transfer

Figure 5.10 Temperature profiles of balanced parallel flow heat exchanger.



uniform heat transfer ______ non-uniform heat transfer Figure 5.11 Temperature profiles of unbalanced parallel flow heat exchanger.

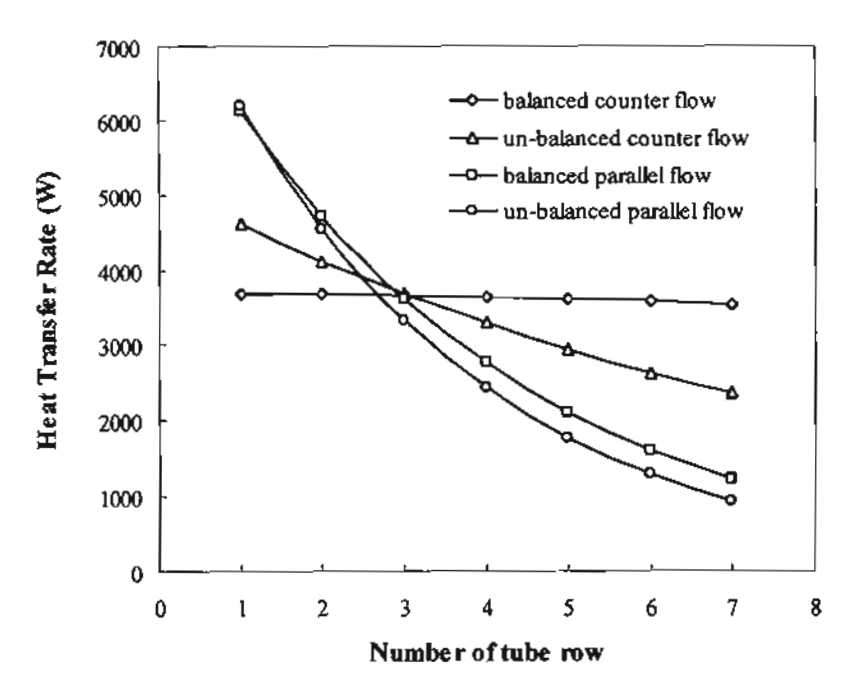


Figure 5.12 Heat transfer rate at each row of the thermosyphon heat exchanger.

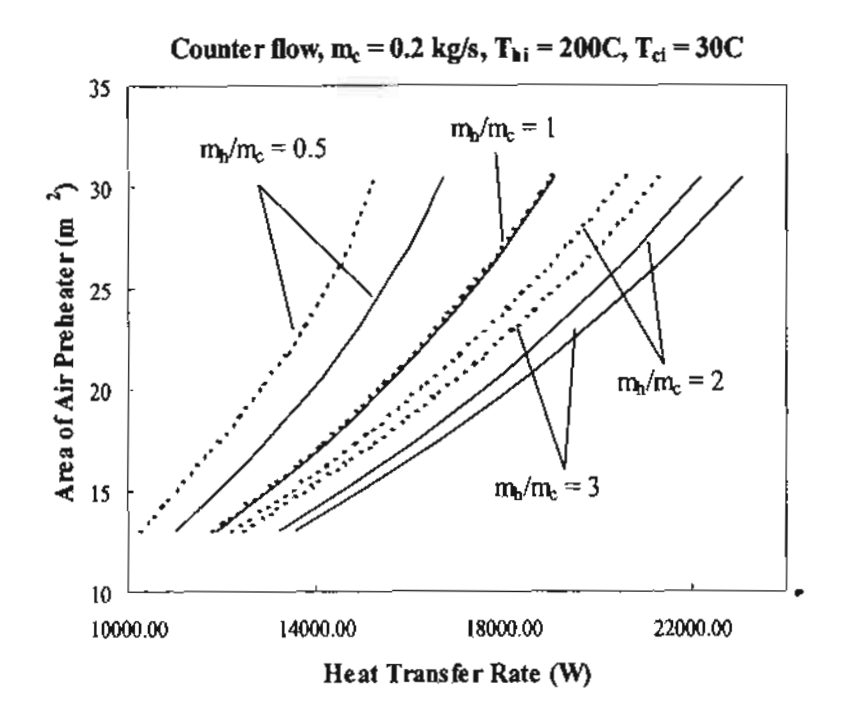


Figure 5.13 Comparisons of heat transfer area calculated by uniform and Non-uniform heat transfer methods.

_____ non-uniform heat transfer

uniform heat transfer

Figure 5.12 shows the heat transfer rate in each row of the thermosyphon heat exchanger calculated by the non-uniform heat transfer method. It is found that in case of balanced counter flow the heat transfer rate is nearly constant and the unbalanced parallel flow gives the highest change of heat transfer rate along the heat exchanger. Figure 5.13 shows the heat transfer areas calculated from both methods. It is found that using the uniform heat transfer method requires more area for exchanging heat except in case of balanced counter flow which means that the conventional one gives an overestimated result, this may bring about unnecessary investment cost.

CHAPTER 6

SELECTION OF WORKING FLUIDS FOR AIR-TO-AIR THEMOSYPHON HEAT EXCHANGER

6.1 Introduction

When the temperature is approximately lower than 80°C, water is not appropriate as the working fluid inside. The heat transfer rate is not good because water is difficult to boil. In addition, it is also found that in this temperature range pure ethanol gives higher heat transfer rate than that of water. Ethanol-water mixture in the thermosyphon also gives lower heat transfer rate compared with pure ethanol. So in this temperature application only pure water or pure ethanol is used. In the heat exchanger, the temperature profiles are changing along the heat exchanger, therefore, selecting the suitable working fluid for each row of the thermosyphon is needed to get higher heat transfer rate than using single working fluid for all rows.

For high working temperature or high heat flux, it is found that using Triethylene Glycol (TEG; C₆H₁₄O₄) – water mixture as a working fluid could reduce the flooding phenomenon of the thermosyphon while the heat transfer rate slightly decreases. In this chapter, selection of the suitable fraction of TEG in the working fluid mixture in each row of a thermosyphon air preheater operated at high temperature has also been carried out.

This chapter is divided into two parts, low and high working temperatures.

The details of each part are as follows:

6.2 <u>Selection of Working Fluids for Low Operating Temperature Thermosyphon</u> Heat Exchanger

6.2.1 Simulation Program

The performance of the thermosyphon heat exchanger at low temperature range is investigated (T_{hi} < 100 °C). In this part, the working fluids in the thermosyphons are ethanol and water. As mentioned in the introduction, the thermosyphon heat exchanger that uses water in this range may possess a poor heat transfer characteristics. Therefore, it would be beneficial to use the thermosyphons that containing ethanol in some rows of the heat exchanger because it gives heat transfer performance than water in this temperature range. The simulation program is developed to select the suitable working fluid for each row between water and ethanol. The flow chart for low temperature application can be seen from Figure 6.1.

As seen in Figure 6.1, both counter and parallel flow arrangements are implemented. For the counter flow arrangement at the starting stage of iteration, temperatures of the inlet hot and cold streams are prescribed and the inlet and the outlet temperatures of the fluids at each row are assumed by considering all rows to be water. Iteration then starts by setting ethanol to the first row. Comparison is made with the original water thermosyphon. Ethanol is selected if the related heat transfer performance is better than that of the original water thermosyphon. The selection process continues row by row to the last row. In case of the parallel flow, similar process has been carried out from the first row to the last row. In order to obtain appropriate fluid in every row of the thermosyphon heat exchanger.

Table 6.1 shows related geometrical parameters of thermosyphon heat exchanger. These values are used as the condition for selecting the working fluids (water and ethanol) in the heat exchanger.

Table 6.1 Testing conditions and related geometrical parameters of the thermosyphon heat exchanger.

Items	Conditions
1. Flow arrangement	Parallel and counter flow
2. Temperature of hot air	50-100 °C
3. Temperature of cold air	30 °C
4. Mass flow rate of air	0.1-0.5 kg/s
5. Thermosyphon arrangement	Staggered array
	$S_t = 0.053 \text{ m}, S_d = 0.053 \text{ m}, S_l = 0.046 \text{ m}$
6. Number of tube rows	7
7. Number of tubes in row	7
8. Diameter of thermosyphon (bare tube)	0.027 m
9. Type of fin	Circular fin
10. Size of fin	Fin height = 0.1 m and
	fin pitch = 10 fins/inch
11. Filling ratio of working fluid	50%
12. Material of pipe and fin	Stainless steel 304

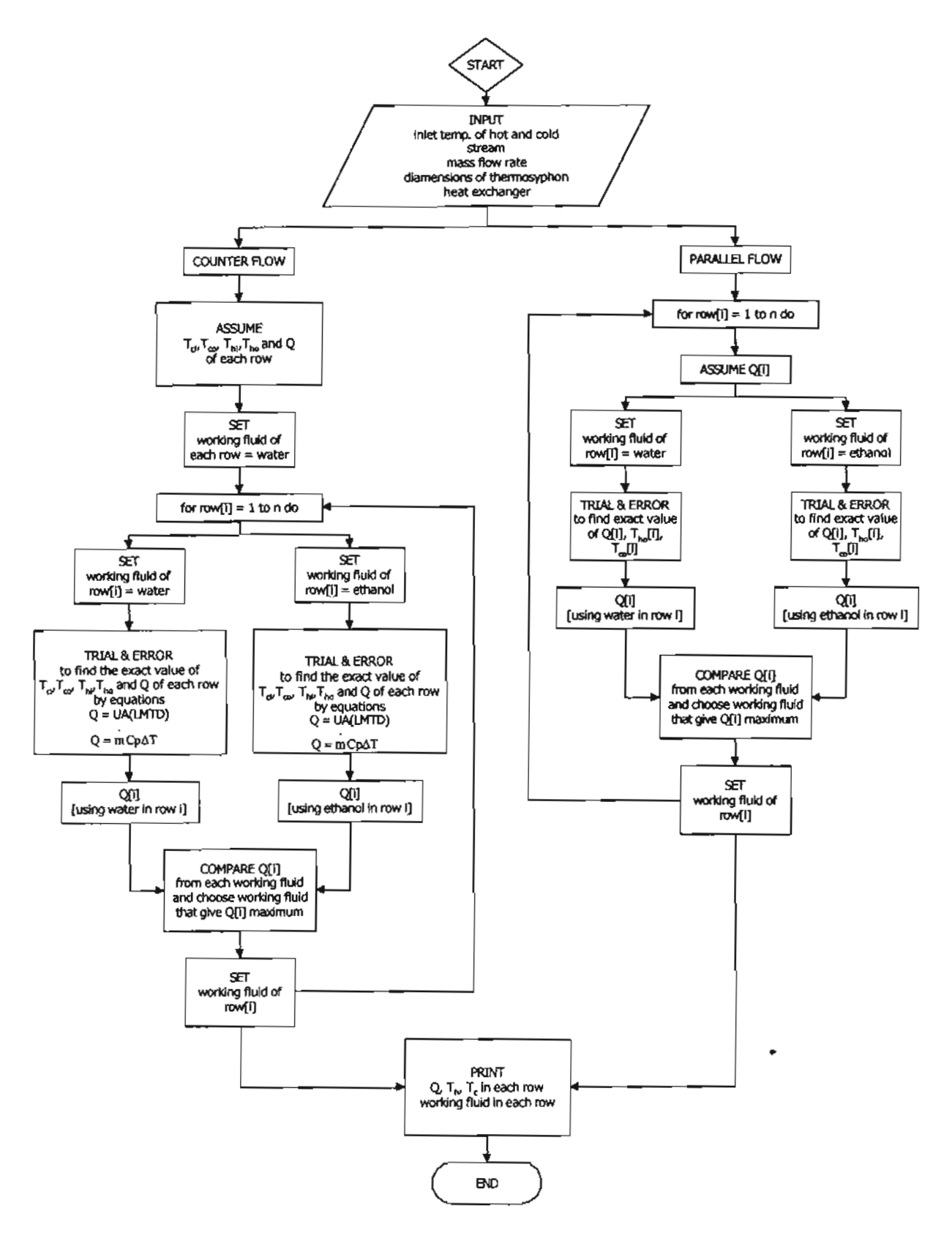


Figure 6.1 The flow chart of the two-fluid thermosyphons in low working temperature.

6.2.2 Simulation Results and Discussion

Table 6.2 shows calculated results from the simulation program in the case of the balanced counter flow arrangement ($\dot{m}_h = \dot{m}_c$) at various working conditions. Calculations are performed at a fixed T_{cl} of 30°C. Range of T_{hi} is from 50°C to 100°C with a mass flow rate of 0.1 to 0.5 kg/s. As seen from Table 6.2, all-water thermosyphons would be the best choice for $T_{hi} = 100$ °C at mass flow rate higher than 0.4 kg/s while all ethanol thermosyphons show the highest performance for $T_{hi} < 60$ °C. For 70 °C < $T_{hi} < 100$ °C, it can be shown that use of both fluids in the thermosyphons would be advantageous. However, only a slight increase of performance is observed. It should be noted that water thermosyphons should be placed at the hot air inlet. Figure 6.2 shows the appropriate number of ethanol thermosyphons in the heat exchanger at various inlet hot gas temperatures.

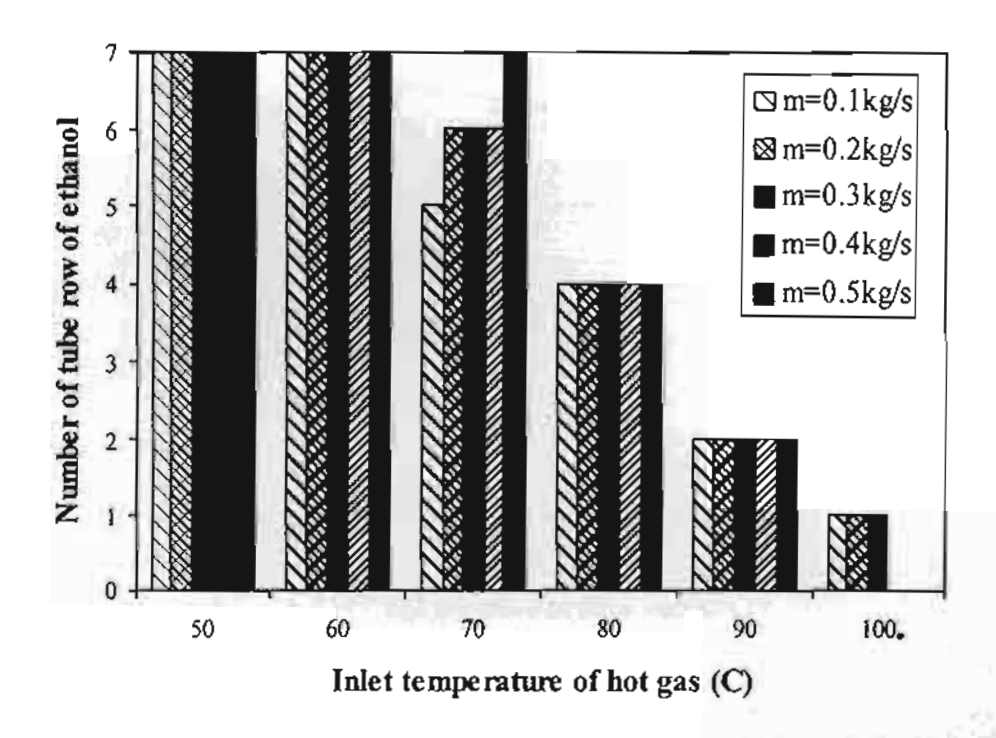


Figure 6.2 Appropriate number of ethanol thermosyphon of balanced counter flow.

The inlet cold air is 30°C.

In case of unbalanced counter flow shown in Table 6.3. It should be noted that, the concept of using 2-kinds of working fluid is still feasible. The heat transfer rate increase approximately 0.1-1.5% compared to those of all water or all ethanol. In this part, the mass flow rate of the hot stream is kept constant at 0.3 kg/s and the temperature of cold air is also fixed at 30°C. It is found that at the same value of inlet temperature of the hot gas, higher mass flow rate of the cold gas results in higher number of ethanol thermosyphon. This result comes from the effect of the inside temperature of the thermosyphon tube. In case of lower mass flow rate of cold gas, the temperature of the cold stream increases easily. Therefore, the inside temperature of the thermosyphon tube is increased; water could be boiled more so that will be appropriate to be filled in the thermosyphon.

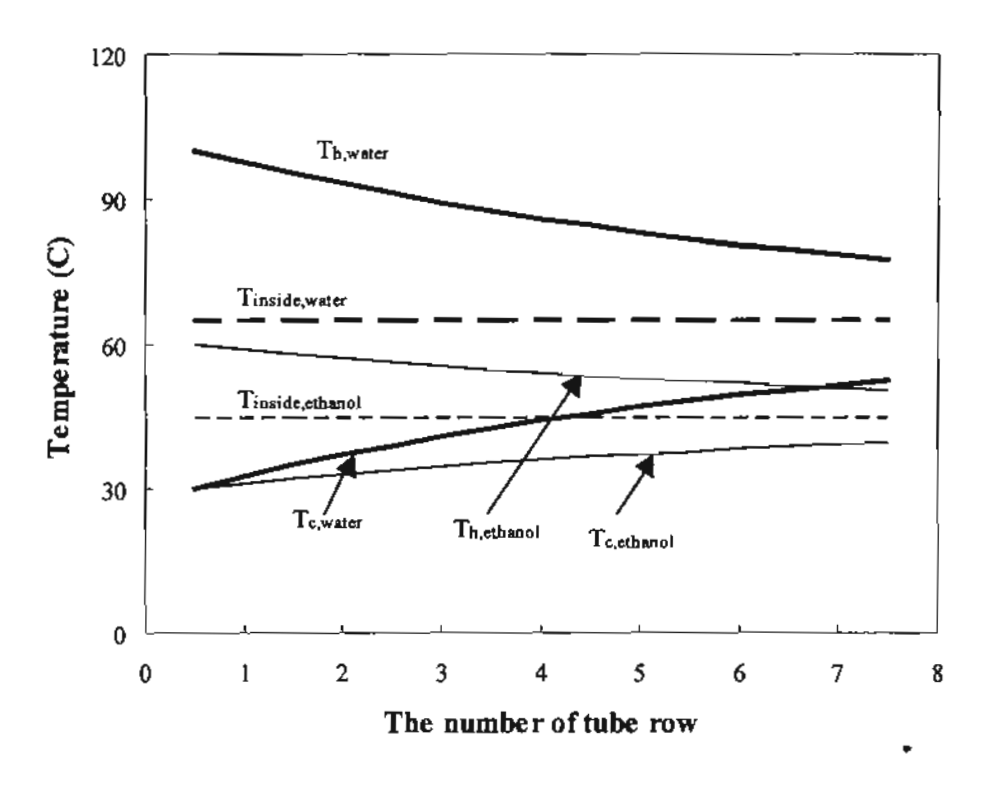


Figure 6.3 Temperature profile of the balanced parallel flow.

In the case of thermosyphon heat exchanger with balanced parallel flow arrangement $(\dot{m}_h = \dot{m}_c)$ shown in Table 6.4, the calculation indicates that use of

ethanol and water is not beneficial throughout the range when compared with all water or all ethanol thermosyphons. Explanation of this phenomenon can be seen from Figure 6.3. As depicted in Figure 6.3, the temperature profiles of the hot and the cold streams are quite symmetry and the inside temperatures of the thermosyphons from the first to the last row are nearly constant. Therefore, this inside temperature is suitable for only one type of working fluid. Consequently, use of two kinds of thermosyphon is not so beneficial when compared to those of the counter flow arrangement.

Unlike those of balanced parallel flow arrangement, for the case of unbalanced parallel flow thermosyphon heat exchanger ($\dot{m}_h \neq \dot{m}_c$) shown in Table 6.5, the temperature profiles of the hot and the cold streams are not symmetry. The concept of employing the two-fluid thermosyphons gives a little advantage. Table 6.5 shows one result of using two-kinds of working fluid (\dot{m}_h =0.3 kg/s with \dot{m}_c = 0.1 kg/s and T_{hl} = 70°C).

It can be noted that the suitable working fluid inside the thermosyphon tube depends on the inside temperature of the thermosyphon tube. This temperature depends on the temperature of the hot and the cold streams, the mass flow rate and the flow direction. The effect of these parameters can be concluded that, if the temperature of the hot and the cold gases are high, all water thermosyphon is better than all ethanol thermosyphon. However in other case all ethanol thermosyphon is better. If the mass flow rate is low, the temperature is easy to change and it has an opportunity to use 2-kinds of working fluid. For the effect of the flow direction, counter flow has an opportunity to use 2-kinds of working fluid because the inside temperature changes along the heat exchanger. However, in case of parallel flow, the temperature profile of the hot and the cold streams are nearly symmetry and tend to be constant inside temperature of the thermosyphon tube. Therefore, using 2-kinds of working fluid is not feasible.

Table 6.2 Results of simulation in the case of balanced counter flow arrangement for low temperature application.

		\neg									_												_	_								
% increase	relative to	ethanol	0.00	0.00	0.00	00.0	0.00	00.0	0.00	0.00	0.00	0.00	0.11	0.11	0.16	0.20	0.00	0.20	0.39	0.55	69.0	0.81	0.37	0.70	66:0	1.25	1.75	0.48	0.92	1.29	1.87	2.21
% increase	relative to	water	3.01	3,54	3.76	3.85	3.87	2.25	2.48	2.47	2.39	2.27	1.26	1.54	1.42	1.25	1.24	0.82	0.75	0.62	0.46	0.31	0.34	0.28	0.19	60.0	0.00	0.14	0.10	0.04	0.00	0.00
(jo		7	щ	щ	Э	Э	ப	ш	ы	ш	ÜΪ	Ш	щ	щ	ŒĴ	ш	ŒΪ	ш	щ	ш	ഥ	ш	ш	щ	ш	Щ	ш	щ	щ	IIJ	≱	≱
= ethanol)		9	щ	Œ	ū	ш	щ	Э	ш	ш	ш	ជា	Щ	ш	Щ	ш	ш	Щ	Э	田	щ	四	功	ъ	可	щ	政	≱	B	≱	≱	≱
Д Ш		5	ш	Э	ш	ш	Ξ	Э	出	Э	വ	田	ш	3	ম	叫	н	田	ы	ш	Ξ	ជា	≩	≱	≽	≯	≱	≱	≱	≽	≱	≱
V ≃ water,	in each row	4	Ξì	Э	щ	Э	Э	ш	ш	ш	Э	凶	Э	Э	Ш	Щ	щ	Ή	凹	凶	ш	Э	≱	≱	≱	≱	≱	≩	≱	≽	≱	≱
	. s	3	ш	ш	ш	ш	щ	Э	Э	田	ធ	<u> </u>	Э	ш	ш	Э	Э	≱	≱	≱	≱	≱	≱	≱	⋧	≱	≩	≱	≱	≱	≱	≱
working fluid		2	Ξ	ជ	ப	田	ш	Щ	Щ	Щ	Щ	ப	×	Ξ	Ξ	ы	Ħ	≱	≱	≱	≱	≱	≩	≱	≱	≱	≱	≱	≱	≱	≱	≱
ĭo M		_	四	ы	ш	П	щ	щ	ш	ш	田	ш	≱	≱	≱	≱	ш	≱	≱	≱	≱	≱	≱	≱	≱	≱	≱	≽	≱	×	≱	≱
(Swaier-ethanol	<u></u>	946.39	1552.23	2024.75	2416.79	2753.64	1422.08	2331.29	3039,51	3626.51	4130.40	1901.66	3116.25	4063.29	4848.28	5509.03	2383.51	3911.71	5104,37	6094.56	6945.99	2870.22	4716.00	6159.83	7360.94	8418.11	3358.57	5522.14	7216.60	8648.18	9872.30
(Cerhanol	(<u>k</u>	946.39	1552.23	2024.75	2416.79	2753.64	1422.08	2331.29	3039.51	3626.51	4130.40	1899.53	3112.75	4056.76	4838.46	5509.03	2378.77	3896.66	5076.62	6052.93	88.6889	2859.76	4683,05	6099.15	7270.00	8273.10	3342.52	5471.90	7124.38	8489.72	628.79
(Cwater	3	918.73	1499.10	1951.36	2327.22	2651.03	1390.80	2274.98	2966.16	3541.85	4038.68	1877.99	3069.10	4006.55	4788.37	5441.44	2364.24	3882.45	5073.06	6066.42	6924.61	2860.58	4702.98	6148.28	7354.02	8417.77	3353.86	5516.72	7213.40	8648.18	9872.30
Ŀ	I ci	(၃)	30	30	30	30	30	30	30	30	30	30	30	30	30	30	30	30	30	30	30	30	30	30	30	30	30	30	30	30	30	30
Ę	I hi	(30)	20	20	20	20	20	09	9	09	9	09	70	20	70	20	70	80	80	80	80	80	8	6	8	06	8	100	100	100	001	100
	m _c	(x/8x)	0.1	0.2	0.3	9.4	0.5	0.1	0.2	0.3	4.0	0.5	0.1	0.2	0.3	4.0	0.5	0.1	0.2	0.3	0.4	0.5	0.0	0.2	0.3	4.0	0.5	0.1	0.2	0.3	0.4	0.5
			-		_			_	_		_				_		<u></u>			~	-	٠-	_	~	_	-		_			_	0.5

Table 6.3 Results of simulation in the case of unbalanced counter flow arrangement for low temperature application.

																		_							
% increase	ethanol	0.00	0.00	0.00	00.0	0.00	00.0	00.00	00.00	0.29	0.25	00.0	00.0	0.52	0.58	0.62	0.46	0.70	96'0	1.11	86.0	0.78	1.23	4.	1.55
% increase	water	3.09	3.49	3.68	3.71	2.26	2.41	2.39	2.36	0.61	1.18	1.54	1.47	0.14	0.47	0.59	0.67	0.00	0.10	0.18	0.23	0.00	0.00	0.04	0.04
(io	7	ш	ш	ы	щ	Œ	വ	ш	ш	щ	ш	Œ	ш	Э	Э	口	ы	≥	щ	щ	ш	≱	≥	ш	Œ
working fluid (W = water, E = ethanol) in each row	9	Ю	ங	ш	ш	ш	ш	Щ	Э	Ш	ш	щ	ш	≥	凹	ш	ш	≱	≱	ப	ш	≱	∌	≩	≱
er, E= w	S	ш	щ	ш	ш	щ	Э	ш	Œ	田	щ	臼	Э	≩	Щ	щ	щ	≱	≱	≥	щ	≱	≥	≱	≱
(W = water in each row	4	Э	щ	щ	Э	ш	ш	ш	щ	≱	щ	团	ш	≱	≱	ш	Щ	×	≥	≱	≽	≥	≥	≱	≱
w) bid in e	6	ш	щ	ш	ш	ш	Э	щ	ш	≯	ш	Ш	Œ	≥	≱	≯	Ш	≱	≱	≱	≱	≽	≥	≱	≱
ing flu	7	ш	щ	ш	щ	ш	ш	щ	ш	3	≱	Щ	ш	≥	≥	≱	≥	≱	≥	≽	≥	≱	≽	≥	≱
work	-	Э	Œ	ш	ш	ш	ш	凶	щ	≱	≱	Œ.	Э	≱	≱	≽	≩	≱	*	≩	3	≱	≱	≩	≥
Quaterethanol	(8)	1197.27	1717.67	2231.96	2383.11	1798.02	2578.86	3350.32	3577.04	2407.32	3450.86	4471.37	4773.83	3020.11	4332.85	5629.89	66.0009	3635.26	5225.61	6797.16	7247.23	4250.29	6120.12	7965.45	8512.97
Qeshanol	-S	1197.27	1717.67	2231.96	2383.11	1798.02	2578.86	3350,32	3577.04	2400.39	3442.23	4471.37	4773.83	3004.41	4307.86	5595.32	5973.73	3610.11	5175.78	6722.24	7176.83	4217.47	6045.98	7852.12	8383.16
Qwater	(s)	1160.25	1657.64	2149.83	2294.80	1757.38	2516.65	3270.32	3492.69	2392.60	3410.13	4402.54	4703.56	3016.03	4312.37	5596.79	5960.89	3635.26	5220,53	6785.02	7230.35	4250.29	6120.12	7962.32	8509.96
T_{ci}	(2)	30	30	30	30	30	30	30	30	30	30	30	30	30	30	30	30	30	30	30	30	30	30	30	30
T_{hi}	(00)	20	20	20	20	9	09	9	9	70	20	70	70	80	80	80	80	8	8	96	9	001	001	100	100
m _c	(kg/s)	0.1	0.2	0.4	0.5	0.1	0.2	4.0	0.5	0.1	0.7	0.4	0.5	0.1	0.5	4.0	0.5	0.1	0.7	0.4	0.5	0.1	0.2	0.4	0.5
m _h	(kg/s)	0.3	0.3	0.3	0.3	0.3	0.3	0.3	0.3	0.3	0.3	0.3	0.3	0.3	0.3	0.3	0.3	0.3	0.3	0.3	0.3	0.3	0.3	0.3	0.3
-								_	_	_	_	_					_		_						

Table 6.4 Results of simulation in the case of balanced parallel flow arrangement for low temperature application.

						_																		_	_				_		
% increase relative to	ethanol	00.0	0.00	0.00	0.00	0.00	0.00	0.00	0.00	0.00	0.00	0.00	0.00	0.00	0.00	0.00	0.25	0.64	1.00	1.33	1.63	0.30	0.73	1.14	1.50	1.83	0.34	0.82	1.26	1.65	2.01
% increase	water	2.47	3.24	3.58	3.74	3.80	1.88	2.32	2.41	2.38	2.29	1.51	1.73	1.67	1.52	1.33	0.00	0.00	0.00	0.00	0.00	0.00	0.00	0.00	0.00	0.00	0.00	0.00	00'0	0.00	0.00
ol)	7	Ü	ы	Щ	ш	Œ	Ή	ш	ш	щ	щ	Œ	ш	ਜ਼	Ħ	īī	≱	≱	≱	≱	≱	≩	≱	≱	≯	≽	≩	≥	≱	≱	≱
= ethanol)	9	ш	ш	ш	ш	ш	ш	ш	ш	ĭΞ	ш	Щ	ш	ш	ш	ப	≩	≥	≩	≱	≩	≱	≱	≱	€	≱	≱	≱	≱	≱	≩
	٧	Э	Щ	щ	ш	ш	Э	ω	Œ	ш	ш	മ	Э	ш	ш	Э	≩	≩	×	≱	≱	₹	≩	≩	¥	≱	≥	≩	≱	≽	≱
(W = water in each row	4	ш	ப	ш	ш	ш	Щ	ш	Щ	ы	щ	щ	Щ	ш	凹	ធា	≩	≽	≩	≱	≩	≱	≥	≩	≱	≱	≱	≩	≥	≱	≱
luid (V	3	ы	m	Щ	ш	щ	Œ	ш	ப	凹	щ	ш	Ή	ы	μì	Э	≩	≱	≱	≱	≱	≱	≱	≱	≩	≱	≩	≩	≩	≩	≱
working fluid (W = water, E in each row	2	ïЛ	凹	凹	ш	凹	山	ш	可	Э	Э	ា	ш	ш	ш	ப	⋧	≽	≱	⋧	≱	≱	≱	≩	≱	≥	≱	≱	≱	≱	≱
Μ.	-	Э	ш	Ш	Э	Э	ш	ъ	ப	ம்	ш	ш	凹	ы	ш	田	≱	≱	_ ≱	¥	≱	≩	<u>-</u> ≽	≱	¥	×	≱	≱	≱	≱	≱
Quaterethanol	<u></u>	836.66	1440.12	919.49	2319.63	2664.18	1256.66	2162.63	2881.47	3480.87	3996.49	1677.84	2887.12	3845.68	4644.24	5330.64	2105.57	3636.81	4860.58	5887.50	6775.95	2531.37	4374.05	5846.90	7082.88	8152.15	2958.65	5114.24	6837.40	8283.39	9534.37
ð		∞	17	=	7	14			•						•										•	00	` '	۷,	Ū		
Qethanol Qu	%	836.66 8	_	_	_	_	1256.66		_	_	3996.49	1677.84	2887.12	3845.68	_	5330.64	2100.24	3613.63	4812.25	5809.97	86.9999	2523.84	4342.19	5781.19	6978.15	8005.63	_	5072.80		8148.83	9346.69
		836.66	1440.12	1919.49	2319.63	2664.18	1256.66	2162.63	2881.47	3480.87	_	_	2887.12	3845.68	4644.24	_		_	_		_	_	_		6978.15	8005.63	2948.63	5072.80	6752.58	8283.39 8148.83	
Quoter Deshanol	*	816.51 836.66	1394.90 1440.12 1	1853.16 1919.49 1	2236.10 2319.63	2566.62 2664.18	1233.42 1256.66	2113.62 2162.63	2813.53 2881.47	3399.84 3480.87	3906.84	1652.84	2838.03 2887.12	3782.54 3845.68	4574.88 4644.24	5260.84	2105.57	3636.81	4860.58	5887.50	6775.95	2531.37	4374.05	5846.90	7082.88 6978.15	8152.15 8005.63	2958.65 2948.63	5114.24 5072.80	6837.40 6752.58	8283.39	9534.37
Quoter Deshanol	(M) (W)	816.51 836.66	30 1394.90 1440.12 1	30 1853.16 1919.49 1	30 2236.10 2319.63	30 2566.62 2664.18	30 1233,42 1256,66	30 2113.62 2162.63	30 2813.53 2881.47	30 3399.84 3480.87	30 3906.84	30 1652.84	30 2838.03 2887.12	30 3782.54 3845.68	30 4574.88 4644.24	30 5260.84	30 2105.57	30 3636.81	30 4860.58	30 5887.50	30 6775.95	30 2531.37	30 4374.05	30 5846.90	30 7082.88 6978.15	30 8152.15 8005.63	30 2958.65 2948.63	30 5114.24 5072.80	30 6837.40 6752.58	30 8283.39	30 9534.37
Thi Tc Quater Quitor	(M) (W)	30 816.51 836.66	50 30 1394.90 1440.12 1	50 30 1853.16 1919.49 1	50 30 2236.10 2319.63	50 30 2566.62 2664.18	60 30 1233.42 1256.66	60 30 2113.62 2162.63	60 30 2813.53 2881.47	60 30 3399.84 3480.87	60 30 3906.84	70 30 1652.84	70 30 2838.03 2887.12	70 30 3782.54 3845.68	70 30 4574.88 4644.24	70 30 5260.84	80 30 2105.57	80 30 3636.81	80 30 4860.58	80 30 5887.50	80 30 6775.95	90 30 2531.37	90 30 4374.05	90 30 5846.90	90 30 7082.88 6978.15	90 30 8152.15 8005.63	100 30 2958.65 2948.63	*100 30 5114.24 5072.80	100 30 6837.40 6752.58	100 30 8283.39	100 30 9534.37

Table 6.5 Results of simulation in the case of unbalanced parallel flow arrangement for low temperature application.

m, m									_			_										_	_				_
m_c T_{hi} T_{ci} Q_{water} $Q_{water-clifumed}$ $working fluid (W = water, E = ethanol)$ 0.21 50 7	% increase	ethanol	0.00	0.00	00'0	0.00	0.00	0.00	0.00	0.00	0.15	00:0	0.00	0.00	0.48	08'0	0.00	0.00	0.56	16'0	1.29	1.41	0.63	1.01	1.42	1.55	
m_c T_{iv} T_{ci} $Q_{colorer}$	% increase relative to	water	2.93	3.40	3.67	3.72	2.16	2.37	2.41	2.40	0.70	1.72	1.61	1.55	0.00	00.0	1.03	0.94	0.00	0.00	0.00	0.00	0.00	0.00	0.00	00.00	
m_c T_{iv} T_{ci} Q_{water} $Q_{$	(loi	7	ш	Щ	凹	Э	ш	凹	щ	Э	≱	田	ш	ш	≩	≩	ப	ш	≥	≥	≱	≱	≱	×	≱	≱	_
m_c T_{ii} T_{ci} Q_{water} $Q_{water-channel}$		9	Э	ы	凹	ш	Щ	ш	ш	Щ	≱	ш	щ	ш	≱	≱	ш	Ħ	≱	≱	≱	≱	≱	}	≱	≱	
m _c T _k i T _c i Q _{water} Q _{cthornol} Q _{water-cthornol} (4g8) (***) (***) (***) (***) 0.1 50 30 1092.68 1124.71 11124.71 0.2 50 30 1565.58 1618.77 1618.77 0.4 50 30 2051.96 2127.25 2127.25 0.5 50 30 2199.69 2281.55 2281.55 0.1 60 30 2051.96 2127.25 2127.25 0.1 60 30 2199.69 2281.55 2281.55 0.1 60 30 2373.96 2430.31 2430.31 0.2 60 30 2373.96 2430.31 2434.62 0.3 3117.89 3193.15 3193.15 3193.15 0.4 60 30 2373.98 2254.38 2257.75 0.2 60 30 2422.09 2254.38 2434.62 0.7		5	щ	щ	Э	ш	Щ	ш	ш	ய	≩	团	<u>ы</u>	ப	≱	≱	<u>ы</u>	ப	≱	≱	<u>≽</u>	≱	≱	≱	≩	≱	
m _c T _k i T _c i Q _{water} Q _{cthornol} Q _{water-cthornol} (4g8) (***) (***) (***) (***) 0.1 50 30 1092.68 1124.71 11124.71 0.2 50 30 1565.58 1618.77 1618.77 0.4 50 30 2051.96 2127.25 2127.25 0.5 50 30 2199.69 2281.55 2281.55 0.1 60 30 2051.96 2127.25 2127.25 0.1 60 30 2199.69 2281.55 2281.55 0.1 60 30 2373.96 2430.31 2430.31 0.2 60 30 2373.96 2430.31 2434.62 0.3 3117.89 3193.15 3193.15 3193.15 0.4 60 30 2373.98 2254.38 2257.75 0.2 60 30 2422.09 2254.38 2434.62 0.7	V = wa each r	4	ш	ш	E	Ш	ш	ធា	ப	Щ	ш	ш	ы	ш	≱	≱	ш	щ	≱	≱	≱	≱	≩	≩	≩	≩	
m _c T _k i T _c i Q _{water} Q _{cthornol} Q _{water-cthornol} (4g8) (***) (***) (***) (***) 0.1 50 30 1092.68 1124.71 11124.71 0.2 50 30 1565.58 1618.77 1618.77 0.4 50 30 2051.96 2127.25 2127.25 0.5 50 30 2199.69 2281.55 2281.55 0.1 60 30 2051.96 2127.25 2127.25 0.1 60 30 2199.69 2281.55 2281.55 0.1 60 30 2373.96 2430.31 2430.31 0.2 60 30 2373.96 2430.31 2434.62 0.3 3117.89 3193.15 3193.15 3193.15 0.4 60 30 2373.98 2254.38 2257.75 0.2 60 30 2422.09 2254.38 2434.62 0.7	V) biuf in	3	ы	Щ	ш	Э	Ш	ш	Э	Э	Ш	ш	Ш	ш	≩	≩	ш	ы	≩	≱	<u>≽</u>	≩	≱	≱	≱	≽	
m _c T _k i T _c i Q _{water} Q _{cthornol} Q _{water-cthornol} (4g8) (***) (***) (***) (***) 0.1 50 30 1092.68 1124.71 11124.71 0.2 50 30 1565.58 1618.77 1618.77 0.4 50 30 2051.96 2127.25 2127.25 0.5 50 30 2199.69 2281.55 2281.55 0.1 60 30 2051.96 2127.25 2127.25 0.1 60 30 2199.69 2281.55 2281.55 0.1 60 30 2373.96 2430.31 2430.31 0.2 60 30 2373.96 2430.31 2434.62 0.3 3117.89 3193.15 3193.15 3193.15 0.4 60 30 2373.98 2254.38 2257.75 0.2 60 30 2422.09 2254.38 2434.62 0.7	rking f	2	ப	ш	<u> </u>	ш	ш	ш	ы	ш	щ	ш	ш	ш	≱	⋧	വ	ш	≱	≱	≱	≩	≱	≱	≱	≩	
mc T _{ii} T _c Qwarer Qestannol (kg/s) (°C) (°C) (°N) (N) 0.1 50 30 1092.68 1124.71 0.2 50 30 1565.58 1618.77 0.4 50 30 2051.96 2127.25 0.5 50 30 2199.69 22281.55 0.1 60 30 2173.96 22281.55 0.1 60 30 2173.96 22281.55 0.1 60 30 2173.96 22281.55 0.1 60 30 2173.96 22281.55 0.1 60 30 2373.96 22430.31 0.2 60 30 2242.09 22281.55 0.1 70 30 2242.09 2254.33 0.2 70 30 4194.00 4261.51 0.2 80 30 2834.98 2821.34 0.2 80 30	om		ш	Э	Э	Щ	Э	团	щ	ப	ш	ш	凹	Щ	≱	≱	ш	凹	≩	≱	≱	≱	≩	≩	<u>≽</u>	≩	
mc Th Tc Qwater (kg/s) (°C) (°C) (°A) 0.1 50 30 1092.68 0.2 50 30 1565.58 0.4 50 30 2199.69 0.1 50 30 2199.69 0.1 60 30 2373.96 0.2 60 30 2373.96 0.2 60 30 2373.96 0.2 60 30 3117.89 0.2 60 30 2373.96 0.1 70 30 2242.09 0.2 70 30 4194.00 0.2 70 30 4500.40 0.2 70 30 4500.40 0.1 80 30 5278.30 0.2 80 30 5278.30 0.2 80 30 5665.61 0.1 90 30 4921.18 0.2 90 <td>Qwater-ethanol</td> <td>(34)</td> <td>1124.71</td> <td>1618.77</td> <td>2127.25</td> <td>2281.55</td> <td>1688.86</td> <td>2430.31</td> <td>3193.15</td> <td>3424.62</td> <td>2257.75</td> <td>3243.75</td> <td>4261.51</td> <td>4570.31</td> <td>2834.98</td> <td>4091.76</td> <td>5332.48</td> <td>5718.83</td> <td>3408.64</td> <td>4921.18</td> <td>6488.91</td> <td>6967.02</td> <td>3984.33</td> <td>5753.88</td> <td>7589.09</td> <td>8149.01</td> <td></td>	Qwater-ethanol	(34)	1124.71	1618.77	2127.25	2281.55	1688.86	2430.31	3193.15	3424.62	2257.75	3243.75	4261.51	4570.31	2834.98	4091.76	5332.48	5718.83	3408.64	4921.18	6488.91	6967.02	3984.33	5753.88	7589.09	8149.01	
mc T _p T _c (kgb) (C) (C) 0.1 50 30 0.2 50 30 0.4 50 30 0.5 50 30 0.1 60 30 0.2 60 30 0.1 60 30 0.2 70 30 0.1 70 30 0.2 70 30 0.1 80 30 0.2 80 30 0.1 90 30 0.2 80 30 0.1 90 30 0.2 100 30 0.2 100 30 0.2 100 30 0.2 100 30 0.2 100 30	Qethanol	€	1124.71	1618.77	2127.25	2281.55	1688.86	2430.31	3193.15	3424.62	2254.38	3243.75	4261.51	4570.31	2821.34	4059.18	5332.48	5718.83	3389.71	4876.62	6406.13	6870.28	3959.52	5696.11	7482.52	8024.71	
0.1	Qwaler	<u>&</u>	1092.68	1565.58	2051.96	2199.69	1653.19	2373.96	3117.89	3344.35	2242.09	3188.98	4194.00	4500.40	2834.98	4091.76	5278.30	5665.61	3408.64	4921.18	6488.91	6967.02	3984,33	5753.88	7589.09	8149.01	
(Keg/s) 0.1 0.2 0.2 0.4 0.0 0.0 0.0 0.0 0.0 0.0 0.0	T_{cr}	(0,0)	30	30	30	30	30	30	30	30	30	30	30	30	30	30	30	30	30	30	30	30	30	30	30	30	
	T_{hi}	(00)	50	20	50	20	09	09	90	09	70	70	70	70	80	80	80	80	8	06	06	06	100	100	100	100	
0.3 0.3 0.3 0.3 0.3 0.3 0.3 0.3 0.3 0.3	m _c	(kg/s)	0.1	0.2	0.4	0.5	0.1	0.2	0.4	0.5	0.1	0.2	0.4	0.5	0.1	0.5	0.4	0.5	0.1	0.2	0.4	0.5	0.1	0.2	4.0	0.5	
	mh	(kg/s)	0.3	0.3	0.3	0.3	0.3	0.3	0.3	0.3	0.3	0.3	0.3	0.3	0.3	0.3	0.3	0.3	0.3	0.3	0.3	0.3	0.3	0.3	0.3	0.3	

6.2.3 Testing of Thermosyphon Heat Exchanger

In this part, the experiments have been conducted to find out the performance of the thermosyphon heat exchanger that uses various types of working fluids. The testing conditions of this part are shown in Table 6.6 The inlet and the outlet temperatures of the hot and the cold streams and also the mass flow rate of both sides have been measured in order to calculate the rate of heat transfer of the heat exchanger.

Table 6.6 Testing conditions of the thermosyphon air preheater.

Items	Conditions
Flow arrangement	Parallel and counter flow
2. Temperature of hot air	50-80 °C for low temperature
3. Temperature of cold air	Ambient temperature
4. Mass flow rate of air	0.1-0.28 kg/s
5. Thermosyphon arrangement	Staggered array
	$S_t = 0.053 \text{ m}, S_d = 0.053 \text{ m}, S_l = 0.046 \text{ m}$
6. Number of tube rows	7
7. Number of tubes in row	7
8. Diameter of thermosyphon (bare tube)	0.027 m
9. Type of fin	Circular fin
10. Size of fin	Fin height = 0.1 m and
	fin pitch = 10 fins/inch
11. Filling ratio of working fluid	50%
12. Material of pipe and fin	Stainless steel 304
13. Working fluids	٠
Pure working fluids	Water, ethanol
Binary working fluid	Water-ethanol at 1:1 by volume
2-kinds working fluids	Number of water rows = $2,3,4,5$
	(the rest rows are ethanol)

From the experiments it is found that the simulation program gives over prediction of heat transfer rate of the thermosyphon air preheater and the result is shown in Figure 6.4. Note that in the simulation program, the correlations of Brigg & Young [32] and Hewitt et al [30] have been used to calculate the outside heat transfer coefficient between air and heat pipes of the heat exchanger. The correlation of Brigg & Young and Hewitt et al are shown in Equations (6.1) and (5.7) respectively.

$$j = 0.134 Re^{-0.319} \left(\frac{f_s}{f_h}\right)^{0.2} \left(\frac{f_s}{f_t}\right)^{0.11}, \tag{6.1}$$

where

$$j = \frac{h_o}{\rho V_{max} C p} P r^{2/3},$$

$$Nu = 0.242 Re^{0.658} \left(\frac{f_s}{f_h}\right)^{0.297} \left(\frac{S_t}{S_I}\right)^{-0.091} Pr^{0.333} . \qquad (5.7)$$

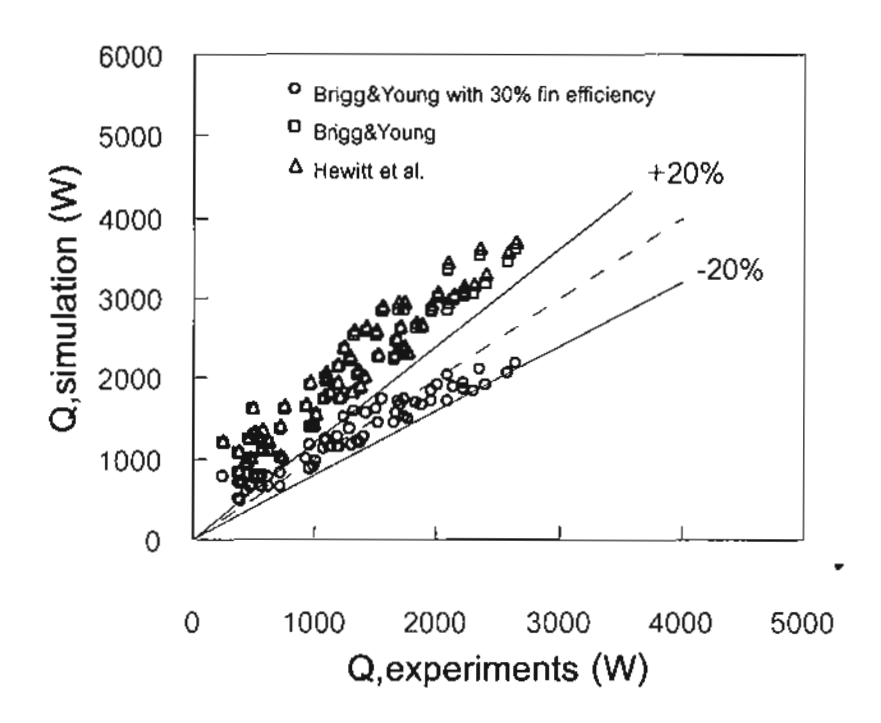


Figure 6.4 The comparison of heat transfer rate from the experimental results and simulations.

From Figure 6.4 it is found that the correlations of Brigg & Young and Hewitt et al give the same result and they over-predict the heat transfer compared with the experimental results. This phenomenon comes from;

- The shape of fin that is used in the correlations of Brigg and Young and Hewitt et al are agree well with circular fin. However, the fin used in this experiment is spiral fin thus the performance deviates from those predicted by the above correlations.
- 2. The attachment between the fin and the tube is not so good, therefore there is a contact resistance between the fin and the tube.

To over come this problem, the fin efficiency is reduced from normal value (~70-80%) to 30% and it was found that the correlation of Brigg & Young can predict the experimental results very well. However if the fin efficiency reduce to 30% it means that the total outside resistance of the heat exchanger is very high compared to the inside resistance due to boiling or condensation inside the tubes.

Figure 6.4 also shows the results of the simulation program when fin efficiency is reduced to 30% and using water and ethanol are used as working fluids. It is found that the heat transfer rate of each fluid is the same. So with this fin type, there is no difference between the working fluids from the experiment.

6.3 Selection of TEG Content in Thermosyphon Heat Exchanger

6.3.1 Simulation Program

This part is the case study of using TEG-water as a working fluid in the thermosyphon air preheater. Table 6.7 shows testing conditions and related geometrical parameters of the thermosyphon air preheater used in the simulation program. The concept of the program is to find out the suitable mixture content of TEG-water in each row of the air preheater. Note that the contents of TEG used in the binary mixture are 0, 25, 50, 75 and 100% by volume.

Figure 6.5 shows the flow chart of the calculation method. It can be divided into two parts, counter flow and parallel flow. The procedure in the counter flow

part, starts by inputting all of working conditions and also dimensions of the air preheater then assuming values of inlet and outlet temperatures of the hot and the cold streams and also heat transfer rate in each row. Next, set the working fluid of each row as water and using trial and error technique to find out the real value of the temperatures and the heat transfer rate of each row. After that check the critical heat flux of each row is checked and the suitable working fluid which gives the highest heat transfer rate is selected. The computational values are re-calculated until they are constant. The calculation continues until the last row of the heat exchanger.

For the parallel flow part, the procedure starts from row 1 by assuming the value of Q and using water as working fluid. Then, by using the trial and error technique, the real value of the outlet temperature of the hot and the cold air and also the heat transfer rate are obtained. Next the critical heat flux of this row is checked and the heat transfer rate is computed. Then the suitable mixture content is selected and the whole process is re-calculated again until every value is steady. The same method is used with every row.

Note that this chapter not only deals with the simulation program for finding the suitable mixture content of TEG in each row but also compare the performance with dowtherm A, a common working fluid for high operating temperature. ESDU [8,33] proposed the correlation for evaluating the boiling and the condensation heat transfer coefficients of the thermosyphon in form of thermal resistances as follow:

Thermal resistance due to pool boiling $(Z_{ei,p})$ in the evaporator section is

$$Z_{e',p} = \frac{1}{\phi_1 g^{0.25} Q^{0.4} (\pi D_i L_e)^{0.6}}, \tag{6.2}$$

where

$$\phi_1 = 0.32 \frac{\rho_I^{0.65} k_I^{0.3} C p_I^{0.7}}{\rho_V^{0.25} \lambda^{0.4} \mu_I^{0.1}} \left[\frac{P_V}{P_A} \right]^{0.23}.$$
 (6.3)

Thermal resistance due to falling film evaporation $(Z_{ei,f})$ in the evaporator section is

$$Z_{ei,f} = \frac{0.235Q^{1/3}}{D_i^{4/3}g^{1/3}L_e\phi_2^{4/3}},$$
(6.4)

$$\phi_2 = \left(\frac{\lambda k_i^3 \rho_i^2}{\mu_i}\right)^{1/4}.$$
 (6.5)

The total thermal resistance due to boiling in the evaporation (Z_{ei}) can be calculated as

$$Z_{el} = Z_{el,f}(1-F) + Z_{el,p}F,$$
 (6.6)

where F is filling ratio of the working fluid.

Thermal resistance in the condenser (Z_{ci}) is

$$Z_{o'} = \frac{0.235Q^{1/3}}{D_{l}^{4/3}g^{1/3}L_{c}\phi_{2}^{4/3}}.$$
 (6.7)

Table 6.7 Testing conditions and related geometrical parameters of the thermosyphon heat exchanger.

Items	Conditions
1. Flow arrangement	Parallel and counter flow
2. Temperature of hot air	300-400 °C
3. Temperature of cold air	30 °C
4. Mass flow rate of air	0.1-0.5 kg/s
5. Thermosyphon arrangement	Staggered array
	$S_t = 0.02 \text{ m}, S_d = 0.02 \text{ m}, S_l = 0.0173 \text{ m}$
6. Number of tube rows	6
7. Number of tubes in row	10
8. Diameter of thermosyphon (bare tube)	0.0095 m
9. Type of fin	Plain plate fin
10. Size of fin	fin pitch = 6 fins/inch
	fin thickness = 0.0005 m
11. Filling ratio of working fluid	50%
12. Material of pipe and fin	Copper for pipe and Aluminum for fin

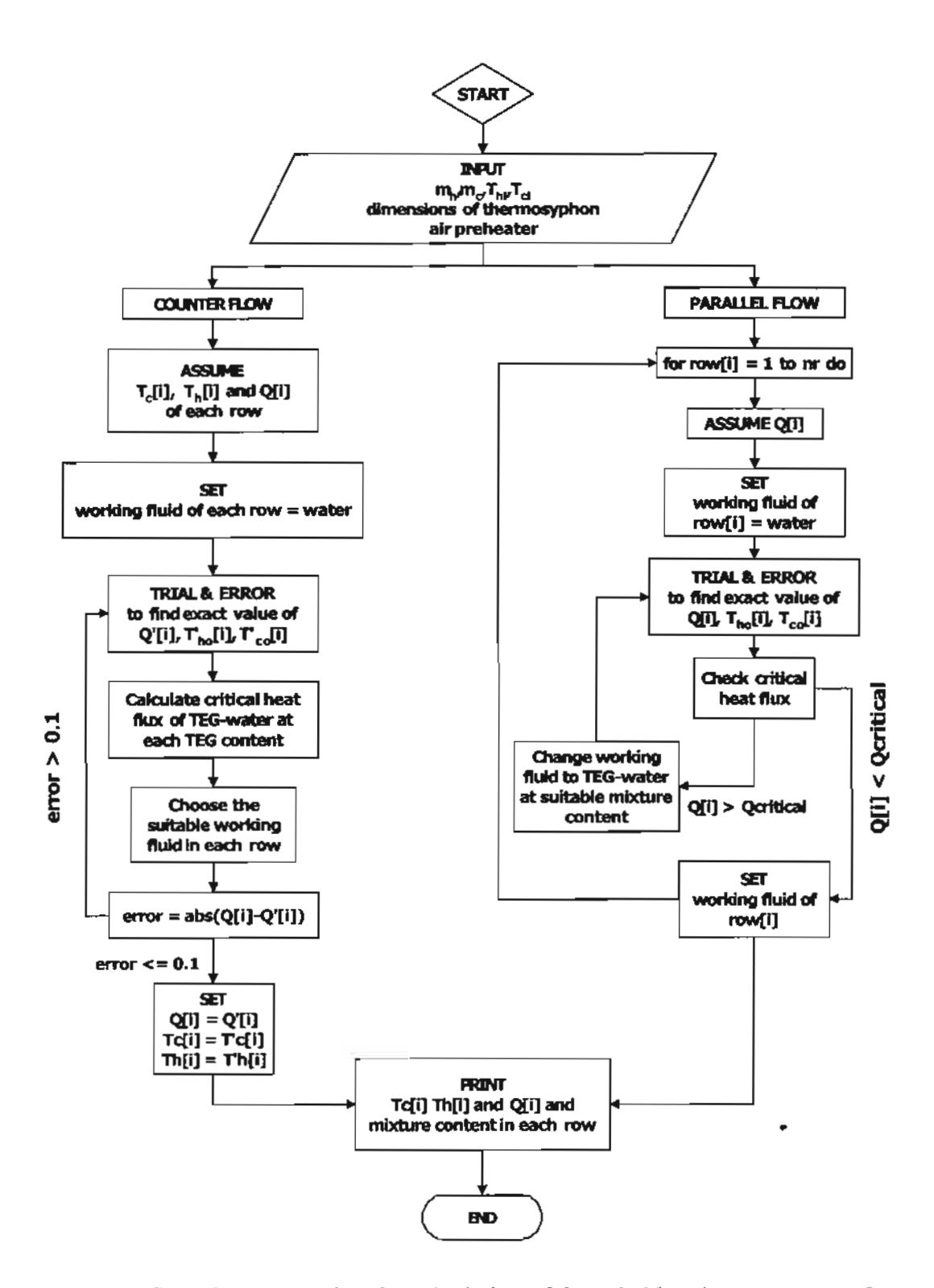


Figure 6.5 A flow chart presenting the calculation of the suitable mixture content of TEG-water in each row of the thermosyphon heat exchanger.

6.3.2 Results and discussion

Tables 6.8 and 6.9 show the results of the simulation program for the parallel flow and the counter flow respectively. It is found that the heat transfer rate increases significantly in some conditions compared with pure TEG with suitable mixture content in each row of the heat exchanger. Normally water cannot be used as a working fluid in this temperature range (300-400°C) because of its flooding limit. However, TEG-water can extend this limit and the performance increases approximately 30-80% for parallel flow and 60-115% for counter flow compared with pure TEG. When compared with a common working fluid, dowtherm A, it is also found that using TEG-water can also increases the heat transfer rate approximately 80-160% for parallel flow and 140-220% for counter flow configurations.

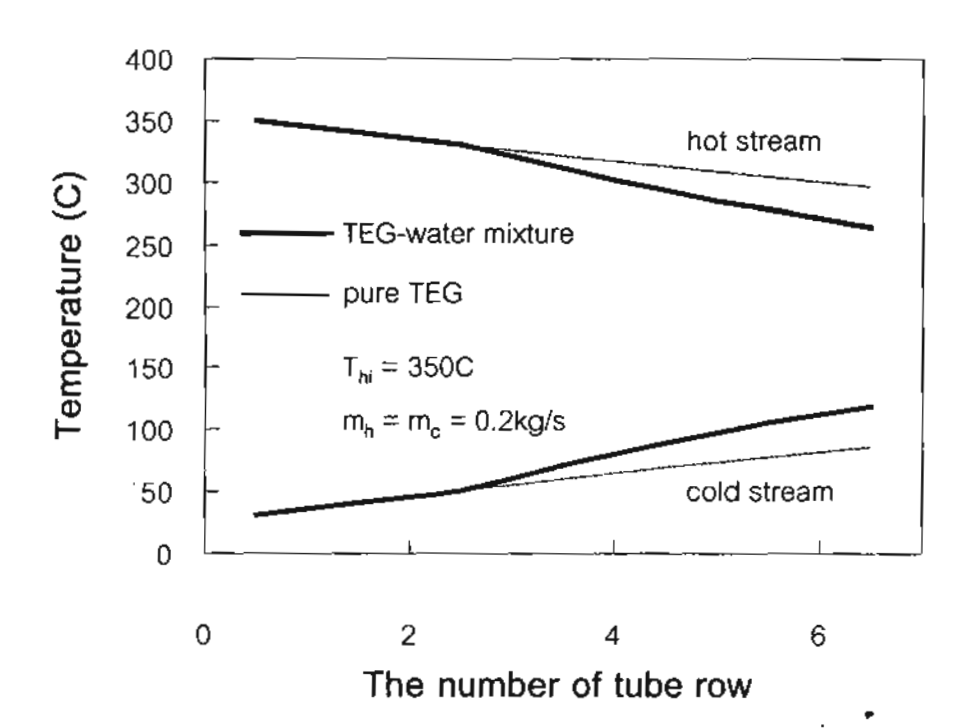


Figure 6.6 A comparison of temperature profile of parallel flow thermosyphon air preheater between using TEG-water mixtures and pure TEG (no. 7 in Table 6.8).

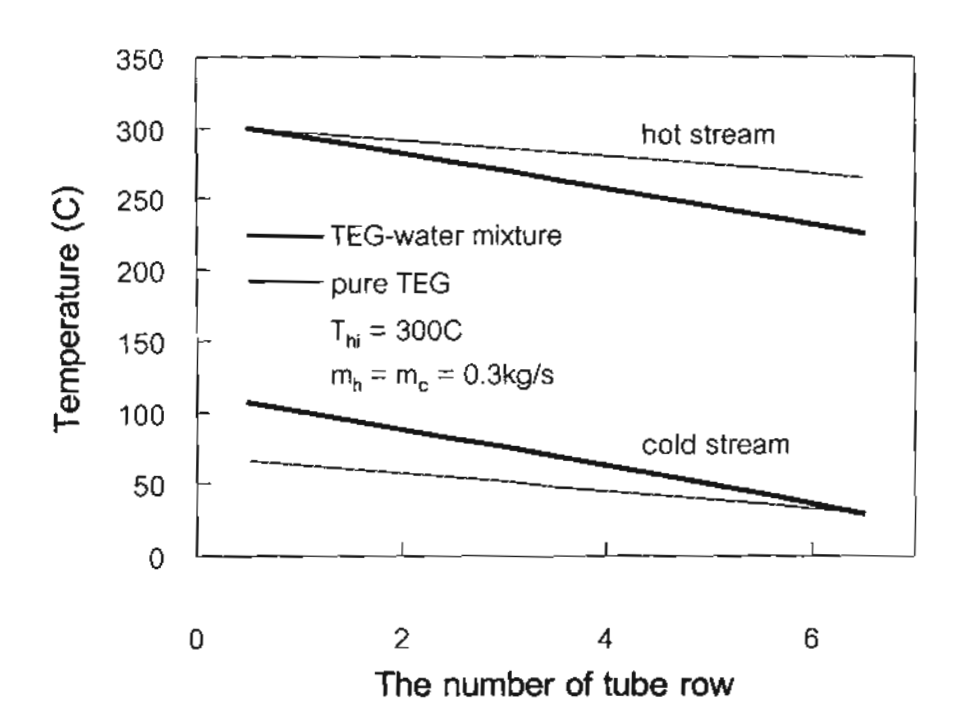


Figure 6.7 A comparison of temperature profile of balance counter flow thermosyphon air preheater between using TEG-water mixtures and pure TEG (no. 3 in Table 6.9).

In case of parallel flow, it is found that the content of TEG should be high in the first row and water is a good working fluid in the last rows. These results can be explained by Figure 6.6 which shows the temperature profiles of the parallel flow air preheater. Normally the temperature difference between the hot and the cold streams is large at the initial rows and narrow at the last rows. Consequently the heat transfer rate of the initial row is higher than that of the last row and it has a high opportunity to reach the critical limit. Therefore high content of TEG or pure TEG are the suitable working fluids in this range. However, water or lower content of TEG in the mixture is suitable for the last rows. Figure 6.6 also shows the comparison between TEG-water and pure TEG. This result comes from the simulation result shown in Table 6.8 (No.7). It is found that by using 75% and 25% of TEG in rows 3 and 4 and pure water in row 5 and 6, the

temperature difference between the hot and the cold air streams is considerably smaller significantly compared with pure TEG; therefore, higher heat exchange is obtained.

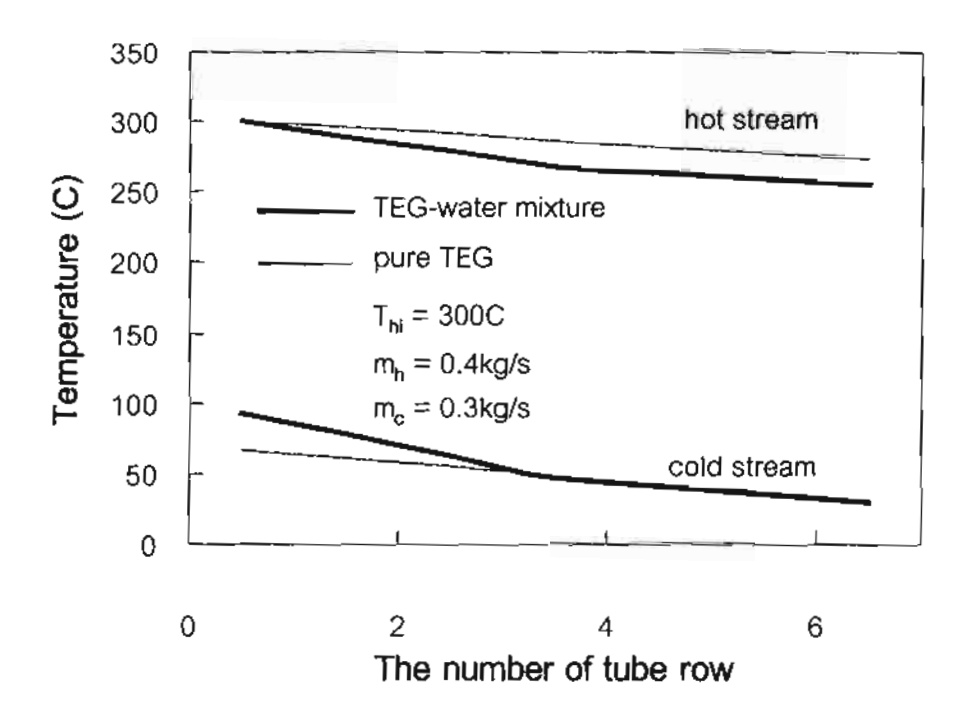


Figure 6.8 A comparison of temperature profile of unbalance counter flow thermosyphon air preheater between using TEG-water mixtures and pure TEG (no.18 in Table 6.9).

In case of counter flow, Table 6.9, it is found that in case of balanced counter flow $(\dot{m}_h = \dot{m}_c)$ the mixture content in each row is nearly the same. This phenomenon can be explained in Figure 6.7 which shows the comparison of temperature profiles of balanced counter flow between using TEG-water mixture and pure TEG. Actually in this case the temperature difference of the hot and the cold streams is nearly constant. Consequently the heat transfer rate of each row is nearly constant and this value is suitable for only single fluid thermosyphon. However, in case of unbalanced counter flow $(\dot{m}_h \neq \dot{m}_c)$, neither the temperature difference nor the heat transfer rate is constant, therefore, the content of the mixture in each row will affect the performance.

Figure 6.8 shows the results obtained from Table 6.9 (No.18). Use of TEG content of 75% in row 1-3 and 100% in rows 4-6 shows better heat exchange compared with pure TEG in all rows.

It could be seen that the system performance when using TEG-mixture is also higher than using only dowtherm A, which is a common working fluid of high temperature. From Tables 6.8 and 6.9, the performance increases about 80-160% for parallel flow and 140-220% for counter flow.

6.4 Conclusion

In this chapter, the concepts of using ethanol or water in some rows for low temperature application and TEG-water for high operating temperature in the thermosyphon heat pipe have been studied. Major results are summarized as follow:

- 6.4.1 Using ethanol or water in the appropriate rows of the thermosyphon can increase the heat transfer rate approximately 0-2% compared to using water or ethanol in all rows of thermosyphon.
- 6.4.2 The concept of two-kinds of working fluid (ethanol-water) is feasible in case of counter flow and unbalanced parallel flow, however, in case of balanced parallel flow it is not feasible because of uniform inside temperature of all rows of thermosyphon.
- 6.4.3 Using TEG-water can extend the critical limit due to flooding inside the thermosyphon and the limit is directly proportional to the content of TEG in the mixture.
- 6.4.4 Suitable mixture content of TEG-water in each row of the thermosyphon air preheater can increase the performance of the system approximately 30-80% for parallel flow and 60-115% for counter flow compared with pure TEG.
- 6.4.5 The heat exchanger with suitable content of TEG-water also shows better performance than that with dowtherm A.

Table 6.8 Results of simulation in the case of parallel flow arrangement; inlet temperature of cold air = 30°C.

Γ		$\overline{}$	_	_																						_			
% increase	Relative to	07 01	10.70	159.92	111.21	53.74	57.04	86'38	128.48	49.53	54.16	57.44	91.36	87.10	50.31	54.94	58.21	124.20	164.71	51.42	52.98	126.11	96.75	51.84	53.39	115.85	46.35	52.62	54.15
% inc	Relative to	75.00	45,00	83.16	41.68	00:00	0.00	46.49	60.52	0.00	0.00	0.00	47.34	30.74	0.00	0.00	0.00	64.15	82.41	00.0	0.00	65.10	35.16	00.0	0.00	56.83	00.0	00'0	0.00
	Edowitherm A (W)	5277	1766	9699	7263	7626	7871	6371	7846	8539	8952	9231	7340	8990	9758	10215	10521	6102	6917	7459	7586	7227	8151	8757	6688	8324	9338	9994	10146
,	§ §	7007	0334	9446	10827	11724	12361	8236	11168	12768	13801	14533	9533	12865	14668	15827	16646	8335	10038	11294	11605	8686	11866	13297	13650	11456	13666	15253	15640
	KTEG-water (W)	10055	CCOOL	17301	15340	11724	12361	12065	17926	12768	13801	14533	14046	16820	14668	15827	16646	13681	18311	11294	11605	16341	16038	13297	13650	1367	13666	15253	15640
	9	•	>	0	25	100	001	0	0	100	100	001	0	25	100	001	100	0	0	100	100	0	25	100	100	0	100	100	100
*	5	<	>	0	75	100	100	0	0	001	100	100	0	75	100	001	100	0	0	100	100	0	75	100	100	0	100	001	100
each ro	4		> -	0	100	001	100	0	25	100	100	100	0	100	001	100	100	0	0	100	100	0	100	001	100	0	100	100	100
% TEG in each row	3	<	>	0	100	100	001	0	75	100	<u>8</u>	100	0	100	100	100	100	0	25	100	100	0	100	100	100	52	100	100	100
6	2	•	> ;	25	100	100	100	0	100	001	100	8	0	100	100	100	100	0	75	100	001	0	9	100	8	75	901	100	100
	1		> 1	20	100	100	100	0	100	100	100	100	25	100	100	001	100	<u> </u>	100	100	100	20	100	100	100	100	100	100	100
£	(\$C)	300	300	300	300	300	300	350	320	350	350	350	400	400	400	400	400	300	300	300	300	350	350	320	350	400	400	400	400
;	(kg/s)	-	1.0	0.2	0.3	0.4	0.5	0.1	0.2	0.3	0.4	0.5	0.1	0.2	0.3	0.4	0.5	0.3	0.3	0.3	0.3	0.3	0.3	0.3	0.3	0.3	6.3	0.3	0.3
3	(kg/s)	-	5.	0.2	0.3	4.0	0.5	0.1	0.2	0.3	4.0	0.5	0.1	0.2	0.3	0.4	0.5	0.1	0.2	0,4	0.5	0.1	0.2	9.4	0.5	0.1	0.2	0.4	0.5
	ž	-	- 1	7	m	4	S	9	7	∞	6	10	=	12	13	14	15	16	17	18	61	20	21	22	23	24	25	56	27

Table 6.9 Results of simulation in the case of counter flow arrangement; inlet temperature of cold air = 30°C.

Γ	Γ				_	_		_				_		_	_		_	_					_		_				
% increase	Relative to	dowtherm A	82.66	176.24	220.70	54.09	57.29	102.76	167.03	50.03	54.50	57.68	106.36	166.20	50.81	55.27	58.45	133.11	192.47	154.16	92.46	135.00	187.72	52.27	53.74	136.89	47.00	53.03	54.49
% in	Relative to	TEG	52.86	93.49	114.37	00.0	0.00	54.75	86.47	0.00	00'0	00.0	56.77	84.92	0.00	00'0	0.00	69.59	100.63	67.38	25.51	70.50	96.76	00.0	00.0	71.02	00'0	0.00	0.00
(Zdowtherm A	(w)	5448	6684	7278	7635	7878	6452	7877	8555	8962	9237	7429	9023	9776	10225	10529	6133	6937	7470	7596	7262	8174	8770	8910	8362	9362	10008	10157
	25.50	(*)	7120	9543	10888	11765	12391	8453	11280	12836	13847	14566	8778	12989	14743	15877	16682	8430	10113	11344	11648	10009	11952	13354	13698	11582	13762	15314	15692
	CTEG-water (M)	(w)	10884	18465	23340	11765	12391	13081	21033	12836	13847	14566	15330	24019	14743	15877	16682	14296	20290	18987	14619	17065	23517	13354	13698	19808	13762	15314	15692
	,	9	0	0	20	100	100	0	25	001	100	100	0	75	100	100	100	0	0	100	100	0	22	100	100	0	100	100	100
A	4	r -	0	0	20	100	100	0	25	00	100	100	0	75	100	100	100	0	0	001	100	0	20	001	100	0	100	001	100
each ro	, <i>V</i>	t	0	0	20	100	100	0	25	100	100	001	0	75	100	901	100	0	0	100	100	0	20	100	001	0	100	100	100
% TEG in each row	,	S	0	0	20	100	100	0	25	100	100	00	0	75	001	100	001	0	25	75	100	0	50	100	100	0	100	100	100
8	۲	7	0	0	20	001	100	0	25	100	100	100	0	20	100	100	100	0	25	75	100	0	75	100	100	22	100	100	100
	_	-	0	0	20	001	100	0	25	100	100	100	0	20	100	100	100	0	25	75	75	. 25	75	100	100	20	100	100	90
 -	3 2		300	300	300	300	300	350	350	350	350	350	400	400	400	400	400	300	300	300	300	350	350	350	350	400	400	400	400
 	(ko/e)	(c/gu)	0.1	0.2	0.3	4.0	0.5	0.1	0.2	0.3	0.4	0.5	0.1	0.2	0.3	0.4	0.5	0.3	0.3	0.3	0.3	0.3	0.3	0.3	0.3	0.3	0.3	£.0	0.3
1	(ko/c)	(r (Gu)	0.1	0.2	0.3	4.0	0.5	0.1	0.2	0.3	4.0	0.5	0.1	0.2	0.3	0.4	0.5	0.1	0.2	0.4	0.5	0.1	0.2	0.4	0.5	0.1	0.2	0.4	0.5
	%		_	7	m	4	S	9	7	∞	σ.	01	=	12	13	4	12	16	11	8	61	70	21	77	23	24	25	26	27

CHAPTER 7

SECOND LAW ANALYSIS OF THERMOSYPHON HEAT EXCHANGER

7.1 Introduction

In this chapter the 2nd law of thermodynamic has been used as a parameter for evaluating the performance of the thermosyphon heat exchanger in both cases of low and high temperature applications. From the previous chapter, it is found that using ethanol or water in some rows gives higher heat transfer rate than using only pure water or ethanol in all rows. For high temperature or high heat flux application, it is found that flooding phenomenon may occur when using the water thermosyphon, however, using TEG-water mixture can extend this limit. The suitable content of TEG in the binary mixture should be determined first to get the higher heat flux of the thermosyphon in each row.

7.2 Theoretical Background

Figure 7.1 shows the heat exchanger. The second law efficiency of thermodynamic of this heat exchanger is defined as the ratio of flow availability of cold stream to hot stream which is

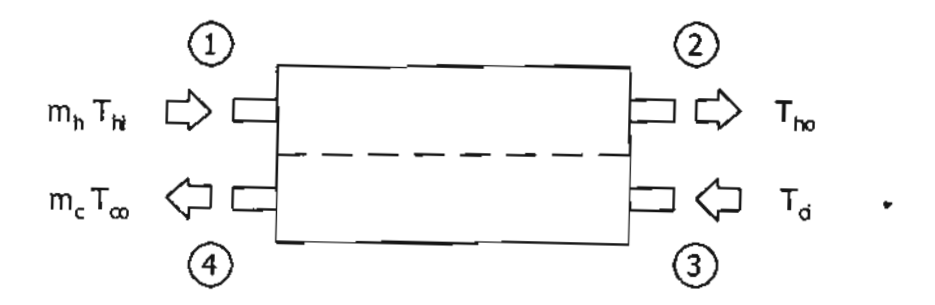


Figure 7.1 Counter flow heat exchanger.

$$\varepsilon = \frac{\dot{m}_c \left(a_{f4} - a_{f3} \right)}{\dot{m}_h \left(a_{f1} - a_{f2} \right)},\tag{7.1}$$

where

 $\varepsilon = 2^{nd}$ law efficiency

 a_f = flow availability (J/kg).

The flow availability in case of steady state and control volume can be calculated as

$$a_f = (h - h_o) - T_o(s - s_o) + 0.5V^2 + gZ$$
 (7.2)

where

h = enthalpy (J/kg)

s = entropy (J/kgK)

V = velocity (m/s)

Z = elevation (m)

 T_o = temperature at dead state (K)

Note that subscript "o" means the dead state and the temperature at this state in this research is set as 30°C. If the pressure drop in the heat exchanger, the velocity and the level of the inlet and the outlet stream are neglected, equation (7.2) can be written in form of

$$a_f = C_\rho \left(\left(T - T_o \right) - T_o \ln \left(T / T_o \right) \right). \tag{7.3}$$

Therefore equation (7.1) can be arranged as

$$\varepsilon = \frac{\dot{m}_{c}C_{pc}\left(\left(T_{co} - T_{cl}\right) - T_{o} \ln\left(\frac{T_{co}}{T_{cl}}\right)\right)}{\dot{m}_{h}C_{ph}\left(\left(T_{hl} - T_{ho}\right) - T_{o} \ln\left(\frac{T_{hl}}{T_{ho}}\right)\right)}.$$
(7.4)

7.3 Second Law Efficiency of Thermosyphon Heat Exchanger

7.3.1 Low operating temperature

Tables 7.1-7.4 show the calculated results of the 2nd law efficiency of the balanced counter and parallel flows and the unbalanced counter and parallel flows, respectively. All the data come from the simulation results in Chapter 6. It should be pointed out that using ethanol or water in some suitable rows (2-kinds) gives higher 2nd

law efficiency compared to that of pure water or ethanol (approximately 0-1.8%). However for balanced parallel flow, there is no improvement compared with that of single working fluid. Some of results from Tables 7.1-7.4 are shown in Figures 7.2-7.7. The inlet temperature of the hot air and the mass flow rate of air affect the 2nd law efficiency. It is found that the counter flow heat exchanger gives higher 2nd law efficiency than that of parallel flow. This result is not surprising because normally counter flow heat exchanger gives higher heat transfer rate than that of parallel flow, therefore, higher efficiency is obtained. It is also found that higher mass flow rate gives lower efficiency and higher inlet temperature of hot air gives higher efficiency. Figure 7.8 shows an effect of the mass flow rate on the performance of water thermosyphon in case of balanced counter flow. The gap of the temperature of the hot and the cold streams is reduced when the mass flow rate decreases. Therefore the quality of the cold stream outlet in case of lower mass flow rate is better than that of higher mass flow rate because the outlet temperature of the cold stream of the lower mass flow rate is higher.

The inlet temperature of hot air has an effect on the 2nd law efficiency of the heat exchanger. This result comes from the increase of heat transfer coefficient of boiling inside the thermosyphon. Higher inlet temperature of hot stream results in increasing in boiling heat transfer coefficient and more heat transfer performance is obtained. However, the inlet temperature of hot gas has a little effect compared to the effect of mass flow rate since the performance of the heat exchanger is controlled by the air-side thermal resistance.

Figure 7.9 is the example of the comparison of 2nd law efficiency of using all water, all ethanol and water or ethanol in some proper rows (2-kinds). It is found that using 2-kinds of working fluid give the highest efficiency compared to that of all water or all ethanol. However, only slight improvement is found because the boiling and condensation heat transfer coefficients of water and ethanol are nearly the same.

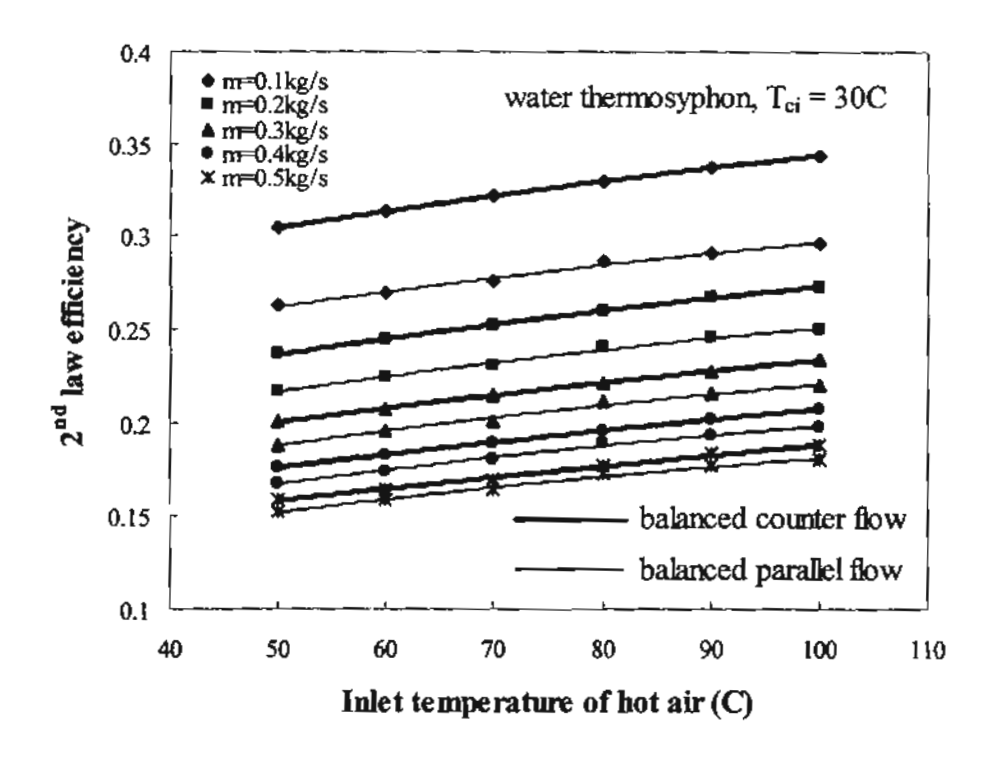


Figure 7.2 The effect of inlet temperature of hot air and mass flow rate on the 2nd law efficiency; water balanced counter & parallel flows.

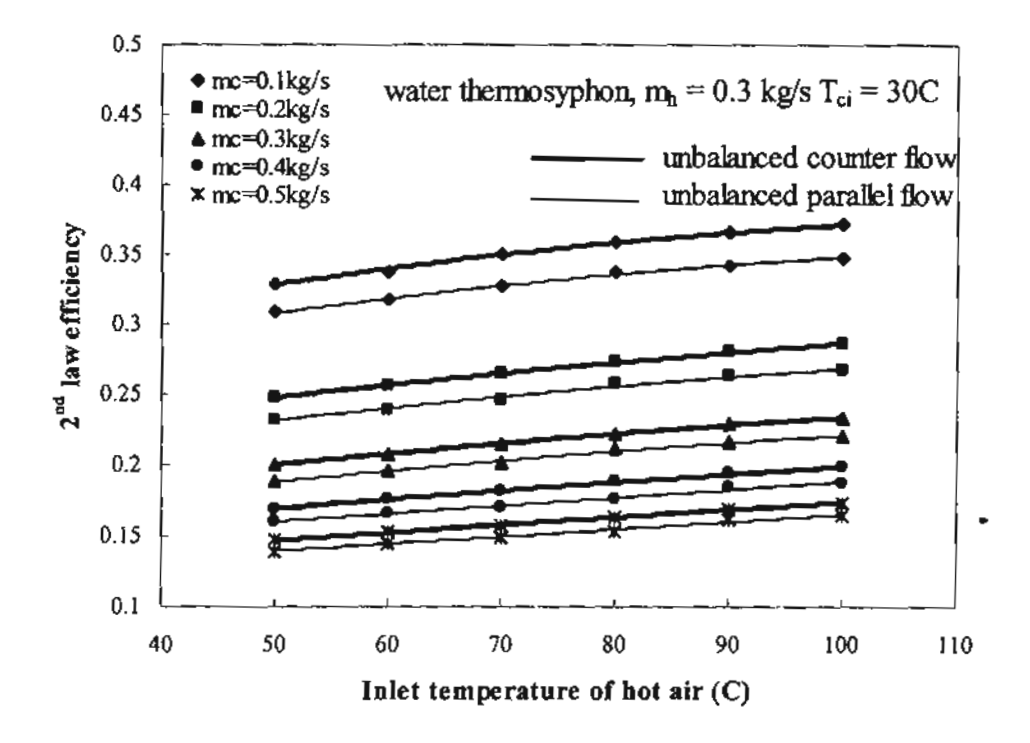


Figure 7.3 The effect of inlet temperature of hot air and mass flow rate on the 2nd law efficiency; water unbalanced counter & parallel flows.

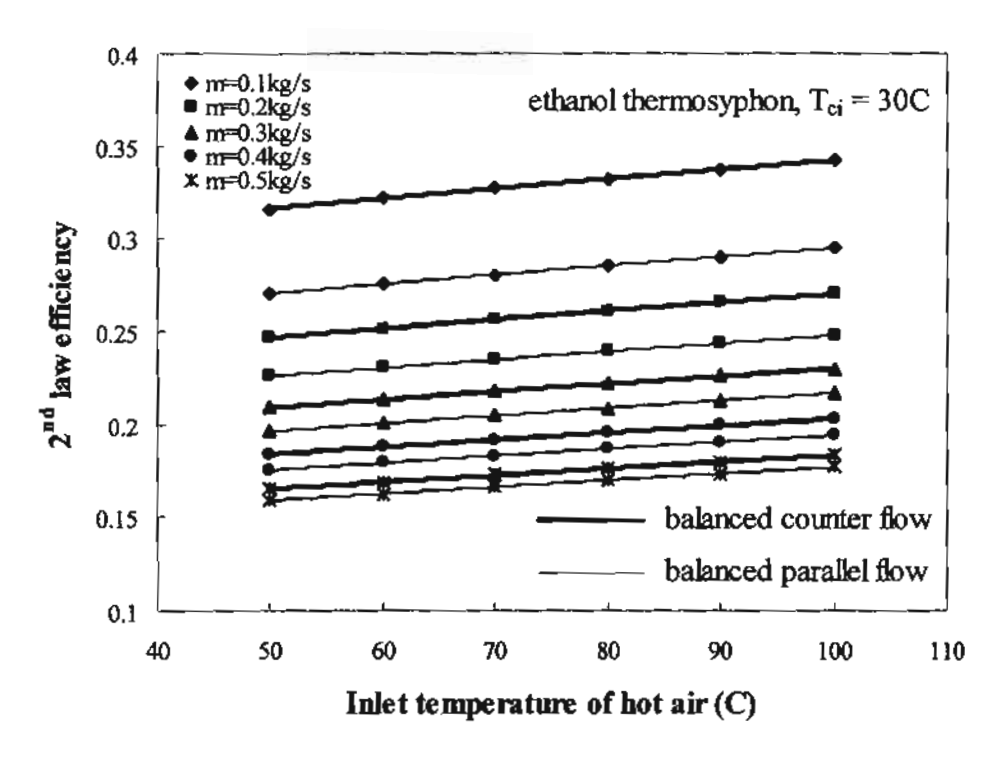


Figure 7.4 The effect of inlet temperature of hot air and mass flow rate on the 2nd law efficiency; ethanol balanced counter & parallel flows.

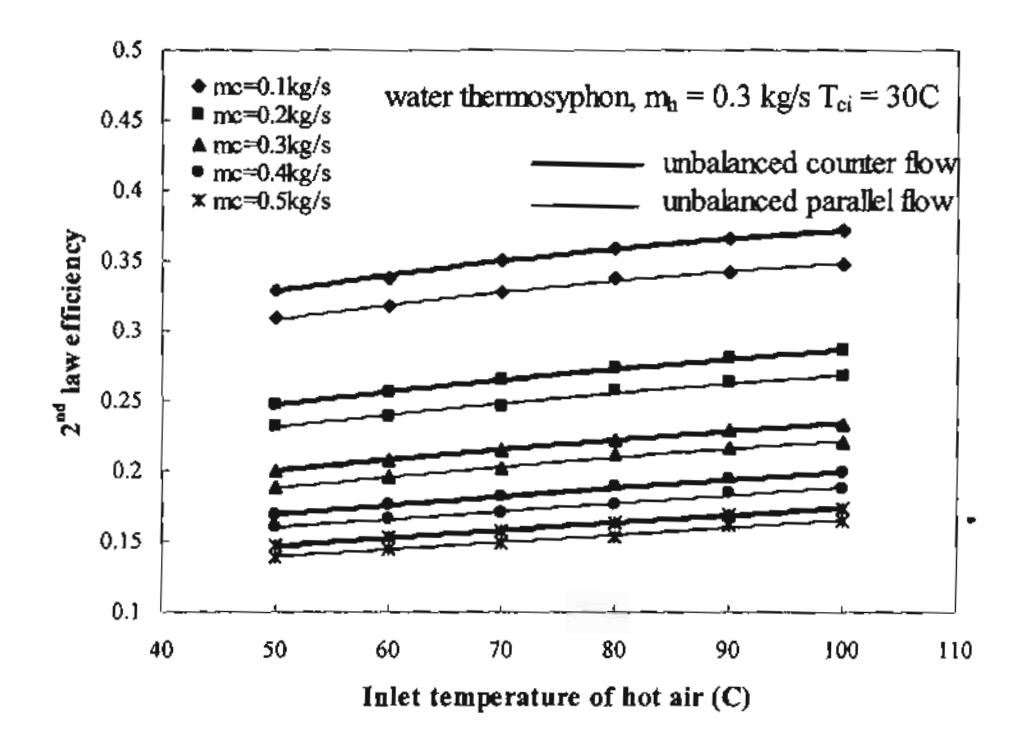


Figure 7.5 The effect of inlet temperature of hot air and mass flow rate on the 2nd law efficiency; ethanol unbalanced counter & parallel flows.

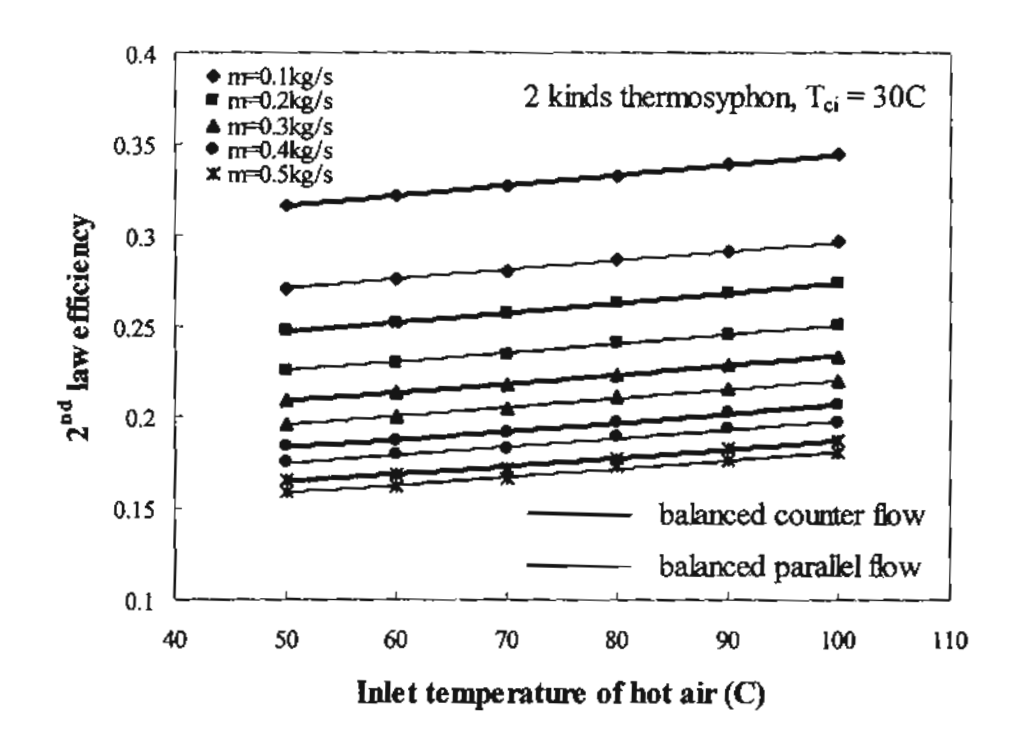


Figure 7.6 The effect of inlet temperature of hot air and mass flow rate on the 2nd law efficiency; 2-kinds and balanced counter & parallel flows.

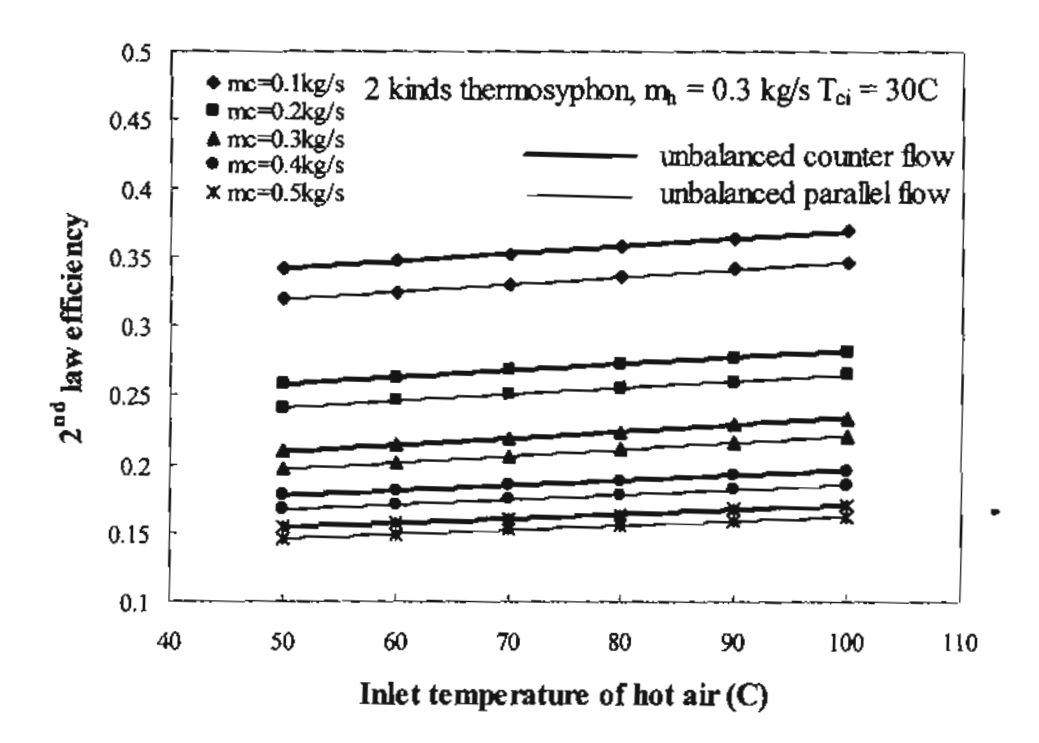


Figure 7.7 The effect of inlet temperature of hot air and mass flow rate on the 2nd law efficiency; 2-kinds and unbalanced counter & parallel flows.

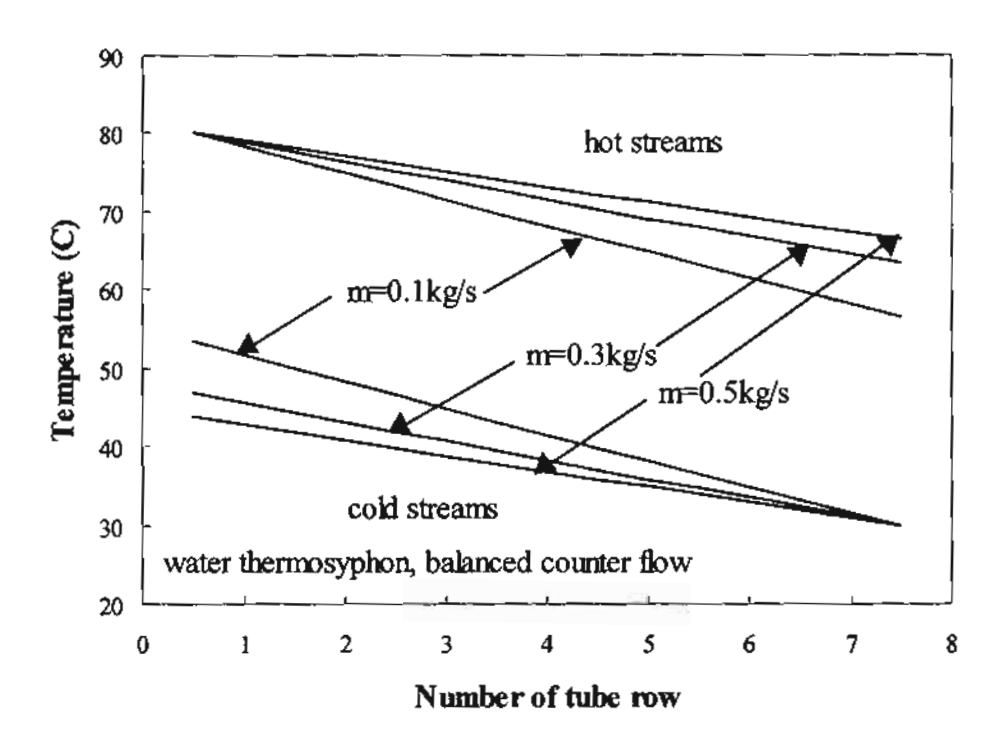


Figure 7.8 A temperature profile of water thermosyphon at various mass flow rate.

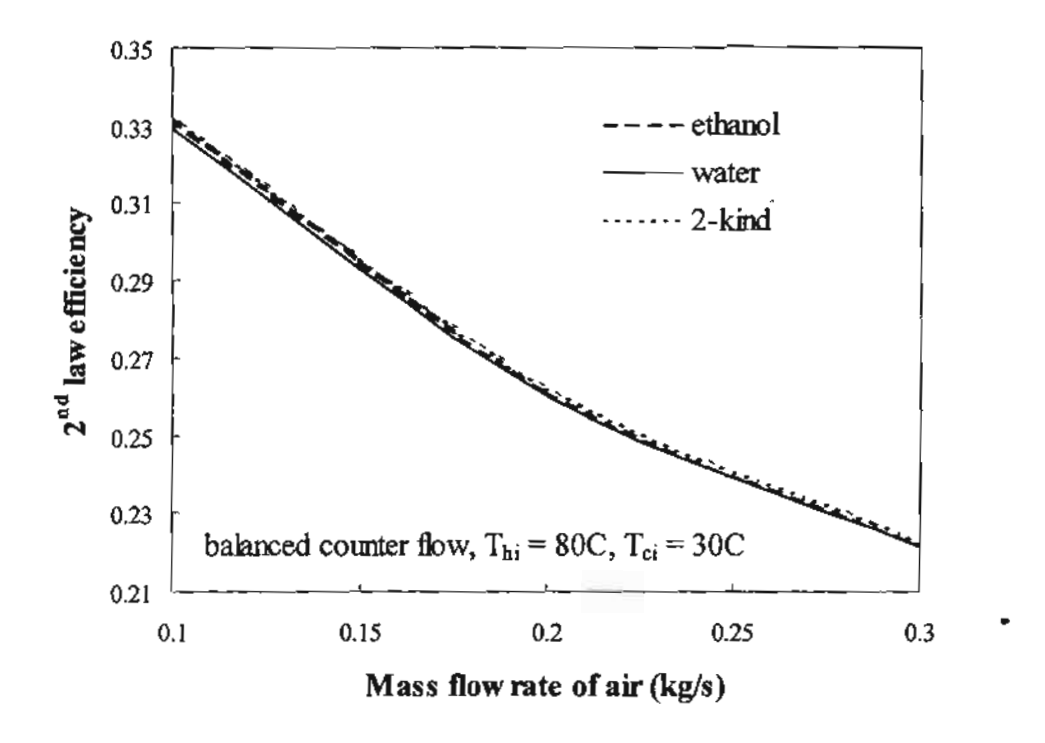


Figure 7.9 A comparison of 2nd law efficiency at various kinds of working fluids.

7.3.2 High Operating Temperature

Tables 7.5-7.6 show the 2nd law efficiency when using TEG-water, dowtherm A and TEG in case of parallel flow and counter flow heat exchangers respectively. It is found that with suitable mixture content of TEG-water mixture, the 2nd law efficiency increases drastically compared to pure TEG or dowtherm A (approximately 27-77% relative to TEG and 77-60% relative to dowtherm A for parallel flow and 70-106% relative to TEG and 140-204% relative to dowtherm A for counter flow).

Some of the results are shown in Figures 7.10-7.11 in case of balanced counter flow and balanced parallel flow, respectively. It is found that the 2nd law efficiency increases drastically when using binary working fluid in the thermosyphon because of its high heat transfer performance compared to those of TEG or dowtherm A. The effects of the mass flow rate and the inlet temperature of hot stream are also the same as the low operating temperature.

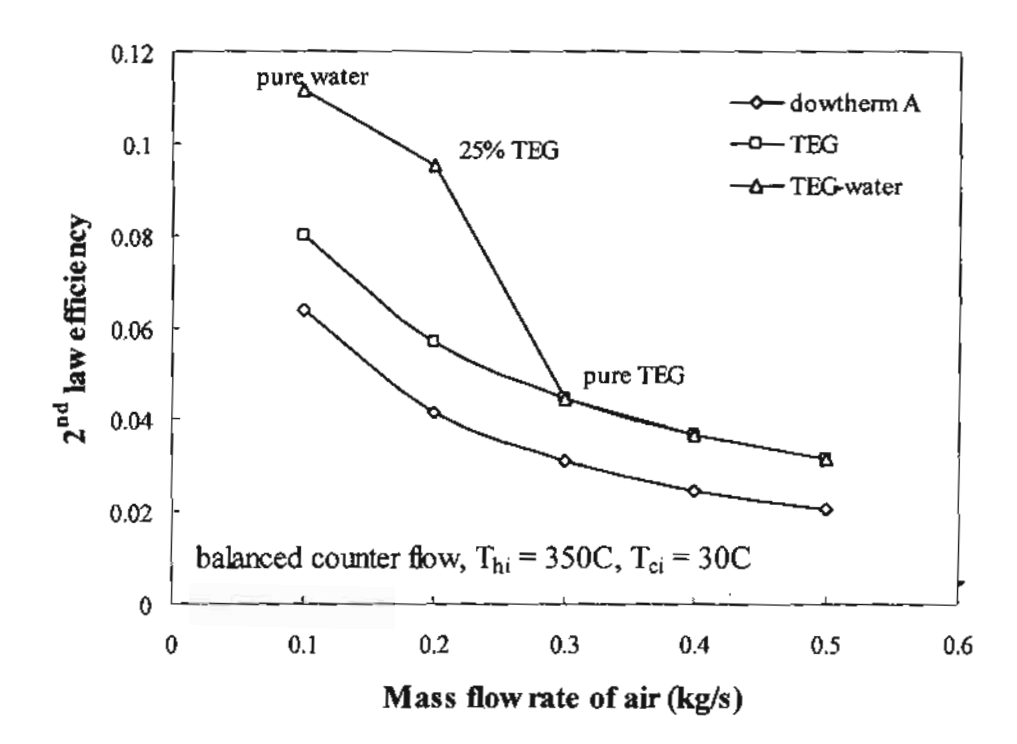


Figure 7.10 The 2nd law efficiency of various kind of working fluids of balanced counter flow heat exchanger operating at high temperature.

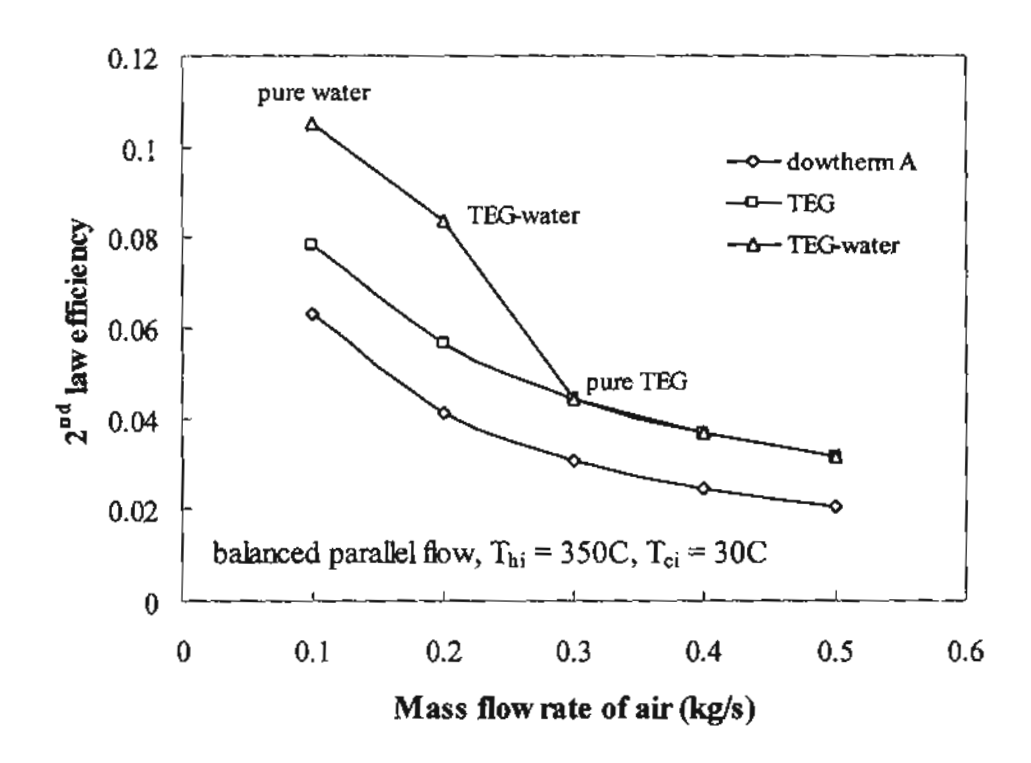


Figure 7.11 The 2nd law efficiency of various kind of working fluids of balanced parallel flow heat exchanger operating at high temperature.

Table 7.1 The 2nd law efficiency in the case of balanced counter flow arrangement for low temperature application.

	% increase relative to	ethanol	0.00	0.00	00'0	00.0	00:0	00.0	00:0	00.00	00.0	00.0	0.13	0.03	0.32	0.12	00.0	0.26	0.38	0.61	0.75	68.0	0.43	0.89	1.13	1.42	1.95	0.58	1.06	1.52	1.88	2.05
	% increase relative to	water	3.70	4.24	4.25	4.25	4.16	2.83	2.80	2.85	2.74	2.53	1.64	1.79	1.72	1.27	1.35	1.00	0.81	89.0	0.52	0.32	0.43	0.38	0.22	0.12	0.00	0.12	0.13	0.05	0.00	0.00
19	101)	7	Ē	щ	Ш	щ	щ	ш	Щ	ш	ப	ш	H	ш	ш	ш	ш	щ	ш	ш	Œλ	ы	Э	щ	Ħ	ľΩ	ш	ш	ш	щ	≱	3
= otheroll		9	Ε	щ	ы	ធា	ш	щ	Щ	Œ	ш	ш	Э	臼	ш	Ш	ш	П	Щ	ш	ធា	田	凶	щ	щ	Œ	ш	≱	≱	≩	≱	≱
= woter B		5	ы	ш	Э	щ	Э	ш	ш	Э	त्त	ជា	Э	Ш	Э	щ	ш	ш	ш	ш	山	田	×	≩	3	≱	×	3	≽	≱	⋧	€
$\langle W \rangle = v_{\rm so}$	row (4	മ	ш	ធា	ய	ш	ш	田	Э	ъ	μì	ш	ш	ш	ш	ப	ш	ш	បា	ъ	Э	≱	≥	≱	≱	≩	≱	⋧	*	≱	∌
	n each	ю	ய	ы	ш	ш	ம	ш	ഠ	ы	H	ш	ш	ш	ப	Ш	ш	≩	≩	≩	≱	≱	≱	≱	≱	≱	≱	≱	≱	*	≽	≱
Working fluid	1	2	ы	щ	ы	щ	Э	ш	щ	ப	Э	ш	≩	ш	Э	<u>ш</u>	ш	≱	≱	≩	≩	≱	≱	*	≱	≱	≱	≱	≱	≱	≱	≱
Š	\$	1	ធ	ш	ப	щ	ы	щ	ы	ш	ম	щ	≩	≱	≱	≱	Э	≱	≱	≱	≱	≱	≽	≱	3	≱	∌	≱	≱	≩	*	≱
30,	ng fluids	2 kinds	0.316	0.247	0.209	0.184	0.165	0.322	0.252	0.213	0.188	0.169	0.327	0.257	0.218	0.192	0.172	0.333	0.262	0.223	0.197	0.178	0.338	0.268	0.228	0.202	0.183	0.344	0.273	0.234	0.207	0.188
30 Isyn efficiency of	various kinds of working fluids	ethanol	0.316	0.247	0.209	0.184	0.165	0.322	0.252	0.213	0.188	0.169	0.327	0.257	0.217	0.191	0.172	0.332	0.261	0.222	0.195	0.176	0.337	0.266	0.226	0.199	0.180	0.342	0.270	0.230	0.203	0.183
l puc	various k	water	0.305	0.237	0.200	0.176	0.159	0.313	0.245	0.207	0.183	0.165	0.322	0.252	0.214	0,189	0.170	0.329	0.260	0.222	0.196	0.177	0.337	0.267	0.228	0.202	0.183	0.343	0.273	0.233	0.207	0.188
	I_{ct}	(°C)	30	30	30	30	30	30	30	30	30	30	30	30	30	30	30	30	30	30	30	30	30	30	30	30	30	30	30	30	30	30
	T_{hl}	(၃)	50	20	20	20	20	9	09	09	9	9	70	20	70	92	70	80	80	80	80	80	8	06	8	06	8	100	100	100	100	100
	m _c	(kg/s)	0.1	0.2	0.3	4.0	0.5	0.1	0.2	0.3	0.4	0.5	0.1	0.2	0.3	4.0	0.5	0.1	0.2	0.3	0.4	0.5	0.1	0.2	0.3	0.4	0.5	0.1	0.5	0.3	4.0	0.5
	mh	(kg/s)	0.1	0.2	0.3	4.0	0.5	0.1	0.2	0.3	0.4	0.5	0.1	0.2	0.3	4.0	0.5	0.1	0.2	0.3	0.4	0.5	0.1	0.2	0.3	0.4	0.5	0.1	0.2	0.3	9.4	0.5

Table 7.2 The 2nd law efficiency in the case of balanced parallel flow arrangement for low temperature application.

	% increase relative to	ethanol	00'0	0.00	0.00	0.00	0.00	0.00	0.00	00.0	00.00	00.0	00.0	00.0	00'0	0.00	00'0	0.38	0.67	1.14	1.48	1.76	0.30	9.76	1.34	1.67	2.01	0.33	86.0	1.40	1.80	2.17
, , 0	% increase relative to	water	3.05	4.08	4.19	4.35	4.23	2.29	2.70	2.73	2.70	2.46	1.84	1.93	1.92	1.69	1.49	0.00	0.00	0.00	0.00	0.00	0.00	0.00	0.00	0.00	0.00	0.00	0.00	0.00	0.00	0.00
Clos	ì	7	Э	щ	ш	щ	ш	Э	மு	ப	ш	ш	Э	ш	ш	ы	ш	¥	≱	≱	≱	≱	≩	≱	≱	≥	≱	*	∌	≯	≩	≩
= ethanol)	_	9	ы	щ	Э	ш	щ	ы	<u>(11</u>	ы	ш	ப	щ	щ	ш	ц	ш	≱	≱	≱	≩	≱	≱	≱	≱	≱	≱	∌	≱	≱	≱	≱
ļį.	힐	8	ъ	ш	ы	ш	Œ	Э	ш	ш	ы	田	Э	田	ш	ப	山	≱	≱	≱	∌	≱	≩	≱	≱	≱	≱	⋧	8	≽	≱	≩
V = water	row (4	ъ	퍼	ш	щ	ল	Œ	យ	ш	ធា	П.	<u> </u>	щ	ш	ш	Щ	≱	≩	≱	≱	≩	≱	≱	≩	≱	≱	≩	≩	≩	≱	≽
working fluid (W	in each	3	Э	Э	Œ	ഥ	ΙΞÌ	ম	ъ	ш	ы	т)	Э	ш	ш	ш	Э	≱	≱	≱	⋧	≱	≩	≩	≱	≱	≽	≱	⋧	≩	≱	≥
rking f	1 I	2	ш	щ	ப	ш	ш	മ	щ	ш	ப	Щ	Э	щ	ы	щ	Э	≱	≱	≱	≽	≽	≩	≱	3	≩	≱	≱	≱	≩	≱	≱
8	2	1	3	щ	ப	ш	ш	ы	ш	Э	ш	凹	Ħ	П	ш	Щ	ш	≱	≱	≱	≥	≱	≱	≱	≱	≩	∌	≱	≱	≱	≽	≱
Jo A	ng fluids	2 kinds	0.270	0.226	0.196	0.175	0.159	0.276	0.230	0.200	0.179	0.163	0.280	0.235	0.205	0.183	0.166	0.286	0.241	0.211	0.189	0.173	0.291	0.245	0.216	0.194	0.177	0.296	0.250	0.220	0.198	0.181
2nd law efficiency of	various kinds of working fluids	ethanol	0.270	0.226	0.196	0.175	0.159	0.276	0.230	0.200	0.179	0.163	0.280	0.235	0.205	0.183	0.166	0.285	0.239	0.209	0.187	0.170	0.290	0.244	0.213	0.190	0.173	0.295	0.248	0.217	0.194	0.177
2nd	various k	water	0.262	0.217	0.188	0.168	0.153	0.270	0.224	0.195	0.174	0.159	0.275	0.230	0.201	0.180	0.164	0.286	0.241	0.211	0.189	0.173	0.291	0.245	0.216	0.194	0.177	0.296	0.250	0.220	0.198	0.181
	T_{ci}	(2)	30	30	30	30	30	30	30	30	30	30	30	30	30	30	30	30	30	30	30	30	30	30	30	30	30	30	30	30	30	30
	7,	() ()	20	20	20	20	20	9	09	09	9	8	70	2	70	20	70	08	08	08	08	80	8	06	8	90	8	100	001	001	100	0 0 0
-	JE .	(kg/s)	0.1	0.5	0.3	0.4	0.5	0.1	0.2	0.3	0.4	0.5	0.1	0.2	0.3	0.4	0.5	0.1	0.7	0.3	0.4	0.5	0.1	0.5	0.3	0.4	0.5	0.1	0.2	0.3	0.4	0.5
	ш	(kg/s)	0.1	0.2	0.3	0.4	0.5	0.1	0.2	0.3	0.4	0.5	0.1	0.2	0.3	4.0	0.5	0.1	0.2	0.3	0.4	0.5	0.1	0.2	0.3	0.4	0.5	0.1	0.2	0.3	0.4	0.5

Table 7.3 The 2nd law efficiency in the case of unbalanced counter flow arrangement for low temperature application.

_					_		_				_																_
	relative to	ethanol	0.00	0.00	0.00	00'0	0.00	0.00	0.00	00.00	0.35	0.31	0.00	0.00	0.52	0.62	99.0	0.65	0.65	1.05	1.22	1.18	0.70	1.12	1.67	1.88	
0, 10	relative to	water	3.55	3.91	4.48	4.95	2.49	2.87	2.75	2.71	99.0	1.34	1.82	1.61	0.17	0.56	99.0	0.82	0.00	0.05	0.21	0.39	0.00	0.00	0.07	60.0	
(0	ì	7	ш	ш	Щ	Œ	ū	Щ	Ξ	ш	ш	m	ш	ഥ	ш	Щ	ы	Щ	≱	щ	ш	ш	≯	≱	Э	凶	
working fluid (W = water E = ethanol)		9	Œ	Щ	Щ	ш	щ	П	Œ	ш	Ξ	П	Ш	ធា	≱	ш	ш	ш	≱	≥	ш	ш	≥	3	≽	*	
F	n each row (2 kinds	2	ய	Э	ш	П	Щ	凹	田	Ξ	山	ш	ш	ш	≱	Э	щ	山	≱	≱	¥	ш	≱	` ≱	≱	≱	
A	row (2	4	ш	Ш	Щ	ш	Щ	ចា	Э	Ξ	*	Ш	山	ш	≱	≱	П	山	≩	≱	≩	≩	≩	≱	≱	≱	
luid (V	n each	m	Ю	凶	Э	ш	ш	щ	ш	ш	≱	田	凶	щ	≱	×	*	Ш	≱	≽	×	≱	≩	×	≱	≱	
king f	.=	7	щ	щ	ш	ш	ш	Œ	ш	ы	≱	≱	Щ	Ξ	≱	∌	≱	≽	≱	≱	≥	≥	≥	≽	≱	≩	
NO.		_	ïП	ω	щ	ш	Щ	щ	ш	щ	₹	¥	ш	щ	≱	≱	*	≽	*	≱	*	×	≩	×	≱	≱	
, of	ng fluids	2 kinds	0.341	0.257	0.177	0.154	0.346	0.262	0.180	0.157	0.353	0.268	0.184	0.160	0.359	0.274	0.189	0.164	0.365	0.280	0.194	0.169	0.371	0.285	0.199	0.173	
2nd law efficiency of	various kinds of working fluids	ethanol	0.341	0.257	0.177	0.154	0.346	0.262	0.180	0.157	0.352	0.267	0.184	0.160	0.357	0.272	0.188	0.163	0.363	0.277	0.192	0.167	0.368	0.282	0.195	0.170	
1 puc	various ki	water	0.329	0.248	0.169	0.147	0.338	0.255	0.176	0.153	0.351	0.265	0.181	0.157	0.359	0.272	0.188	0.163	0.365	0.280	0.194	0.168	0.371	0.285	0.199	0.173	
	$T_{c'}$	<u>ق</u>	8	30	30	30	30	30	30	30	30	30	30	30	30	30	30	30	30	30	30	30	30	30	30	30	
	T_{hi}	(ĵ	50	20	20	20	09	9	09	9	70	70	70	70	80	80	80	80	90	8	06	8	8	100	100	100	
	mc	(kg/s)	0.1	0.2	4.0	0.5	0.1	0.2	0.4	0.5	0.1	0.2	0.4	0.5	0.1	0.2	0.4	0.5	0.1	0.2	0.4	0.5	0.1	0.2	4.0	0.5	
	m	(kg/s)	0.3	0.3	0.3	0.3	0.3	0.3	0.3	0.3	0.3	0.3	0.3	0.3	0.3	0.3	0.3	0.3	0.3	0.3	0.3	0,3	0.3	0.3	0.3	0.3	

Table 7.4 The 2nd law efficiency in the case of unbalanced parallel flow arrangement for low temperature application.

0/ 120000	relative to	ethanol	00'0	0.00	0.00	00.0	0.00	0.00	00.0	0.00	0.14	00.0	0.00	00.0	0.51	0.95	0.00	00.0	0.52	1.02	1.57	1.63	99.0	1.12	1.60	1.76	
0,000	relative to	water	3.34	3.67	4.09	4.41	2.37	2.73	2.67	2.95	0.71	2.01	1.96	1.89	0.00	0.00	1.12	1.17	0.00	0.00	0.00	0.00	0.00	0.00	00'0	0.00	
(log	,	7	Э	ш	ш	Э	ш	ш	ш	Œ	≱	ш	ш	凶	≱	≩	ш	щ	3	≱	≱	≱	A	≽	≩	≩	_
= ethanol)	(9	9	ш	口	ы	Ш	田	ш	Э	Ø	≩	Ш	ш	ਸ਼	≩	∌	ш	ঘ	¥	≱	≩	≩	≱	*	×	8	
working fluid (W = water. E =	each row (2 kinds	\$	ធា	ш	ш	ш	Щ	ш	Э	Э	≩	田	Э	ш	≩	≱	四	凹	≩	≱	≱	≩	*	≱	3	≱	_
\\\\\\\\\\\\\\\\\\\\\\\\\\\\\\\\\\\\\\	row (4	ਯ	Щ	ш	Ē	ш	щ	Щ	ш	m	ш	ш	Ιī	≱	≱	Э	Э	≱	≱	≩	≱	≱	≱	≱	≱	
fluid (in each	Э	ш	ш	ĬΞĴ	Ю	ш	щ	山	ш	ш	ш	m	M	≱	≱	ъ	ш	≱	≱	≱	≱	≱	*	≱	≩	
rking	0	7	ங	ш	ш	Ħ	ш	щ	m	ш	ш	ъ	臼	Ш	3	≱	ш	ш	≱	≱	}	≱	≱	≱	≱	≱	_
*		-	ш	ïП	щ	ы	ш	ш	山	ы	Э	ш	Œ	ш	≱	≩	Œ	凹	≱	≱	≱	≱	≱	≩	≩	≱	
Jo A	ing fluids	2 kinds	0.318	0.240	0.167	0.145	0.324	0.246	0.170	0.149	0.330	0.250	0.174	0.152	0.337	0.257	0.178	0.155	0.342	0.262	0.184	0.161	0.348	0.267	0.188	0.164	
2nd law efficiency of	various kinds of working fluids	ethanol	0.318	0.240	0.167	0.145	0.324	0.246	0.170	0.149	0.329	0.250	0.174	0.152	0.335	0.255	0.178	0.155	0.340	0.260	0.181	0.158	0.346	0.264	0.185	0.162	
2 nd	various k	water	0.308	0.232	0.160	0.139	0.316	0.239	0.166	0.145	0.327	0.245	0.171	0.149	0.337	0.257	0.176	0.153	0.342	0.262	0.184	0.161	0.348	0.267	0.188	0.164	
	T_{ci}	(,C)	30	30	30	30	30	30	30	30	30	30	30	30	30	30	30	30	30	30	30	30	30	30	30	30	_
	T_{hi}	ပ္မ	20	20	50	20	9	09	09	09	92	70	20	20	80	80	80	08	8	90	8	96	001	001	100	001	
_	m _c	(kg/s)	0.1	0.5	0.4	0.5	0.1	0.2	0.4	0.5	0.1	0.2	0.4	0.5	0.1	0.2	0.4	0.5	0.1	0.7	0 .4	0.5	0.1	0.2	4.0	0.5	
	т,	(kg/s)	0.3	0.3	0.3	0.3	0.3	0.3	0.3	0.3	0.3	0.3	0.3	0.3	0.3	0.3	0.3	0.3	0.3	0.3	0.3	0.3	0.3	0.3	0.3	0.3	

Table 7.5 The 2nd law efficiency in case of parallel flow arrangement; inlet temperature of cold air = 30°C.

% increase	Relative to dowtherm A	80.67	147.94	105.17	51.77	55.39	79.16	115.38	46.66	51.48	55.03	77.35	77.28	46.60	51.43	55.14	134.23	160.62	48.69	49.91	132.03	92.17	48.32	49.43	116.89	43.72	48.28	49.29
% inc	Relative to TEG	42.00	77.32	39.51	0.00	0.00	41.48	54.59	0.00	0.00	0.00	40.39	27.37	0.00	00.0	0.00	69.92	80.72	0.00	0.00	68.74	33.59	0.00	0.00	57.84	0.00	0.00	0.00
cy of king fluids	TEG-water	0.329	0.286	0.174	0.102	980.0	0.350	0.268	0.134	0.110	0.093	0.370	0.235	0.144	0.118	0.100	0.174	0.213	0.129	0.131	0.187	0.170	0.138	0.141	0.188	0.136	0.148	0.151
2 nd law efficiency of various kinds of working fluids	dowtherm A	0.182	0.115	0.085	0.067	0.056	0.196	0.124	0.091	0.073	090.0	0.208	0.133	860.0	0.078	0.065	0.074	0.082	980.0	0.088	0.081	0.088	0.093	0.094	0.087	0.095	0.100	0.101
varic	TEG	0.232	0.161	0.125	0.102	980.0	0.248	0.173	0.134	0.110	0.093	0.263	0.185	0.144	0.118	0.100	0.103	0.118	0.129	0.131	0.111	0.127	0.138	0.141	0.119	0.136	0.148	0.151
	9	0	0	25	100	001	0	0	100	100	100	0	25	100	001	100	0	0	001	100	0	25	100	001	0	100	100	100
wo.	5	0	0	7.5	100	9	0	0	001	100	100	0	75	100	100	100	0	0	100	100	0	75	100	100	0	100	00 100	100
each r	4	0	0	100	100	100	0	25	100	100	100	0	100	100	001	100	0	0	100	100	0	001	100	100	0	100	100	100
% TEG in each row	rs.	0	0	100	100	001	0	75	100	100	100	0	100	100	001	100	0	25	100	100	0	100	100	100	25	100	100	100
%	2	0	25	100	100	20	0	100	100	100	100	0	100	100	100	001	0	75	100	100	0	100	001	100	75	001	100	100
	1	0	20	100	100	100	0	100	100	100	100	25	001	100	100	100	0	001	100	100	20	100	100	100	001	100	100	100
T_{hi}	(°C)	300	300	300	300	300	350	350	320	350	350	400	400	400	400	400	300	300	300	300	320	350	350	350	400	400	400	400
m _c	(kg/s)	0.1	0.5	0.3	0.4	0.5	0.1	0.2	0.3	4.0	0.5	0.1	0.2	0.3	0.4	0.5	0.3	0.3	0.3	0.3	0.3	0.3	0.3	0.3	0.3	0.3	0.3	0.3
mh	(kg/s)	0.1	0.2	0.3	0.4	0.5	0.1	0.2	0.3	0.4	0.5	0.1	0.2	0.3	0.4	0.5	0.1	0.7	0.4	0.5	0.1	0.2	0.4	0.5	0.1	0.2	0.4	0.5
2	25	_	2	m	4	'n	9	7	00	6	10	=	12	13		15	91	17	18	61	20	21	22	23	24	25	76	27

Table 7.6 The 2nd law efficiency in the case of counter flow arrangement; inlet temperature of cold air = 30°C.

	Relative to dowtherm A	2.32	162.60	04.60	52.11	5.46	0.55	148.12	17.08	1.87	55.30	39.26	41.91	17.07	16.18	55.23	44.89	87.76	41.65	\$5.92	41.92	76.71	18.60	19.71	39.14	4.33	18.54	19.62
% іпстеаѕе	Rel dow	5	_	2	4 ,	4 1		_	_	4,	<u> </u>		_	_		41	_		_	_	_		_	_		_		
, i %	Relative to TEG	49.29	86.73	106.40	00:0	0.00	48.67	77.12	0.00	0.00	0.00	48.09	72.89	00.0	0.00	0.00	76.48	98.72	62.04	23.71	74.95	91.63	0.00	0.00	73.02	0.00	0.00	0.00
y of ing fluids	TEG-water	0.355	0.304	0.259	0.102	0.087	0.377	0.309	0.135	0.110	0.094	0.399	0.323	0.144	0.118	0.100	0.183	0.236	0.209	0.163	0.196	0.245	0.139	0.142	0.208	0.137	0.149	0.151
2 nd law efficiency of various kinds of working fluids	dowtherm A	0.185	0.116	0.085	0.067	0.056	0.198	0.125	0.092	0.073	090:0	0.211	0.133	860.0	0.078	0.065	0.075	0.082	0.087	0.088	0.081	0.089	0.093	0.095	0.087	0.095	0.100	0.101
vario	TEG	0.238	0.163	0.125	0.102	0.087	0.254	0.175	0.135	0.110	0.094	0.269	0.187	0.144	0.118	0.100	0.104	0.119	0.129	0.132	0.112	0.128	0.139	0.142	0.120	0.137	0.149	0.151
	9	0	0	20	100	100	0	25	100	100	100	0	75	100	100	100	0	0	100	100	0	25	100	100	0	100	100	100
*	5	0	0	20	100	100	0	25	001	100	001	0	75	100	100	100	0	0	100	001	0	20	100	100	0	001	100	001
% TEG in each row	4	0	0	20	100	001	0	25	001	100	100	0	75	100	100	100	0	0	100	100	0	20	001	100	0	001	100	100
TEG in		0	0	20	100	100	0	25	100	100	100	0	75	100	100	100	0	25	75	100	0	20	100	100	0	100	100	001
%	2	0	0	20	100	901	0	25	001	100	100	0	20	100	100	100	0	25	75	100	0	75	100	100	25	100	100	001
		0	0	20	100	001	0	25	100	001	100	0	20	100	100	100	0	25	75	75	25	75	100	100	20	100	001	100
T_{h_t}	(၃)	300	300	300	300	300	350	350	320	350	350	400	400	400	400	400	300	300	300	300	320	350	350	350	400	400	400	400
m _c	(kg/s)	0.1	0.2	0.3	4.0	0.5	0.1	0.2	0.3	4.0	0.5	0.1	0.2	0.3	0.4	0.5	0.3	0.3	0.3	0.3	0.3	0.3	0.3	0.3	0.3	0.3	0.3	 0,3
m,	(kg/s)	0.1	0.2	0.3	0.4	0.5	0.1	0.2	0.3	0,4	0.5	0.1	0.2	0.3	4.0	0.5	0.1	0.2	0.4	0.5	0.1	0.7	0.4	0.5	0.1	0.2	4.0	0.5
- 7	2	1	7	m	4	2	9	7	00	6	0	1	12	13	4	15	91	17	81	- 19	20	21	22	73	24	25	56	27

CHAPTER 8

CONCLUSION

8.1 Summary of the Research Work

Performance of the air-to-air thermosyphon heat exchanger using binary working fluid has been investigated in this research work. It can be divided into two parts, the heat transfer behavior of the thermosyphon heat pipe using binary working fluids and the performance of the thermosyphon heat exchanger using various kinds of working fluids. The main results of each part could be summarized as follows;

8.1.1 Thermal Behavior of the Thermosyphon Heat Pipe Using Binary Mixtures

Thermal performance of thermosyphon heat pipe using ethanol-water and TEG-water are presented. The affecting parameters such as the mixture content, the pipe aspect ratio and the working temperature have been studied in this part. From the experiments, it is found that at low temperature of heat source ethanol-water mixture has higher heat transfer rate than that of water. However, it is lower than that of pure ethanol. In case of TEG-water mixture, the heat transfer rate of the thermosyphon varies with the content of TEG in the mixture and it is found that, TEG in the mixture can increase the critical heat flux due to the flooding limit of the small size of the thermosyphon.

The boiling equation of Rohsenow and the condensation equation of Nusselt are modified to predict the heat transfer coefficients of the boiling and the condensation inside the thermosyphon. In case of the binary mixtures, it is found that the weighted average of the heat transfer coefficient of each component can be used to predict the total heat transfer coefficient. Furthermore, it is found that ESDU's equation

can be used to predict the critical heat flux due to the flooding limit of the thermosyphon with pure working fluids and binary mixtures.

8.1.2 <u>Performance Analysis of Thermosyphon Heat Exchanger Using</u> <u>Various Kinds of Working Fluids</u>

In this part, the concept of introducing two-fluid thermosyphons is examined. Calculations are performed for both low and high temperature ranges with parallel and counter flow arrangements.

For lower temperature application, (T_{hi} < 100°C), use of ethanol or water in the suitable row of thermosyphon can slightly improve the associated heat transfer performance for counter flow arrangement. However, for balanced parallel flow arrangement, the concept of using two-fluid thermosyphons may not feasible. But in case of unbalanced parallel flow this concept still feasible. The use of two-fluid thermosyphons is especially advantageous for high temperature application.

For thermosyphon air preheater at high temperature applications, it is found that with selected mixture content of TEG-water in each row of the thermosyphon the performance of the system could be increased approximately 30-80% compared with pure TEG for parallel flow and 60-115% for counter flow configurations. The performances also increase approximately 80-160% for parallel flow and 140-220% for counter flow compared with those of pure dowtherm A which is the common working fluid at high temperature applications.

8.2 Recommendation

The performance improvement of the thermosyphon heat exchanger by change the type of working fluid by consider the heat load at each row of thermosyphon tube in case of low operating temperature can slightly improves the performance. Since the heat transfer rate of the heat exchanger is controlled by the air-side thermal resistance. Therefore, in this case, the outside heat transfer coefficient should be improved to get higher performance of the system.

In case of high operating temperature of the thermosyphon heat exchanger, the application of TEG-water mixture should be applied to recover heat from the waste heat of the boiler or furnace having high exhaust temperature and enormous heat transfer rate is obtained compared to using dowtherm A or pure water.

The application of TEG-water mixture should be investigated in case of electronic cooling heat pipe. Since, this kind of heat pipe has very high heat flux (because of its very small diameter).

REFERENCES

- 1. Chi, S.W., 1976, Heat Pipe Theory and Practice, Washington, Hemisphere, 242p.
- Faghri, A., 1995, Heat Pipe Science and Technology, Philadelphia, Taylor & Francis, 874p.
- Peterson, G.P., 1994, An Introduction to Heat Pipes Modeling, Testing and Applications, New York, John Wiley & Sons, 356p.
- Peterson, P.F., Hijikata, K. and Tien, C.L., 1990, "Variable-Conductance Behavior in Two-Phase Binary Thermosyphons," Journal of Thermophysics, Vol. 4, No. 3, pp. 325-331.
- Wei, Q. and Yuan, L., 1999, "Heat Transfer Characteristics of a Closed Two-Phase Thermosiphon Working with a Binary Mixture at Different Incline Angles," Proceeding of the 11th International Heat Pipe Conference, Tokyo, Japan, pp. 110-115.
- Fox, R., Nagasaki, T., Hijikata, K. and Peterson, P.F., 1993, "Reflux Condensation of Binary Mixtures in a Two-Phase Thermosyphon," HTD-Vol. 242: Phase Change Heat Transfer, ASME, pp. 65-73.
- 7. Korner, M., 1977, Heat Atlas, Association of German Engineers, 3rd ed.
- Engineering Sciences Data Unit Item Number 81038, 1983, Heat Pipes-Performance of Two-Phase Closed Thermosyphons, London.
- Shiraishi, M., Kikuchi, K. and Yamanishi, T., 1982, "Investigation of Heat
 Transfer Characteristics of a Two-Phase Closed Thermosyphon", Advances in
 Heat Pipe Technology: The 4th International Heat Pipe Conference, London,
 Pergamon Press, pp. 95-104.
- 10. Hahne, E. and Gross, U., 1982, "The Influence of the Inclination Angle on the Performance of a Closed Two-Phase Thermosyphon", Advances in Heat Pipe Technology: The 4th International Heat Pipe Conference, London, Pergamon Press, pp. 125-136.

- Rohsenow, W.M., 1952, "A Method of Correlating Heat Transfer Data for Surface Boiling of Liquids", Transaction of ASME, Vol. 74, pp. 969-975.
- Nusselt, W., 1916, "Die Oberflachenkondensation des Wasserdampfes,"
 Zeitschr. Ver. Deutsch. Ing., Vol. 60, pp. 541-569.
- Tanthapanichakoon, W., 1986, Design of Heat Pipe Heat Exchanger (in Thai),
 Chulalongkorn University, 21p.
- 14. Bezrodnyi, M.K. and Alekseenko, D.B., 1977, "Investigation of the Critical Region of Heat and Mass Transfer in Low-Temperature Wickless Heat Pipes," High Temperature, Vol. 15, pp. 399-405.
- 15. Shiraishi, M., Yoneya, M. and Yabe, A., 1984, "Visual Study of Operating Limit in the Tow-Phase Closed Thermosyphon," Proceeding of the 5th Int. Heat Pipe Conference, Grenoble, France, pp. 10-17.
- Nuntaphan, A., 1998, Thermal Behavior Analysis of Thermosyphon Heat Pipe
 Using Binary Working Fluids, Special Study Report, King Mongkut's University
 of Technology Thonburi, 66p.
- Yaws, C.L., 1996, Handbook of Thermodynamic Diagrams, Vol. 2, Houston, Gulf Publishing, pp. 240-378.
- Perry, R.H. and Chilton, C.H., 1973, Chemical Engineer's Handbook, 5th Edition, New York, McGraw Hill.
- Reid, R.C., Pransnitz, J.M. and Poling, B.E., 1986, The Properties of Gases&Liquids, 4th ed., New York, McGraw Hill, 741p.
- 20. Kohl, A.L. and Riesenfeld, C.F., 1979, Gas Purification, 3rd ed., Houston, Gulf Publishing, pp. 595-629.
- Jamieson, D.T., Irving J.B. and Tudhope, J.S., 1973, Liquid Thermal Conductivity a Data Survey to 1973, Edinburgh, National Engineering Laboratory, p. 140.
- Kuong, J.F., 1965, Applied Nomography, Vol. 1, Houston, Gulf Publishing, pp. 114-115.

- Wadowski, T., Akbarzadeh, A. and Johnson, P., 1991, "Characteristics of a Gravity Assisted Heat Pipe Based Heat Exchanger," Heat Recovery Systems&CHP., Vol. 11, No. 1, pp. 69-77.
- 24. Terdtoon, P., Chaitep, S., Soponpis, N. and Groll, M., 1996, "Thermosyphon Economiser for Package Boiler: A Case Study of Northern Thailand,"
 Proceeding of the 5th International Heat Pipe Symposium, Melbourne,
 Australia, pp. 267-272.
- Dube, V., Sauciuc, I., Akbarzadeh, A. and Devis, A., 1996, "Design Construction and Testing of a Thermosyphon Heat Exchanger for Medium Temperature Heat Recovery," Proceeding of the 5th International Heat Pipe Symposium, Melbourne, Australia, pp. 273-279.
- 26. Hsing, S.S. and Huang, D.C., 1990, "Comparison of Thermal Performance and Pressure Drop of Counter Flow and Parellel Flow Heat Pipe Heat Exchangers with Aligned/Staggered Tube Rows," Energy Conversion and Management, Vol. 30, No. 4, pp. 357-368.
- Wuttijumnong, V., 1999, A Design and Construction of Heat Pipe Air Pre-heater for Package Boiler, Master of Engineering Thesis, Chiang Mai University, 197p.
- 28. ANSI/ASHRAE 41.2-1987, 1987, Standard Methods for Laboratory Air-Flow Measurement, American Society of Heating Refrigerating and Air-Conditioning Engineers Inc.
- Incropera, F.P. and DeWitt, D.P., 1990, Fundamentals of Heat and Mass Transfer, 3rd ed., Singapore, John Wiley & Sons, 919p.
- Hewitt, G.F., Shires, G.L. and Bott, T.R., 1994, Process Heat Transfer, Boca Raton, CRC Press, 1042p.
- Schmidt, Th. E., 1949, Heat Transfer Calculations for Extended Surfaces,
 Refrigerating Engineering, pp. 351-357.
- Webb, R.L., 1993, Principles of Enhanced Heat Transfer, New York, John Wiley
 & Sons, 556p.

33. Engineering Science Data Unit No.80017, 1980, Thermophysical Properties of Heat Pipe Working Fluids: Operating Range Between -60°C and 300°C, ESDU Int. Plc., London, UK.

APPENDIX A SIMULATION PROGRAMS

A.1 Simulation Program for Selecting the Suitable Working Fluids for Low Operating Temperature Thermosyphon Heat Exchanger

1. Method for Using Program

The simulation program is developed by using Turbo Pascal for Windows version 1.5. This program is used to calculate the suitable working fluids between ethanol and water in each row of the thermosyphon heat exchanger operating at low temperature heat source (especially lower than 100°C). When the program is run the display will show the primary data as follow;

PROGRAM HEAT PIPE 001

This program is used for calculating performance of the thermosyphon heat exchanger operating at low temperature with 2-kinds of working fluids (water-ethanol)

Developed by Atipoang Nuntaphan, Ph.D. student Thermal Technology Division, School of Energy and Materials, King Mongkut's University of Technology Thonburi

Then, the program will ask the input parameter as follow;

Please enter informations below

- 1. Heat exchanger informations
 - 1.1 Input number of rows
 - 1.2 Input number of column
 - 1.3 Input outside diameter of tube (m)
 - 1.4 Input inside diameter of tube (m)
 - 1.5 Input evaporator length (m)

- 1.6 Input condenser length (m)
- 1.7 Input type of fin
 - 1. bare tube 2, circular finned 3, plain plate finned
- 1.8 Input fin thickness (m) (input 0 for bare tube)
- 1.9 Input fin gap (m) (input 0 for bare tube)
- 1.10 Input fin height (m) (input 0 for bare tube)
- 1.11 Input number of fins (fin/inch) (input 0 for bare tube)
- 1.12 Input pipe arrangement
 - 1. aligned 2. staggered
- 1.13 Input transverse pitch (St) (m)
- 1.14 Input longitudinal pitch (Sl) (m)
- 1.15 Input directional pitch (Sd) (m) (input 0 for aligned)
- 1.16 Input cross section area of duct (m^2)

2. Working conditions

- 2.1 Input inlet temperature of hot gas (C)
- 2.2 Input inlet temperature of cold gas (C)
- 2.3 Input mass flow rate of hot gas (kg/s)
- 2.4 Input mass flow rate of cold gas (kg/s)
- 2.5 Input flow pattern
 - 1. parallel flow 2. counter flow

Then the simulation program will calculate the suitable working fluids between water and ethanol in each row of the thermosyphon and also calculate the heat transfer and the inlet and the outlet temperatures of the hot and the cold air streams in each row of the thermosyphon heat exchanger.

2. Detail of the Program

```
Program
               Heat Pipe 001; {heat transfer rate at low operating temperature}
Uses
               Wincrt:
Var
               Thi, Tci, Qtotal: real;
               mh,mc,Le,Lc,fs,fh,ft,St,Sd,Sl,od,fn,id,Qw,Qe: real;
               Q : array[1..100] of real;
              Th : array[1..100] of real;
              Tc : array[1..100] of real;
              Imtd, Thow, Tcow, Thoe, Tcoe: real;
               fintype,arrangement,flowpattern,cross section area: real;
              a,nr,nc,i,j,k: integer;
              wc: array[1..100] of real;
Function den_air(T:real):real; {calculate density of air}
  Begin
      den air := 0.000005*sqr(T+273.15)-0.0063*(T+273.15)+2.6043;
Function vis_air(T:real):real; {calculate viscosity of air}
  Begin
      vis air := (-0.0003*sqr(T+273.15)+0.6361*(T+273.15)+17.349)/10000000;
 End:
Function Cp air(T:real):real; {calculate Cp of air}
 Begin
      Cp air := (0.0000004*sqr(T+273.15)-0.0002*(T+273.15)+1.0324)*1000;
Function k air(T:real):real; {calculate thermal conductivity of air}
 Begin
      k air := (-0.00003*sqr(T+273.15)+0.0955*(T+273.15)+0.24)/1000;
 End:
Function Pw(T:real):real; {vapor pressure of water}
 Var Pc, Tc, b1, b2, b3, b4, Tr: real;
 Begin
      Pc := 22.093*1000000;
                                    Tc := 647.25;
      b1 := -7.78747;
                                    b2 := 1.50255;
      b3 := -2.81152;
                                    b4 := -1.22268;
      Tr := (T+273.15)/Tc;
      Pw := \exp(\ln(Pc) + (1/Tr) + (b1 + (1-Tr) + b2 + \exp((3/2) + \ln(1-Tr)))
            +b3*exp(3*ln(1-Tr))+b4*exp(6*ln(1-Tr)));
 End:
Function Dwl(T:real):real; {density of liquid water}
 Var dc, Tc, b1, b2, b3, b4, Tr: real;
 Begin
```

```
Tc := 647.25;
     dc := 315.5:
     b1 := 2.24670:
                            b2 := -2.09405:
     b3 := 2.73700;
                            b4 := -1.74750;
     Tr := (T+273.15)/Tc;
     Dwl := dc*exp(b1*exp((1/3)*ln(1-Tr))+b2*exp((2/3)*ln(1-Tr))
             +b3*(1-Tr)+b4*exp((4/3)*ln(1-Tr)));
 End:
Function Dwg(T:real):real; {density of vapor water}
 Var dc, Tc, b1, b2, b3, b4, Tr: real;
 Begin
                            Tc := 647.25:
     dc := 315.5;
                            b2 := -6.06253;
     b1 := -1.38200;
                            b4 := -6.68477;
     b3 := 5.91090;
     Tr := (T+273.15)/Tc;
     Dwg := dc*exp(b1*exp((1/3)*ln(1/Tr-1))+b2*exp((2/3)*ln(1/Tr-1))
             +b3*(1/Tr-1)+b4*exp((4/3)*ln(1/Tr-1)));
 End;
Function Lw(T:real):real; {latent heat of water}
 Var Tc,b1,b2,b3,b4,Tr: real;
 Begin
     Tc := 647.25;
     b1 := 1.7035*100000;
                                   b2 := 1.12332*100000000;
     b3 := -1.47041*100000000;
                                   b4 := 6.35750*1000000;
     Tr := (T+273.15)/Tc;
     Lw := b1*exp((1/3)*ln(1-Tr))+b2*exp((2/3)*ln(1-Tr))
           +b3*(1-Tr)+b4*exp((4/3)*ln(1-Tr));
Function Cpw(T:real):real; {density of liquid water}
 Var Tc,b1,b2,b3,b4,Tr: real;
 Begin
     Tc := 647.25;
     b1 := -1.4995*10000;
                                  b2 := 8.8*0.01:
     b3 := -6.82*0.1;
                                  b4 := -7.05*0.1;
     Tr := (T+273.15)/Tc;
     Cpw := b1*(1+b2*exp((-2/3)*ln(1-Tr))+b3*exp((-1/3)*ln(1-Tr))
            +b4*exp((1/3)*ln(1-Tr)));
Function Vwl(T:real):real; {dynamic viscosity of liquid water}
 Var Tc,b1,b2,b3,b4,Tr: real;
 Begin
     Tc := 647.25;
     b1 := -1.01083*10;
                                  b2 := 1.39621;
     b3 := 4.8431*0.1;
                                   b4 := 7.1019*0.1:
     Tr := (T+273.15)/Tc;
```

```
Vwl := \exp(b1+b2*\exp((1/3)*\ln(1/Tr-1))+b3*\exp((4/3)*\ln(1/Tr-1))
             +b4*exp((7/3)*ln(1/Tr-1));
 End:
Function Vwg(T:real):real; {dynamic viscosity of vapor water}
  Var Tc,b1,b2,b3,b4,Tr: real;
 Begin
     Tc := 647.25:
     b1 := -1.0373*10;
                                  b2 := -8.6737*0.1;
                                 b4 := 9.051*0.01;
     b3 := -2.9699*0.1;
     Tr := (T+273.15)/Tc;
      Vwg := \exp(b1+b2*\exp((1/3)*\ln(1/Tr-1))+b3*\exp((4/3)*\ln(1/Tr-1))
             +b4*exp((7/3)*ln(1/Tr-1)));
 End:
Function kw(T:real):real; {thermal conductivity water}
  Var Tc,b1,b2,b3,b4,b5,Tr: real;
 Begin
     Tc := 647.25;
     b1 := -1.63975;
                                  b2 := 1.11421*10:
                                b4 := 1.67447*10;
     b3 := -2.00805*10;
     b5 := -5.78763;
     Tr := (T+273.15)/Tc;
     kw := b1+b2*Tr+b3*Tr*Tr+b4*Tr*Tr+b5*Tr*Tr*Tr*Tr;
  End:
Function tanh(x:real):real; {calculate hyperbolic tangent}
 Begin
     tanh := (exp(x)-exp(-x))/(exp(x)+exp(-x));
 End,
Function Sw(T:real):real; {surface tension water}
  Var Tc,b1,b2,b3,b4,Tr : real;
 Begin
     Tc := 647.25;
     b1 := 2.358*0.1;
                            b2 := -6.25*0.1;
     b3 := 1.256;
     Tr := (T+273.15)/Tc;
     Sw := b1*exp(b3*ln(1-Tr))*(1+b2*(1-Tr));
 End:
Function Pe(T:real):real; {vapor pressure of ethanol}
 Begin
     Pe := \exp(0.23584*100-(3814/(T+273.15-46.29)));
 End:
Function Del(T:real):real; {density of liquid ethanol}
 Begin
     Del:= 1/((1000/46)*(0.69186/1000)*exp((1+exp(0.2857*)
            ln(1(T+273.15)/516.15))*ln(0.25041)));
```

```
End:
Function Deg(T:real):real; {density of vapor ethanol}
 Begin
     Deg:= 0.0001*exp(0.0278*(T+273.15));
 End;
Function Lae(T:real):real; {latent heat of ethanol}
 Begin
     Lae := 2393.4*(516-T-273.15)+442271;
 End;
Function Cpe(T:real):real; {density of liquid ethanol}
 Begin
     Cpe := 1000*((108.6-0.2068*(273.15+T)+0.0002197*(273.15+T)*(273.15+T)
             +(1.73529/1000000)*(273.15+T)*(273.15+T)*(273.15+T))/46);
Function Vel(T:real):real; {dynamic viscosity ofliquid ethanol}
 Begin
      Vel:= \exp(-12.888+1950.174/(24.124+(T+273.15)));
 End:
Function Veg(T:real):real; {dynamic viscosity of vapor ethanol}
 Var Tc,b1,b2,b3,b4,Tr: real;
 Begin
     Tc := 512.64;
     b1 := -1.06045*10; b2 := -8.74383*0.1;
     b3 := -2.80468*0.1; b4 := 6.1553*0.01;
     Tr := (T+273.15)/Tc;
     Veg:= \exp(b1+b2*\exp((1/3)*\ln(1/Tr-1))+b3*\exp((4/3)*\ln(1/Tr-1))
           +b4*exp((7/3)*ln(1/Tr-1));
 End:
Function ke(T:real):real; {thermal conductivity ethanol}
 Begin
     ke := 0.253-(2.81/10000)*(T+273.15);
 End:
Function Se(T:real):real; {surface tension ethanol}
 Begin
     Se := 0.04678-0.0000832*(T+273.15);
 End:
Function C staggered(Re,St,Sl:real):real; {Zhukauskas factor}
 Var s: real;
 Begin
     If Re<100 then C staggered := 0.9
        Begin
           If Re<1000 then C_staggered := 0.51
          Else
```

```
Begin
                s := St/Si;
                If Re<200000 then
                  Begin
                     If s < 2 then C_staggered := 0.35*exp(0.2*ln(s))
                     else C_staggered := 0.4;
                  End
                Else
                  Begin
                     If Re<1000000 then C_staggered := 0.022;
                  End;
             End;
        End:
 End;
Function m staggered(Re:real):real; {Zhukauskas factor}
 Begin
     If Re<100 then m_staggered := 0.4
     Else
        Begin
           If Re < 1000 then m staggered := 0.5
           Else
             Begin
                If Re < 200000 then m_staggered := 0.6
                Else
                   Begin
                      If Re<1000000 then m_staggered := 0.84;
                   End;
             End;
        End:
 End;
Function C_aligned(Re:real):real; {Zhukauskas factor}
     If Re<100 then C_aligned := 0.8
     Else
        Begin
           If Re<1000 then C_aligned := 0.51
           Else
             Begin
                If Re<200000 then C_aligned := 0.27
                Else
                   Begin
                      If Re < 1000000 then C_aligned := 0.21;
                   End;
             End;
```

```
End;
 End:
Function m aligned(Re:real):real; {Zhukauskas factor}
     If Re < 100 then m_aligned := 0.4
     Else
        Begin
           If Re < 1000 then m aligned := 0.5
           Else
             Begin
                If Re < 200000 then m aligned := 0.63
                   Begin
                      If Re < 1000000 then m aligned := 0.84;
             End;
        End:
 End:
Function UA001(Th, Tc, mh, mc, Q, nc:real):real; {calculate UA of water}
          k = 14.9; {thermal conductivity of metal}
 Var
        Aeo, Aei, Aco, Aci, Afe, Afc, Abe, Abc, heo, hei, hco, hci, mfac, mfae,
        Vmaxe, Vmaxc, Ree, Rec, Pre, Prc, Nue, Nuc, w, effe, effc, Zc, Zef, Zep,
        phe2,phe3,T,Z,Re,a: real;
        del Tsat,x,y,heif,heip,Pr,fp: real;
        Ve, Vc, Vmaxe1, Vmaxe2, Vmaxc1, Vmaxc2: real;
 Begin
        If arrangement = 1 then
          Begin
            If fintype = 1 then
              Begin
                 Abe := nc*Le*3.14159*od;
                 Abc := nc*Lc*3.14159*od;
                 Afe := 0;
                 Afc := 0;
                 Ve := mh/(den air(Th)*cross section area);
                 Vc := mc/(den air(Tc)*cross section area);
                 Vmaxe := St*Ve/(St-od);
                 Vmaxc := St*Vc/(St-od);
                 Ree := den_air(Th)*Vmaxe*od/vis_air(Th);
                 Rec := den air(Tc)*Vmaxc*od/vis air(Tc);
                 Pre := Cp air(Th)*vis air(Th)/k air(Th);
                 Prc := Cp air(Tc)*vis air(Tc)/k air(Tc);
                 Nue := C_aligned(Ree)*exp(m_aligned(Ree)*in(Ree))
                          *exp(0.36*ln(Pre));
```

```
Nuc := C aligned(Rec)*exp(m aligned(Rec)*ln(Rec))
                *exp(0.36*ln(Prc));
        heo := Nue*k_air(Th)/od;
        hco := Nuc*k air(Tc)/od;
        effe := 0:
        effc := 0:
     End:
   If fintype = 2 then
     Begin
        Afe := ((nc*Le*3.14159)/(fs+ft))*(0.5*(sqr(od+2*fh)-sqr(od))
                +(od+2*fh)*ft);
        Abe := ((nc*Le*3.14159)/(fs+ft))*od*fs;
        Afc := ((nc*Lc*3.14159)/(fs+ft))*(0.5*(sqr(od+2*fh)-sqr(od))
                +(od+2*fh)*ft);
        Abc := ((nc*Lc*3.14159)/(fs+ft))*od*fs;
        mfae := nc*Le*(St-od-(2*ft*fh)/(fs+ft));
        mfac := nc*Lc*(St-od-(2*ft*fh)/(fs+ft));
        Vmaxe := mh/(den air(Th)*mfae);
        Vmaxc := mc/(den air(Tc)*mfac);
        Ree := Vmaxe*od*den air(Th)/vis air(Th);
        Rec := Vmaxc*od*den air(Tc)/vis air(Tc);
        Pre := Cp air(Th)*vis air(Th)/k air(Th);
        Prc := Cp air(Tc)*vis air(Tc)/k air(Tc);
        Nue := 0.30*\exp(0.625*\ln(\text{Ree}))*\exp(-0.375*
                 ln((nc*Le*3.14159*od)/(Afe+Abe)))
                 *exp(0.333*ln(Pre));
        Nuc := 0.30*\exp(0.625*\ln(\text{Rec}))*\exp(-0.375*
                 ln((nc*Lc*3.14159*od)/(Afc+Abc)))
                 *exp(0.333*ln(Prc));
        heo := Nue*k air(Th)/od:
        hco := Nuc*k air(Tc)/od;
        w := 0.5*od*(((od+2*fh)/od)-1)*(1+0.35*ln((od+2*fh)/od));
        effe := \frac{(\tanh(\sqrt{t^*k})^*w)}{(\sqrt{t^*k})^*w)}
        effc := (tanh(sqrt(2*hco/(ft*k))*w)/(sqrt(2*hco/(ft*k))*w));
     End:
 End;
If arrangement = 2 then
 Begin
   If fintype = 1 then
     Begin
        Abe := nc*Le*3.14159*od:
        Abc := nc*Lc*3.14159*od;
        Afe := 0;
        Afc := 0;
```

```
Ve := mh/(den air(Th)*cross section area);
    Vc := mc/(den air(Tc)*cross section area);
    Vmaxe1:= St*Ve/(St-od);
    Vmaxc1:= St*Vc/(St-od);
    Vmaxe2:= St*Ve/(2*(Sd-od));
    Vmaxc2:= St*Vc/(2*(Sd-od));
    If Vmaxe1 > Vmaxe2 then Vmaxe := Vmaxe1
    else Vmaxe := Vmaxe2:
    If Vmaxc1 > Vmaxc2 then Vmaxc := Vmaxc1
    else Vmaxc := Vmaxc2;
    Ree := den air(Th)*Vmaxe*od/vis air(Th);
    Rec := den air(Tc)*Vmaxc*od/vis air(Tc);
    Pre := Cp air(Th)*vis air(Th)/k air(Th);
    Prc := Cp air(Tc)*vis air(Tc)/k air(Tc);
    Nue := C \text{ staggered(Ree,St,Sl)*exp(m staggered(Ree)*ln(Ree))}
              *exp(0.36*ln(Pre));
    Nuc := C \text{ staggered(Rec,St,Sl)*exp(m staggered(Rec)*ln(Rec))}
              *exp(0.36*ln(Prc));
    heo := Nue*k air(Th)/od;
    hco := Nuc*k air(Tc)/od;
    effe := 0;
    effc := 0;
 End:
If fintype = 2 then
 Begin
     Afe := ((nc*Le*3.14159)/(fs+ft))*(0.5*(sqr(od+2*fh)-sqr(od))
             +(od+2*fh)*ft);
     Abe := ((nc*Le*3.14159)/(fs+ft))*od*fs;
     Afc := ((nc*Lc*3.14159)/(fs+ft))*(0.5*(sqr(od+2*fh)-sqr(od))
             +(od+2*fh)*ft);
    Abc := ((nc*Lc*3.14159)/(fs+ft))*od*fs;
    mfae := 2*nc*Le*(Sd-od-(2*ft*fh)/(fs+ft));
    mfac := 2*nc*Lc*(Sd-od-(2*ft*fh)/(fs+ft));
     Vmaxe := mh/(den air(Th)*mfae);
     Vmaxc := mc/(den air(Tc)*mfac);
     Ree := Vmaxe*od*den_air(Th)/vis_air(Th);
    Rec := Vmaxc*od*den air(Tc)/vis air(Tc);
    Pre := Cp \operatorname{air}(Th)*\operatorname{vis} \operatorname{air}(Th)/k \operatorname{air}(Th);
    Prc := Cp_air(Tc)*vis_air(Tc)/k_air(Tc);
    Nue := 0.242*\exp(0.658*\ln(\text{Ree}))*\exp(0.297*\ln(\text{fs/fh}))
              *exp(-0.091*ln(St/SI))*exp(0.33333*ln(Pre));
    Nuc := 0.242*\exp(0.658*\ln(\text{Rec}))*\exp(0.297*\ln(\text{fs/fh}))
             *exp(-0.091*ln(St/S1))*exp(0.33333*ln(Prc));
    heo := Nue*k air(Th)/od;
```